The Formation of the Head of Rat Spermatozoa

ABSTRACT

The chronological formation and development of three rat spermatozoon head components - the nucleus, acrosomic system and perinuclear theca - were investigated by electron microscopy during spermiogenesis and transit through the epididymis. Chromatin condensation involves an intermediate step of coarse chromatin filament formation. Coarse filaments aggregate into coarse chromatin clumps which, in turn, fuse into a dense homogeneous mass late in spermiogenesis. The completely formed acrosomic system is composed of the acrosome and head cap, both enclosed in a continuous unit membrane, and a separated portion of the head cap called the ventral flap running on the antero-ventral part of the head. During spermiogenesis, the acrosome and head cap are formed as distinct morphological entities, and the ventral flap is split off from the head cap during step 14 of spermiogenesis. Perinuclear material forms adjacent to the nucleus in three areas which eventually become connected. The material of this continuous layer condenses during the last steps 18 and 19 of spermiogenesis to form the perinuclear theca, a continuous layer over the nucleus except around the attachment site of the flagellum.

Name: Michael F. Lalli

Title of Thesis: The Head of the Rat Spermatozoon and Its Formation during Spermiogenesis: An Electron Microscopic Study

Department: Anatomy

Degree: Doctor of Philosophy

THE HEAD OF THE RAT SPERMATOZOON AND ITS FORMATION DURING SPERMIOGENESIS: AN ELECTRON MICROSCOPIC STUDY

by

Michael F. Lalli

A thesis submitted to the Faculty of Graduate Studies and Research in partial fulfillment of the requirements for the degree of Doctor of Philosophy

Department of Anatomy
McGill University
Montreal, Canada

March, 1972

ACKNOWLEDGEMENTS

I would like to thank Dr. C.P. Leblond, Chairman of the Department of Anatomy, for the privilege of working in his department.

Many thanks to Dr. Y. Clermont, my research director, for his patient and enthusiastic guidance during the course of this work.

Mrs. Magdalena Volkov and Miss Nancy Edson provided technical assistance; I am deeply grateful for their enthusiasm, skill and good nature.

The illustrations are by Mrs. Margot Oeltzschner and the plates were photographed by Mr. Anthony Graham. Some of the reference material was obtained through Mrs. I. Kramer. To these people I extend my appreciation.

I would like to thank my wife, Carol, for help in the preparation of the manuscript and Mrs. J. Streit for the typing.

TABLE OF CONTENTS

CHAPTER I

INTRODUCTION

Morphological studies of spermatozoa effectively commenced with Leeuwenhoek, whose first microscope provided the necessary optical resolution to examine minute objects. His and other early interpretations of sperm morphology have been well chronicled, and the ensuing controversy between the 17th and 18th century "animalculists" and "ovists" is familar to all biologists. With the continuing improvement of light microscopy, considerable knowledge accumulated about the general sperm morphology of many species, culminating with the studies of Retzius in the early 1900s. At about this time, scientific attention became directed more toward the functioning of spermatozoa in fertilization and embryological development than to sperm anatomy, and this trend continued until the advent of electron microscopy in the 1950s. Spermatozoa were again among the first objects to be examined by this new technique, and the capability of resolving subcellular structural details led to a renewed and continuing interest in sperm morphology. The accumulating knowledge of sperm ultrastructure is gradually turning attention back toward fertilization mechanisms, proving once again that only a combination of anatomical and functional data can resolve biological problems.

It was established in the earliest morphological studies that a head and flagellum constituted the basic discernible units of spermatozoa from more common animals. In 1909,

Retzius published one of the most comprehensive studies of the general anatomy of mammalian spermatozoa, illustrating the diversity of the size and shape of spermatozoa from numerous species. Despite this diversity, mammalian sperm heads can be classified into three basic shapes: spatulate, ensiform and falciform. Recent reviews by Bishop and Walton (1960), Hancock (1966) and Fawcett (1958, 1970) have pointed out this trimorphism.

The two main components of the head are the condensed nucleus and the acrosomic system. A perinuclear layer of material may be present between the nucleus and the acrosomic system. This perinuclear layer is especially prominent in some rodent spermatozoa, but it is a matter of controversy whether it is present in those of all mammals. The variability in size and /or shape of these individual components determines head shape.

The spermatozoa of rats, mice, hamsters, lemmings and voles are falciform in shape. These animals all belong to the suborder Myomorpha (families Muridae and Cricetidae) and will be referred to collectively as myomorph rodents in the subsequent discussion. The spermatozoa of these animals were characterized by Retzius (1909) and Friend (1936) by their falciform shape and the presence of a dark staining rod on the concave surface of the anterior part of the head.

Since the present study deals only with ultrastructural changes in the heads of developing rat spermatozoa, the following literature review has been restricted to anatomical

studies of head structures. Each organelle of the spermatozoon head will be described individually. Morphological features will be described as they are seen with both the light and the electron microscope. Where possible, emphasis will be placed upon structures in rat or other myomorph spermatozoa.

Nucleus

Contemporaries of Retzius began studies of rat spermiogenesis, the process by which spermatids of the testis develop into mature spermatozoa (Brown, 1885; Niessing, 1897; Lenhossék, 1898; Duesberg, 1908). These cytologists described the general morphological changes in the size and shape of the nucleus and the development of other organelles during the transformation of the oval spermatid into the falciform spermatozoon. Much later, Leblond and Clermont (1952a, b) precisely described the chronological sequence of this process by using the periodic acid-Schiff histochemical technique, which stains the acrosomic system. They recognized nineteen distinct steps of spermatid maturation (Figs. 1 and 2). The nuclear affinity for basic stains increased and reached a maximum as the nucleus condensed and elongated during steps 12 through 14 of development.

Daoust and Clermont (1955) used the Feulgen technique to study the distribution of DNA in developing spermatids. The nuclei of young spermatids (steps 1-6) contained DNA in fine dust-like granulations and, occasionally, larger granules. In steps 7 and 8, the DNA appeared to disperse into

fine granules which accumulated at opposite nuclear poles, leaving a light equatorial zone. As the nuclei began to elongate in step 9, the Feulgen-positive granules became distributed more evenly throughout the nucleus, but some areas were free of stainable material. These unstained spaces were more apparent in steps 10 and 11 because the stained area was more reactive. The nuclear material became homogeneously stained in step 12 and increased to its maximum staining intensity in steps 13 and 14 as the nucleus attained its sickle-shape. The nuclei of steps 15-19 spermatids had the same intensity of staining as those of steps 13 and 14. The stainable material could be removed from nuclei of steps 1-15 with DNAase. Nuclear material of steps 16-19 was resistant to this treatment, as it was in the mature spermatozoa.

Early electron microscopic investigations (Watson, 1952; Challice, 1953) added little information to the sequence of chromatin condensation as observed by light microscopy. Burgos and Fawcett (1955) and Fawcett and Burgos (1956), using improved techniques, outlined the ultrastructural changes seen in the chromatin during cat and human spermiogenesis as follows: The chromatin appears as finely packed granules (circa 100 A) in the early spermatid. During the elongation phase, these fine granules are replaced by coarse granules with increased osmophilia. The coarse granules become more closely packed as differentiation continues. Late in maturation, these coarse dense granules coalesce into a smooth homogeneous mass which contains some vacuoles. Most

authors consider the nucleus to be without resolvable detail at this time, but Koehler (1970) has shown that the chromatin of the late rabbit spermatid is lamellated. In a brief review of chromatin condensation, Fawcett (1958) pointed out that this process is similar in amphibia, birds and mammals. Others have substantiated these findings in various animals (Horstmann, 1961; Prokof'Yeva-Bel'Govskaya and Chun-He, 1961; Brökelmann, 1963; Franklin, 1968; DeKretser, 1969).

The nucleus of the mature spermatozoon of all studied mammals is covered by an envelope composed of two unit membranes. The inner membrane is closely associated with the condensed chromatin over most of the nuclear surface, with the outer membrane a variable distance from it (Nicander and Bane, 1962, 1966). In the region of the nucleus where the flagellum inserts, the nuclear envelope reflects away from the condensed chromatin and forms long folds of membrane that extend into the neck region of the flagellum (Nicander and Bane, 1962, 1966; Blom and Birch-Anderson, 1965; Wu and Newstead, 1966; Yanagimachi and Noda, 1970a). This redundant nuclear envelope does not always form folds or simple scrolls, but may form very complex scrolls as in the bat (Fawcett and Ito, 1965; Wimsatt et al., 1966) or the two primates, slow loris and bush-baby (Bedford, 1967a). Fawcett (1965) interpreted the simple folds as resulting from the reduction of nuclear volume during spermiogenesis. Franklin (1968) studied the formation of the redundant nuclear envelope in monkey spermatids and agreed with Fawcett's interpretation of the origin of the nuclear

membrane folds. Very prominent nuclear pores are present in these folds in the mature spermatozoon (Nicander and Bane, 1966; Bedford, 1967a; DeKretser, 1969; Pedersen, 1969a; Koehler, 1970; Zamboni et al., 1971).

Lenhossék (1898) commented on the fact that the part of the spermatid nuclear membrane covered by the acrosomic granule appeared to be considerably thicker. Recent investigators have noticed the deposition of material against the inner nuclear membrane in the area of the acrosomic vesicle (Fawcett and Burgos, 1956; Horstmann, 1961; Hopsu and Arstila, 1965; Gardner, 1966; Franklin, 1968). This modified area under the acrosomic vesicle never contains nuclear pores (Franklin, 1968; Sandoz, 1970). Brökelmann (1963) observed that chromatin condensation in rat spermatids begins adjacent to this modified area of the nuclear envelope.

During nuclear elongation and chromatin condensation, areas appearing devoid of nuclear material form in the caudal part of the nucleus. These areas, containing material of low electron density, are formed between the condensing chromatin and the porous nuclear envelope (Burgos and Fawcett, 1955; Brökelmann, 1963; Franklin, 1968). Brökelmann (1963) believed that folds of nuclear envelope containing this low electron density material were budded off into the cytoplasm. These folds were recognized by Franklin (1968) as being the precursors of the redundant nuclear folds of the mature spermatozoon.

In both spermatids and spermatozoa, these nuclear folds contain a material of lower electron density than the chromatin

and, occasionally, a strand of condensed chromatin (André, 1963; Nicander and Bane, 1966; Franklin, 1968). André (1963) suggested that the karyolymph material of low density in the nuclear protrusion of a rat spermatid was in the process of being expelled. Horstmann (1961), studying human spermatids, described two methods whereby electron dense material was transferred from the nucleus to the cytoplasm. In early spermatids, the electron dense material moved from the nucleoplasm to an area of the nuclear envelope and was subsequently budded off as lamellae. Stacks of these lamellae formed the lamellar bodies which were commonly seen in these early human spermatids. This process ceased in later spermatids, and the nuclear material was then removed from the nucleus by a second mechanism. Nuclear vacuoles containing material of low electron density were transferred from the nucleus to the cytoplasm surrounding the caudal part of the nucleus. Many vacuoles of this type were found in the cytoplasm of these spermatids.

Another method for the transfer of nuclear material to the cytoplasm was proposed by Prokof'Yeva-Bel'Govskaya and Chun-He (1961). Tubules, which they considered to be canals of endoplasmic reticulum, supposedly carried nuclear material into the cytoplasm. From their electron micrographs, it appears that these tubules were actually microtubules of the caudal tube.

There is also other evidence for the exchange of material across the nuclear envelope of the late spermatid. Lison (1955) observed an increase in arginine in the nuclei of step 14-19 rat spermatids. Using radioactive labeled ^{3}H-arginine, Monesi

(1964, 1965) observed bound radioactive material in the nuclei of steps 11-15 mouse spermatids. He gave evidence that this was arginine-rich histone replacing lysine-rich histone. By use of histochemical techniques, Vaughn (1966) demonstrated the replacement of lysine-rich histones with those containing predominantly arginine in steps 13-16 rat spermatid nuclei. The replaced lysine-rich histone was later found in the sphere chromatophile of the residual body. The arginine-rich histone does not turn over and is, therefore, found in the mature spermatozoon (Kopečný, 1970).

A modification of the nuclear envelope is found in the implantation fossa of the flagellum. Here the nuclear membranes are regularly spaced with numerous cross bridges between them (Fawcett and Phillips, 1969b; Fawcett, 1970). A thickened layer of material is closely applied to the outer nuclear envelope. This is the basal plate which stains strongly with phospho-tungstic acid (Nicander and Bane, 1962, 1966). The implantation fossa has a species specific shape, but the structural components are similar in all mammals (Blom and Birch-Anderson, 1965; Nicander and Bane, 1966; DeKretser, 1969; Pedersen, 1969a; Zamboni and Stefanini, 1971).

Acrosomic System

The acrosomic system of mammalian spermatozoa covers the lateral and apical surfaces of the nucleus. It usually extends beyond the nucleus in a thickened apical segment of variable volume which depends on the species (Fawcett, 1958, 1970; Fawcett

and Phillips, 1970; Hancock, 1966). For descriptive purposes the acrosomic system can be divided into three regions: the apical projecting anteriorly beyond the edge of the nucleus; the main segment extending back over the anterior and lateral portions of the nucleus; and a thinner equatorial segment caudal to the main segment (Fawcett, 1970; Fawcett and Phillips, 1970). Early electron microscopic studies demonstrated that the acrosomic system is enclosed in a continuous unit membrane (Burgos and Fawcett, 1955; Horstmann, 1961; Nicander and Bane, 1962; Bedford, 1964). Recently Pikó (1969) pointed out that a small separate vesicle resembling the thin lateral surface of the acrosomic system, is located on the ventral surface of the rat and mouse spermatozoon.

Many investigations with the electron microscope have shown that the acrosomic system in the mature spermatozoon of most animals contains an electron dense, homogeneous material. Investigations of the spermatozoa of guinea pigs (Fawcett and Hollenberg, 1963; Fawcett and Phillips, 1969a) and lemmings (Hopsu and Arstila, 1965) have proved an exception to this general finding. In these species, the apical portion of the acrosome has two zones of differing electron density, even in fully mature spermatozoa.

Early investigators, such as Lenhossék (1898) and Duesberg (1908), recognized the association of the Golgi apparatus, more specifically the idiosome, with granules close to the nucleus of the early spermatid. These granules appeared to fuse and form a larger acrosomic granule, which spreads over the nucleus as a nuclear cap (Lenhossék, 1898).

Lenhossék (1898) considered that this granular structure attached to the nuclear envelope should be named by an appropriate Greek term. He chose the name "akrosoma" because of its position over the nucleus. This term was then applied by other authors to the anterior portion of the mature spermatozoon head. This structure was also called the perforatorium by Waldeyer (1906); the use of the term perforatorium will be discussed in more detail later. Bowen (1924) used the term acrosome for the structure originating from the Golgi apparatus. He objected to the term perforatorium and its implied mechanical function, for he assumed that the acrosome had a physiochemical role in fertilization.

Leblond and Clermont (1952a, b) used the histochemical technique, periodic acid-Schiff, to study the formation of the acrosomic system in rodents. This study was later extended to other mammals (Clermont and Leblond, 1955). As a result of their studies, a precise terminology was devised for the head structures in the spermatid and the mature spermatozoon (see glossary in Leblond and Clermont, 1952b).

In the young spermatid, proacrosomic granules are formed in the Golgi apparatus. These granules fuse to form the acrosomic granule which is applied to the nuclear envelope. The acrosomic granule has an outer and an inner zone. The outer zone spreads over the nucleus forming the head cap and the inner zone forms the acrosome proper.

Early electron microscopic studies clearly showed the origin of proacrosomic granules from the Golgi apparatus and

their subsequent fusion into a larger acrosomic granule (Burgos and Fawcett, 1955; Clermont, 1956; Fawcett and Burgos, 1956). The acrosomic granule appeared as a vesicle in electron micrographs. This membrane bound structure has an electron dense, finely granular center which is surrounded by light flocculent and granular material.

In 1965, Fawcett proposed that the term "head cap" be dropped and that the entire acrosomic system be called acrosome or acrosomal cap. His reasons were later given in detail: "... early electron microscopic studies have shown that the acrosome is not a body confined to the tip of the head, but is a membrane-limited structure that forms a cap over the anterior two-thirds of the nucleus. Thus, it becomes obvious that the 'acrosome' and the 'head-cap' of classical cytology are not separate entities but a single cap-like structure investing the anterior portion of the sperm nucleus" (Fawcett and Phillips, 1969a).

This new terminology has not been accepted by some investigators for a number of reasons, some of which will be put forth in the discussion of this thesis. In light of the above discussion, the inner zone of the acrosomic granule obviously corresponds to the electron dense area of the acrosomic vesicle which is called the acrosomic granule. The more electron lucent area of the vesicle corresponds to the outer zone of the acrosomic granule. The difference in histochemical staining of these two zones as seen with light microscopy (Leblond and Clermont, 1952a, b; Clermont and

Leblond, 1955) and electron microscopy (Susi et al., 1971) warrants careful consideration of the roles of these two zones before new terminology is considered. This is especially true in animals such as the guinea pig which has the two distinct morphological zones in the acrosome of the mature spermatozoon (Fawcett and Hollenberg, 1963).

The equatorial segment, a modified portion of the head cap, is another morphologically distinct area of the acrosomic system that has received increasing attention because of its possible role in fertilization. Nicander and Bane (1962, 1966) have investigated this structure in a number of mammalian species. They have detected the equatorial segment with the electron microscope in species in which it had not been reported in previous light microscopic studies. The contents of this thinner segment of the head cap has a greater electron density and a lower affinity for periodic acid-Schiff stain than the contents of the remainder of the acrosomic system (Nicander and Bane, 1966). The formation of the equatorial segment has not been systematically studied, but it appears to form late in spermiogenesis at about the time of sperm release (Fawcett and Phillips, 1969a; Bedford and Nicander, 1971).

Perinuclear Layer (Perforatorium and Postnuclear Cap)

Any discussion of the perinuclear layer becomes extremely confused because of the use of the terms perforatorium and post-nuclear cap. The term perforatorium has been used by light microscopists to designate a structure anterior to the tip of

the nucleus of myomorph spermatozoa. This term has been vigorously attacked by some investigators because of its functional connotation.

The term perforatorium was introduced by Waldeyer (1906) to designate a structure on the anterior tip of the sperm head which he thought had a boring or cutting function. This same structure was called the acrosome by some of his contemporaries (Lenhossék, 1898; Duesberg, 1908). This structure was usually exclusively referred to as the acrosome after Bowen's (1924) description of its formation from the Golgi apparatus, although Brökelmann (1963) considered acrosome and perforatorium synonymous terms in his electron microscopic study.

The structure that is recognized as the perforatorium today was first described as a rod in the anterior portion of the rat sperm head (Niessing, 1897; Duesberg, 1908; Retzius, 1909; Friend, 1936). This rod was called the perforatorium by Blandau (1951) and Odor and Blandau (1951) to describe a structure in the fertilized egg separate from the nucleus. Austin and Sapsford (1952) studied rat spermatozoa which had been digested in NaOH and found a rod-like structure which resisted hydrolysis, but they considered this as part of the acrosome. Leblond and Clermont (1952a, b), in their study of the acrosomic system of rat spermatids and spermatozoa, pointed out an iron hematoxylin staining structure separate from the acrosomic system. They recognized this as the same structure called the perforatorium by Blandau (1951).

The perforatorium of the rat spermatozoon was investigated,

not homogeneous in the hamster but contains an area of greater electron density covered by one of lesser electron density (Franklin et al., 1970a).

It seems quite clear that, in the falciform spermatozoa of myomorph rodents, there is a structure in the anterior tip of the head separate from the acrosomic system and the nucleus. Fawcett (1970) has questioned whether a similar structure is present as a distinct morphological entity in mammalian spatulate spermatozoa, although a number of other investigators have described such a layer at the electron microscopic level in rabbit, boar and bull spermatozoa. It has been suggested that this layer is homologous with the myomorph rodent perforatorium (Moricard, 1961; Nicander and Bane, 1962; Bedford, 1964; Blom and Birch-Andersen, 1965). Hadek (1963) described a cytoplasmic layer between the nucleus and acrosomic system of rabbit spermatozoa. This layer becomes obvious when the spermatozoon is in the vicinity of the vitelline membrane (Hadek, 1969). Bane and Nicander (1963) and Nicander and Bane (1966) found an electron opaque material in the space under the acrosome of a number of mammalian species. They concurred with Austin and Bishop's (1958a) contention that a structure homologous to the perforatorium occurs in all mammalian sperm.

This is at variance with the views of Fawcett (1965) who used the term subacrosomal space to describe this area in sperm of animals other than rodents. He objects to the term perforatorium because of the functional implication. More recently, Fawcett and Phillips (1969a) used the term sub-

using a number of techniques, by Clermont et al. (1955). They concluded that the perforatorium was a triangularly shaped structure, with its three-pronged caudal extension closely applied to the nuclear apex. Because both the nuclear membrane and the perforatorium resisted alkaline hydrolysis and both were acidophilic, they concluded that the perforatorium was an extension of the nuclear membrane. Austin and Bishop (1958a) investigated the perforatoria of a number of murine and cricetine rodents and substantiated the findings of Clermont et al. (1955). They also postulated that the perforatorium might be present in the spermatozoa of all mammalian species, but in a less distinct form.

Electron microscopic investigation of the rat sperm head proved that the above description of the shape and location of the perforatorium had been correct (Pikó and Tyler, 1964a, b). The perforatorium was described as being composed of densely packed fibrous material enclosed by the outer nuclear membrane and inner acrosomal membrane. The diagrams and the few micrographs of Pikó and Tyler failed to substantiate the continuity between the nuclear envelope and the perforatorium.

A more complete electron microscopic description has been given of the perforatorium in hamster spermatozoa (Franklin et al., 1970a, b; Yanagimachi and Noda, 1970b). These workers have described an electron dense layer of material surrounding and extending beyond the anterior tip of the nucleus. As in the rat, this layer of material lies between the inner acrosomal membrane and the outer nuclear membrane. The perforatorium is

acrosomal space in order to de-emphasize the implied homology between the subacrosomic material in other species and the perforatorium of myomorph rodents. These authors suggested that this subacrosomal layer of material is probably concerned with maintaining the cohesion between the nucleus and the acrosomic system, rather than being directly involved in the perforation or lysis of egg membranes during fertilization. Zamboni et al. (1971), discussing human and monkey spermatozoa, agreed with this interpretation. They stated that the material in the subacrosomal space represented a cytoplasmic region which had been trapped between the nucleus and acrosome during sperm differentiation.

The development of that part of the perinuclear layer which forms the so-called perforatorium has been superficially investigated. Leblond and Clermont (1952a, b) observed that a space developed anterior to the tip of the nucleus and under the acrosomic system during step 17 of rat spermiogenesis. The perforatorium formed in this space during the last steps of spermiogenesis. Franklin et al. (1970b) observed that the perforatorium resulted from a lateral (anterior in the terminology used below) extension of the subacrosomal space and its contents late in spermiogenesis. Brökelmann (1963) reported the same phenomenon and mentioned that the space anterior to the tip of the nucleus had a filamentous appearance. He then confused this space with the acrosomic system and, because its shape was similar to that of the perforatorium described by Clermont et al. (1955), he assumed that the perforatorium and the acrosomic system were the same structure.

Hopsu and Arstila (1965) observed that a space developed between the condensing nucleus and the acrosomic system in the late spermatid of the Norwegian lemming. In this space was a large osmophilic formation of tubular and lamellar structures which they identified as the perforatorium. They hypothesized that the material located in this space resulted either from local metabolism or the foldings of nuclear envelope during a late phase of spermiogenesis.

In the early mouse spermatid, Sandoz (1970) observed that a small space containing granular material forms between the developing acrosomic system and the nuclear envelope. As the nucleus condenses, this space expands and at times contains scrolls of nuclear material; the perforatorium forms in this space.

Gatenby and Wigoder (1929) studied guinea pig spermatozoa using a silver staining technique. They demonstrated, for the first time, a distinct layer of material over the posterior part of the sperm nucleus not covered by the acrosomic system. Nicander and Bane (1962, 1966) observed an electron dense, homogeneous layer of material between the tightly adhering plasma membrane and the nuclear envelope in the postacrosomal area of the sperm head. This material is not a complete cap for it does not cover the nucleus at the insertion of the flagellum (Fawcett, 1958,1965, 1970; Nicander and Bane, 1962, 1966). A number of investigators described discrete structures in this postacrosomal dense layer. Blom and Birch-Andersen (1965) and Wu and Newstead (1966) reported tubules in this layer in bull spermatozoa.

Koehler (1969, 1970) described oriented cords of particles in rabbit spermatozoa using the freeze-etch technique. A septate desmosome arrangement has been reported in the postacrosomal layer in the sperm of bats (Fawcett and Ito, 1965), mice (Stefanini et al., 1969) and man and monkeys (Zamboni et al., 1971).

The continuity of this layer of material over the post-acrosomal, or postnuclear, cap region with that layer under the acrosomic system was mentioned by Hadek (1963, 1969), Stefanini et al. (1969), Franklin et al. (1970a), Yanagimachi and Noda (1970a), and Zamboni et al. (1971). The material in these two layers may be chemically similar, for the post acrosomal layer of a variety of sperm (Nicander and Bane, 1962, 1966) and the material under the acrosomic system of human and guinea pig sperm (Gordon, 1969) both stain with phosphotungstic acid.

The caudal tube is a structure associated with the spermatid nucleus during nuclear elongation. The term "caudal tube" derives from a direct translation by Oliver (1913) of Retzius' (1909) "Schwanröhre". The caudal tube arises from the nuclear ring, a ring of cytoplasm encircling the nucleus at the caudal limit of the head cap (Oliber, 1913; Gresson and Zlotnik, 1945; Burgos and Fawcett, 1955). The caudal tube is composed of microtubules which insert in a granular mass of material within the nuclear ring and extend into the caudal cytoplasm forming a sheath around the posterior part of the nucleus (Courot and Flechon, 1966; Fawcett and Phillips, 1967; Kessel and Spaziani, 1969; Pedersen, 1969b). The fate of the caudal tube has not been

completely studied, but Oliver (1913) claimed that it contributed to the formation of the connecting piece of the flagellum, and Brökelmann (1963) observed the breakdown of the microtubules into granules in the region of the neck piece.

Gresson and Zlotnik (1945) concluded that the formation of the postnuclear cap began at the nuclear ring and spread caudally. The most posterior part of the cap was formed by the development of a second nuclear ring around the most posterior part of the nucleus. In the elongated mouse spermatid, a dense layer forms against the plasma membrane, while at the same time a similar layer develops against the nuclear envelope; these two layers compose the postnuclear cap (Sandoz, 1970). Blom and Birch-Andersen (1965) speculated that the tubular components observed in the bull sperm postnuclear cap might be remnants of the caudal tube. Das (1962) confused the caudal tube with the postnuclear cap and assumed that they were the same structure.

Morphological Changes of Spermatozoa during Epididymal Passage

Spermatozoa attain their full fertilizing capacity during passage through the epididymis (Young, 1931). It has been assumed that this involved a physiological or biochemical change in the spermatozoon (Young, 1931; Blandau and Rumery, 1961, 1964). Blandau and Rumery (1964) demonstrated a change in flexibility and patterns of flagellar movement during sperm maturation. A change in position of the cytoplasmic droplet during epididymal passage was observed by Young (1931) and many later investigators.

The first demonstration of a morphological change in the sperm head during epididymal passage was that of Fawcett and Hollenberg (1963). In this and a subsequent study (Fawcett and Phillips, 1969a), it was demonstrated that the apical segment of the guinea pig and chinchilla acrosomic system (acrosome proper of Leblond and Clermont, 1952a, b) was remodeled during epididymal passage. There is a dramatic change in shape of the chinchilla and guinea pig spermatozoon from the time of sperm release from the germinal epithelium until it attains its definitive shape in the cauda epididymidis. A similar, but less dramatic, change takes place in a comparable area of the acrosomic system of the rabbit spermatozoon during transit through the epididymis (Bedford, 1965). The change in the acrosomic system of the guinea pig is closely correlated with a particular region of the epididymal duct (Fawcett and Hollenberg, 1963). The correlation of the change in the acrosome with the level of the duct is not as precise in the rabbit, as there are variations in the shape of the acrosomic system within a particular region of the epididymis (Bedford, 1965).

These studies have demonstrated a morphological characteristic of mature spermatozoa which has only been alluded to in the foregoing discussion; this is the relationship of the plasma membrane to the structures of the head. Bedford (1965) pointed out that the plasma membrane loosely covers the acrosomic system in the mature sperm but is tightly bound to the postnuclear cap, or postacrosomal, area. In the caput

epididymidis, the plasma membrane closely covers the acrosomic system. This loosening of the plasma membrane over the acrosomic system during epididymal passage also was shown by Fawcett and Phillips (1969a).

It is now commonly accepted that the plasma membrane loosely covers the acrosomic system and fits very closely to the postacrosomal or postnuclear cap region in the mature epididymal or ejaculated mammalian spermatozoon. However, Zamboni and Stefanini (1968) studied the configuration of the plasma membrane in the mature epididymal spermatozoon and concluded that the loosening of the plasma membrane observed by other investigators was due to inproper fixation.

Ultrastructural Changes in the Acrosome and Perforatorium (Perinuclear Layer) during Fertilization

The changes in the head components during fertilization have been extensively reviewed (Dan, 1967; Austin, 1968; Hadek, 1969; Pikō, 1969; Bedford, 1970; Franklin, 1970) and will only be commented on briefly here to illustrate the importance of the structures to be dealt with in the present thesis. Most of the material of the sperm acrosomic system is released before, or during, sperm penetration of the cumulus oopherus layer (Austin and Bishop, 1958; Pikō and Tyler, 1964a, b; Bedford, 1967b, 1968; Franklin et al., 1970a; Yanagimachi and Noda, 1970c). The material of the acrosomic system is released from the sperm head by the formation of multiple fusions and vesiculations between the plasma membrane and the outer acrosomal

membrane (Barros et al., 1967). The equatorial segment of the acrosome appears unchanged during the passage through the cumulus (Barros et al., 1967; Bedford, 1967b, 1968; Franklin et al., 1970a). Therefore, after passage through the cumulus, the anterior tip of the sperm is covered by the perfortatorium, which in turn is covered by the inner acrosomal membrane. The plasma membrane fuses to the acrosomal membrane at the anterior border of the acrosomal segment (Bedford, 1970; Franklin et al., 1970a).

Yanagimachi and Noda (1970c) claimed that the equatorial segment contains the zona lysin and that the perforatorium performs an important mechanical function in the penetration of the zona pellucida. However, most authors would probably agree with Bedford (1970) that location and nature of the zona lysin and the function of the perforatorium are not known.

The concept of the acrosome reaction described above has been questioned by Zamboni (1971). He disagrees on the basis that insufficient data are available to determine precisely when the acrosome reaction occurs during the fertilization process. He does agree that the fertilizing spermatozoon lacks an acrosomic system when it contacts the egg membrane.

Sperm entry into the vitellus has been observed by a number of investigators. There is general agreement that fusion takes place in the postnuclear (postacrosomic) cap area of the sperm (Pikō, 1964; Pikō and Tyler, 1964a, b; Stefanini et al., 1969; Yanagimachi and Noda, 1970b, d) or in the comparable "mid-lateral" area (Barros and Franklin, 1968).

The apparently intact perforatorium was recognized in fertilized eggs by Blandau (1951) and Odor and Blandau (1951). A number of investigators have used electron microscopy to follow the fate of the perforatorium in the fertilization process and have seen little or no change in its structure (Pikó, 1964; Pikó and Tyler, 1964a, b; Bedford, 1968; Yanagimachi and Noda, 1970b, c).

Purpose of the Present Study

The purpose of this study was to correlate the ultrastructural appearance of rat spermatids with the light microscopic classification of Leblond and Clermont (1952a, b) in order to follow the chronological development of spermatozoon head components during spermiogenesis. Emphasis was placed upon the description of the formation of the acrosomic system and the changes in nuclear morphology. Particular attention was given to those structures or events which may contribute to an understanding of the structure and formation of that layer adjacent to the nucleus which has been variously called perforatorium, subacrosomic layer and postnuclear cap.

CHAPTER II

MATERIALS AND METHODS

Testicular and epididymal tissues were collected from ten rats of the Sherman strain. They ranged from 90 to 120 days old and weighed approximately 400 g. These animals were housed in metal cages in a temperature controlled room (80°F ± 2°), with lighting on a 12-hour on-off cycle. The diet was Purina Laboratory Chow; food and tap water were available ad libitum.

Tissues were collected in early spring or early fall, with the exception of those from one rat which was sacrificed in late January. The gross anatomical and histological features of the reproductive tract were normal in all animals. For the collection of tissue, animals were anesthetized with ether and a large incision was made in the abdominal mid-line. Each testis and its attached epididymis was pulled gently, and without torsion, into the abdominal cavity by the epididymal fat pad. From this point on, the procedure varied with the type of fixation utilized.

The epididymides were fixed by immersion in all cases. Following ligation of blood vessels, the testis and epididymis were removed in toto from one side of the animal. The epididymis was separated quickly from the testis and cleaned of connective tissue and fat. The testis was processed immediately if it were to be fixed by immersion; if not, it was discarded. The cleaned epididymis then was placed in a large drop of fixative on a strip of dental wax. Each epididymis was cut into cross sections representing five different levels: proximal caput epididymidis; middle caput epididymidis; the area of the distal end of the caput

and proximal end of the corpus; the area of the distal end of the corpus and proximal end of the cauda; and a small area of the distal cauda epididymis. Each tissue block was transferred to a drop of fixative on an individual piece of dental wax, and then cut into smaller pieces by opposing motion of two razor blades. The tissue specimens were flushed into fixative bottles from the wax plates. Care was taken to ensure that spermatozoa from one epididymal level were not transferred mechanically to samples from other levels. In most cases, one testis of each animal was fixed by perfusion and the procedure outlined above was followed to sample the contralateral epididymis.

Samples from one epididymis were fixed for $2\frac{1}{2}$ hours at 4oC in a fixative composed of 2.5% glutaraldehyde in 0.1 M Sörensen's phosphate buffer with a pH of 7.2. All other epididymides were fixed in an undiluted Karnovsky's fixative (1965) at room temperature for $4\frac{1}{2}$ to 5 hours. The fixative was changed in all samples after about one hour. Following fixation, the tissues were washed overnight in three changes of 0.1 M phosphate buffer. The next morning, tissues were postfixed in osmic acid, dehydrated in a graded series of acetone, and embedded in Epon 812.

Testicular tubules from five animals were fixed by immersion for $2\frac{1}{2}$ hours in the mixture of 2.5% glutaraldehyde in 0.1 M Sörensen's phosphate buffer mentioned above. This tubular material was obtained by quickly removing the testicular capsule in a petri dish of ice-cold fixative and teasing small lengths of tubules from the testicular parenchyma. These tubules then were washed, postfixed, dehydrated and embedded as above.

One testis from each of five animals was perfused through the testicular artery, using the method of Christensen (1965). In the rat, the testicular artery enters the superior pole of the testis and follows a straight course along the posterior medial border (Harrison, 1949). It is possible to enter this artery with a cannula made from a blunted 26 gauge hypodermic needle (Dym, personal communication). A normal cannulation procedure consisted of making an incision in the testicular capsule over the testicular artery, placing a loop of thread through the capsule and around the artery distal to the intended entrance point of the cannula, and then placing a loop proximal to this point on the artery entering the testis. Tension was placed on the loop around the entering artery, a small opening was made in the artery between the two loops of thread, and the cannula then was inserted. The cannula was tied into place with the distal loop. The loop proximal to the cannula was also tied off quickly to prevent blood from entering the interstitial space of the testis. The spermatic cord was cut at this time to allow rapid egress of the perfusate through the testicular veins.

Testicular vessels were cleared of blood by perfusing approximately 10 ml of saline solution through the perfusion apparatus ahead of the fixative. The fixative then was perfused for 30 minutes by gravity-feed through a bottle 120-130 cm above the table. The fixative was 2.5% glutaraldehyde in 0.1 M Sörensen's phosphate buffer with a pH of 7.2, or 5% glutaraldehyde in s-collidine buffer (Bennett and Luft, 1959) with an pH of 7.4. Following perfusion, the testis was cut into small blocks which

were put into fresh fixative and stored at 4°C for 30 minutes. The fixative and saline solution were at room temperature until this time. After refrigeration, the material was washed four to five times in one hour with 4°C buffer. Then it either was stored overnight, or processed and embedded the same day.

Tissue blocks were trimmed and sections of 1 μ were cut with glass knives on an LKB ultramicrotome. These sections were affixed to glass slides and stained with toluidine blue. The acrosomic system of the various steps of spermiogenesis could be readily identified in this material, as well as the stages of spermatogenesis described by Leblond and Clermont (1952a, b).

Small pyramid-shaped blocks were trimmed from epididymal and testicular tubules. Thin sections (silver-gray) were cut from these blocks with a diamond knife and placed on copper 300 mesh grids. One thick section was cut from each block and stained with toluidine blue as a record of the stage of spermatogenesis. Thin sections were stained with uranyl acetate (Watson, 1958) followed by lead citrate according to the method of Reynolds (1963) or Venable and Coggeshall (1965). Unstained sections or sections stained with lead citrate alone were used occasionally. All sections were examined in a Siemens Elmiskop I.

Details of Reagents and Technical Procedures

Buffers

1. Sörensen's phosphate buffer, pH 7.5, 0.2 M (Lillie, 1965)

0.2 M NaH_2PO_4	14 parts
0.2 M Na_2HPO_4	86 parts

0.2 M $NaH_2PO_4.H_2O$ = 27.60 g/liter

0.2 M $Na_2HPO_4.7H_2O$ = 53.62 g/liter

Mix in above proportions to obtain a 0.2 M buffer solution of pH 7.5.

2. Sörensen's phosphate buffer, pH 7.2, 0.1 M

0.2 M NaH_2PO_4	24 parts
0.2 M Na_2HPO_4	76 parts

Dilute with an equal volume of distilled water to make a 0.1 M buffer solution of pH 7.2.

3. S-collidine buffer, Eastman Organic Chemicals (Bennett and Luft, 1959)

   a. 2.67 ml of s-collidine in 50 ml of distilled H_2O

   b. Lower pH to 7.4 with 1N HCl

   c. Add H_2O to make total volume 100 ml.

Fixation Procedures

1. Karnovsky's fixative (Karnovsky, 1965)

   a. 2 g of paraformaldehyde

   b. 25 ml of H_2O (60-70°C)

   c. 1-3 drops of 1N NaOH

   d. Cool to room temperature

   e. 5 ml of 5% glutaraldehyde

   f. Add 0.2 M phosphate buffer, pH 7.5, to make volume 50 ml

   g. Final pH should be 7.2, with an osmolality of approximately 2000 milliosmols/kg.

2. The osmolarity of 2.5% glutaraldehyde in phosphate or s-collidine buffer is about 550 milliosmols/kg.

3. Postfixation

The material was postfixed in 1% osmium (OsO_4) after the period of washing mentioned in the text. This was done by mixing equal volumes of 2% OsO_4 solution in distilled water with 0.2 M phosphate buffer or, if the fixation was in s-collidine buffer, two portions of buffer to one of 2% OsO_4 in distilled water. This procedure was carried out at 4°C.

Dehydration

After postfixation, the material was washed in two, one-minute changes of cold 30% acetone. Dehydration was continued in the following graded series of acetone:

a. 50% cold acetone allowed to warm to room temperature for 10 minutes.
b. 70% acetone (room temperature) for 10 minutes.
c. 90% acetone for 10 minutes.
d. 100% acetone, 3 changes of 10 minutes each.
e. One part acetone: 1 part Epon for 1 hour.
f. One part acetone: 2 parts Epon overnight.
g. The next day, two changes of pure Epon of one hour each; then the tissue was embedded.

Stains

1. Uranyl acetate (Watson, 1958)
   a. 100 ml of 70% ethyl alcohol
      4 g of uranyl acetate
   b. Filter before using.

2. Lead citrate (Reynolds, 1963)
   a. 1.33 g lead nitrate
      1.76 g sodium citrate
      30 ml distilled water (boiled and cooled)
   b. Shake intermittently for 30 minutes
   c. Add 8.0 ml of 1N NaOH; shake
   d. When clear, add boiled and cooled distilled H_2O to make 50 ml of solution.

3. Lead citrate (Venable and Coggeshall, 1965)
   a. 0.3 g lead citrate added to 10 ml distilled H_2O in a screw-cap centrifuge tube
   b. Add 0.1 ml 10N NaOH; close tube and shake vigorously until all the lead citrate is dissolved
   c. Use only concentrated NaOH solutions or NaOH pellets to prevent precipitation
   d. Makes 10 ml of stain.

RESULTS

The results will be presented in two separate chapters. The detailed ultrastructure of mature spermatozoa from the cauda epididymidis will be given in the first chapter. In addition, the ultrastructure of the spermatozoa in the caput epididymidis and the morphological changes which take place in the spermatozoa during passage through the epididymis will be discussed. In the second chapter, a description of those structural components of the spermatid which develop into the organelles of the head of the spermatozoon will be systematically examined at the various steps of spermiogenesis. Special attention will be given to the nucleus, the nuclear envelope, the acrosomic system, and that layer of material which is immediately applied to the nucleus and is called the perinuclear layer in this thesis. Parts of this layer have also been called the perforatorium, the postnuclear cap, subacrosomal space, and subacrosomic layer.

CHAPTER III

ULTRASTRUCTURE OF THE HEAD OF THE MATURE, EPIDIDYMAL, RAT SPERMATOZOON

Terminology

It is generally agreed that, in flagellated mammalian spermatozoa, the part of the head closest to the insertion of the flagellum is the caudal region and the opposite end of the head is the anterior region. The orientation of the other surfaces is difficult to determine, and these surfaces have been designated arbitrarily. The descriptive terms used in the following discussion are those used by Leblond and Clermont (1952a, b) to describe the rat spermatozoon.

The head of a rat spermatozoon is falciform or sickle-shaped when viewed on its lateral surface (Fig. 4). The pointed anterior extremity is referred to as the apex, while the wider caudal extremity is at the insertion of the flagellum. The convex surface of the spermatozoon head has been designated as dorsal and the concave surface as ventral. The ventral surface terminates caudally at the ventral angle, that point at which the angle of curvature changes abruptly. On the dorsal surface, the caudal extremity of the head is termed the dorsal angle. The incurved surface between the dorsal and ventral angles is referred to as the caudal surface (Fig. 4). The flagellum inserts into a specialized area of the caudal surface called the implantation fossa. The implantation fossa covers the anterior portion of the caudal surface, with the anterior border of the

fossa at the ventral angle (Fig. 4).

When viewed on the lateral surface, the head of the rat spermatozoon is a long (average size, 12 μ), narrow (averaging 2 μ at its widest part), smoothly curved structure (Figs. 3 and 4). The bulk of the head is made up of the condensed nucleus which has the same falciform shape as the head. The nucleus does not extend into the apex of the head but ends bluntly approximately 3 μ from the apex. The apical portion of the head, surrounding the anterior tip of the nucleus and extending anterior to it, is composed of a dense structure that has been called the perforatorium. Another head structure, the acrosomic system, covers all of the dorsal and lateral surfaces of the perforatorium and most of the nuclear surface. The acrosomic system does not, however, cover a small caudal area of the nucleus. A prominence on the ventral head surface, called the ventral spur, is located approximately 2.5 μ anteriorly to the ventral angle (Figs. 3 and 4).

The anterior one-third of the head of the spermatozoon is triangular in cross section, while the remaining two-thirds are oval in section (Fig. 3). The head is widest in the apical triangular region, becomes narrower at the point where the triangular shape changes to oval, then widens again proximally to the flagellum.

Caudal Epididymal Spermatozoa

Nucleus and Nuclear Envelope

As mentioned previously, the nucleus is a dense structure

comprising the major part of the head of the spermatozoon. The nucleus is falciform-shaped when viewed laterally and is oval in cross-sectional outline (Figs. 7-15). In the apical third of the head, the narrower part of the oval points ventrally (Figs. 8 and 9). In the caudal region of the nucleus, including that part of the nucleus which projects dorsally over the flagellum, the nuclear orientation is reversed with the wider nuclear surface facing ventrally and the narrower surface pointing dorsally (Figs. 14 and 16). In the central region of the head, the nucleus has a symmetrically elliptical shape (Figs. 10 and 13).

The chromatin is compact and extremely electron dense; it is homogeneous and shows no filamentous or crystalline infrastructure. There are, however, small areas of rarefactions in the chromatin which have the appearance of small vacuoles. These areas of rarefaction are not membrane bound and are distributed throughout the nucleus (Figs. 9, 15, 16, and 19). A thin layer of chromatin with increased electron density is found on the inner surface of the nuclear membrane at the implantation fossa (Fig. 16).

The condensed chromatin has a very smooth, clearly delineated border under most of the nuclear surface. The inner unit membrane of the double unit membrane forming the nuclear envelope is applied to the surface of the chromatin with a small space between the irregularities of the membrane and the condensed chromatin. The outer membrane of the nuclear envelope is also irregular and lies at a small variable distance from

the inner membrane. The nuclear envelope is modified at two areas of the nucleus which will be described below.

In the implantation fossa, the membranes of the nuclear envelope become very regular and a narrow regular space is formed between them (Fig. 16). The inner membrane adheres tightly to the chromatin. The chromatin against this inner membrane is modified and forms a thin layer with increased electron density. A thick layer of dense granular material on the outer nuclear membrane forms the basal plate (Figs. 16 and 19).

The second region of modified nuclear envelope encircles the nucleus immediately adjacent to the implantation fossa. This region is circumscribed by a small groove running on the ventral head surface half-way between the ventral angle and the ventral spur. This groove forms a comma-shaped line across the lateral head surfaces and passes under the caudal surface a small distance from the implantation fossa (Figs. 3, 4, 14, 15 and 16). The modified area lies between this line and the implantation fossa, thus forming a collar of modified nuclear envelope around the fossa. For the purposes of description, this modified region will be called the perifossa collar.

The nuclear envelope in the perifossa collar shows several modifications. The space between the unit membranes is wider than elsewhere, and fine granular material is found within this space (Figs. 14, 15 and 16). The nuclear envelope loosely covers the nucleus and occasionally forms long folds that extend into the neck region of the flagellum (Fig. 16). A distinctive

feature of the nuclear envelope in the perifossa collar is the presence of nuclear pores (Figs. 14 and 16).

The surface of the chromatin adjacent to the modified nuclear envelope in the perifossa collar is irregular, in contrast to the smooth chromatin surface in other regions. A fine granular or flocculent material is found in the space between the nuclear envelope and condensed chromatin; this material is also present in the nuclear membrane folds that extend into the neck region of the flagellum (Figs. 14, 15 and 16).

Perinuclear Theca

Examination of a series of cross sections, through various levels of the head of the spermatozoon, reveals an electron dense layer of material adjacent to the nuclear envelope (Figs. 7-17). This layer, that will be called the perinuclear theca, surrounds all of the nucleus except in the perifossa collar and implantation fossa. In the apical third of the head, the perinuclear theca is most prominent where it extends apically beyond the tip of the nucleus. This apical part of the perinuclear theca stained heavily with iron hematoxylin in light microscopic preparations and was called the perforatorium by Leblond and Clermont (1952a, b). In subsequent discussion, only the term perinuclear theca will be used. This term encompasses the apical extension, or perforatorium, the layer adjacent to the nuclear surface under the acrosome, and the postnuclear cap.

The basal plate of the implantation fossa, which in some ways is structurally similar to the perinuclear theca, seems to be more closely related to the flagellum in function and mode of formation (see Chapter IV). Therefore, it will not be considered part of the perinuclear theca in this description.

The perinuclear theca in the apical third of the head is a triangularly shaped structure (Figs. 7, 8, 9 and 18) with a slightly concave ventral surface (Figs. 5, 6a, 6b). The theca is electron dense with a fine granular texture which is homogeneous except in a few small areas where the granules appear less densely packed (Figs. 6b, 7, 8 and 15b). As will be seen later, the theca is closely covered by the acrosomic system and the plasma membrane, but is not delimited by a membrane of its own.

The head has an asymmetrical appearance in the area where its triangular cross-sectional shape changes to oval (Figs. 9 and 18). This results in a thickened ventral layer of the perinuclear theca on the ventral surface of the nucleus.

The quantity of material forming the perinuclear theca in the middle third of the head is considerably less than that in the apical third. The theca is especially thin on the lateral surfaces of the nucleus (Figs. 10, 12 and 13). On the dorsal surface of the nucleus, there is a triangularly shaped thickening of the perinuclear theca with a somewhat distorted apical tip (Figs. 10 and 13). On the rounded ventral surface of the head, which is not covered by acrosomic system, the perinuclear theca is also thicker than on the lateral surfaces

(Figs. 10, 12 and 13). The perinuclear theca is not homogeneous in this thickened ventral layer; that part of the theca against the plasma membrane is slightly denser than that region which lies closer to the nuclear envelope (Figs. 10, 12 and 13). This thickened area of the perinuclear theca forms a localized prominence, the ventral spur (Fig. 13).

In the caudal portion of the head, more of the lateral nuclear surface is covered by a relatively thicker layer of the perinuclear theca (Figs. 14, 15 and 16). As mentioned above, this region of the theca also has a dense layer adjacent to the covering plasma membrane. As can be clearly seen in Figures 14, 15 and 16, the perinuclear theca ends at the groove on the lateral head surface which delineates the perifossa collar. No material comparable to that of the perinuclear theca was seen in the perifossa collar. The perinuclear theca appears to be homogeneous over the most caudal part of the nucleus (Fig.17).

To summarize, the perinuclear theca is a nuclear covering of electron dense granular material. The theca forms a continuous cover over the nucleus except at the implantation fossa and in the perifossa collar. The theca is a prominent triangular structure in the apical region of the head. It extends throughout the mid and caudal head areas as a triangular ridge on the dorsal nuclear surface and as a relatively thick covering on the ventral surface. In these head regions, only a thin layer of theca covers the lateral surfaces of the nucleus.

Acrosomic System

The acrosomic system is a membrane bound organelle covering a large area of the perinuclear theca. As it was pointed out in the introduction, the acrosomic system is derived from a secretory-like granule, the acrosomic vesicle, which is elaborated from the Golgi apparatus. During spermiogenesis, the acrosomic vesicle differentiates into two distinct zones; one zone ultimately forms the acrosome and the other forms the head cap. The fully formed acrosome and head cap of later spermatids and spermatozoa remain bound by a single membrane, but the two regions may have distinctly different cytochemical properties.

The material of the acrosomic system appears homogeneous in electron microscopic preparations of mature spermatozoa. Therefore, an attempt was made to define the two areas of the acrosomic system by shape alone. The acrosome corresponds to the thickened part of the acrosomic system on the dorsal surface of the head (Figs. 6b, 7-10, 13-15, 18). The head cap corresponds to the thinner portions of the acrosomic system on the lateral (Figs. 6-15, LHC) and ventral surfaces (Figs. 6-9, 11, 15b, VHC) of the head.

One surface of the acrosomic system unit membrane always faces the perinuclear theca; this surface is continuous with that facing the plasma membrane (Figs. 9-12). That surface facing the perinuclear theca has been called the inner acrosomic membrane, and the one facing the plasma membrane is the outer acrosomic membrane.

At the apical extremity of the head, the perinuclear theca is covered only by the head cap (Figs. 5 and 6a). More caudally, as the triangular cross-sectional outline of the head becomes larger, two features become apparent (Fig. 6b): firstly, a globular swelling on the dorsal surface which corresponds to the most apical portion of the acrosome; and secondly, a small separate portion of the head cap on the ventral concave surface of the head. This separated ventral portion of the head cap always is the same thickness as the lateral components of the head cap.

Even more caudally, where the nucleus begins to appear in sectioned material, the acrosome is very prominent and forms two thickenings on either side of the dorsal ridge of the perinuclear theca (Figs. 8, 9, 15b, 18). In this same head region, the lateral surfaces of the perinuclear theca are completely covered by the head cap (Figs. 5-8, 15b, 18). The separate ventral portion of the head cap, which has a median position in the apical part of the head, has now shifted to lie laterally of the nucleus (Figs. 6-9, 15b, 18).

The acrosome is still prominent in the middle third of the head, or that region where the head is oval in cross section. However, the shape of the acrosome is changed slightly, and it is larger and also asymmetrical (Figs. 10 and 13). The head cap covers less of the lateral surfaces of the perinuclear theca, and the ventral part of the head cap is absent at this level of the head (Figs. 10, 12 and 13). The lateral components of the head cap are often unequal in size (Figs. 10, 12, 13).

In the caudal third of the head, the acrosomic system decreases in size. The acrosome decreases in volume caudally and ends at the level of the implantation fossa. The head cap covers only a small part of the lateral surfaces of the perinuclear theca (Figs. 14, 15a, 16) and decreases in size caudally, ending slightly anterior to the acrosome caudal extremity.

In summary, the acrosome extends along the dorsal head surface from its apical tip to the level of the implantation fossa. The lateral components of the head cap cover all of the lateral surfaces of the perinuclear theca in the apical triangular region of the head. The head cap covers less of the lateral surfaces in the middle third of the head and only small areas in the caudal third. A small separate portion of the head cap is found on the ventral surface in the apical region of the head.

Plasma Membrane

A plasma membrane covers the whole cell including the flagellum. This membrane has been referred to above as being closely bound to the perinuclear theca in those areas where the theca is not covered by the acrosomic system. The plasma membrane very loosely covers the acrosomic system, including the ventral flap, and lies loosely over the modified nuclear envelope in the perifossa collar. Under the groove delineating the perifossa collar, at the limit of the perinuclear theca, the plasma membrane lies especially close to the nuclear envelope (Figs. 14, 15, 16).

Drawings of a longitudinal section of the rat spermatozoon plus cross section at various levels of the head are shown in Figure 24. The location and extent of the various components of the head can be reviewed in this figure.

Caput Epididymal Spermatozoa

Spermatozoa from the caput epididymidis can be distinguished readily from spermatozoa of the cauda by acrosome size and the relationship of the plasma membrane to the acrosomic system. Based on measurements from electron micrographs, acrosomes of spermatozoa from the caput are approximately twice the height of those of the cauda epididymidis spermatozoa. Cross sections reveal that the acrosome volume is also greater in caput spermatozoa. This feature is even more striking when compared to other acrosomic components, which are morphologically identical in spermatozoa from both epididymal areas. The extent and thickness of the head cap and ventral flap, and the total head area covered by the acrosomic system, remain unchanged during the passage through the epididymis.

Accompanying the change in acrosome size is a change in the tightness of fit of the plasma membrane over the acrosomic system. In the caput epididymidis, the plasma membrane covers the acrosomic system closely with a small space between it and the outer acrosomic membrane. This space widens, with the plasma membrane becoming very loose and irregular in spermatozoa of the cauda epididymidis. In both caput and cauda spermatozoa, the plasma membrane is bound tightly to that perinuclear theca

material not covered by acrosomic system.

The morphology of the perinuclear theca was examined carefully in sections, of various planes of cut, taken from the caput epididymidis. There were no morphological differences in the perinuclear theca of caput and cauda spermatozoa.

Morphological Changes in Spermatozoa during Transit through the Epididymis

The acrosome appears to change very little until the spermatozoa reach the upper part of the corpus epididymidis. During their transit through the corpus, the spermatozoa undergo various changes and attain morphological maturity in the cauda epididymidis. A decrease in acrosome volume is accompanied by a loosening of the plasma membrane overlying the acrosomic system. It should be pointed out that the plasma membrane also becomes looser over the ventral flap, which does not appear to decrease in volume. Sampling of the various areas of the epididymis reveals that, in any one area, the spermatozoa seem to form a homogeneous population; i.e., the maturation gradations, as far as acrosome size is concerned, do not appear to be mixed together.

As mentioned previously, spermatozoa from various levels of the epididymis show no morphological differences in the perinuclear theca or membranes, other than loosening of the plasma membrane. Further, there are no differences in the spatial relationships of the various organelles. The nuclear shape remains constant, as does the general head shape with the exception of

the decreased dorsal ridge due to reduction of the acrosomic volume. Thus, the only major morphological change is the difference in head shape due to the change in the acrosome.

CHAPTER IV

DEVELOPMENT OF HEAD STRUCTURES DURING SPERMIOGENESIS

This chapter will be concerned with the formation and/or transformation of the nucleus, acrosomic system, and perinuclear theca. Organelles which are associated with this developmental process, such as the Golgi apparatus and caudal tube, will be briefly described. The developmental steps of this description will be given in chronological order following the steps of spermiogenesis as described by Leblond and Clermont (1952a, b), and they will be divided into three parts encompassing the four phases of spermiogenesis described by these authors. A phase is a period of spermiogenesis, containing a variable number of steps, in which a dominant event occurs.

Golgi and Cap Phases (Steps 1-7)

Figure 2 shows spermatids in steps 1 through 7 of spermiogenesis, as they are seen with the light microscope. The formation and development of the acrosomic system can be followed in light microscopic preparations of 1 μ thick Epon sections stained with toluidine blue. Images seen with this method are similar to those drawn in Figure 2. Blue-staining granules lie close to the spherical nucleus in the Golgi zone of step 2 spermatids. A large granule composed of two zones forms against the nucleus of step 3 spermatids. This granule spreads over the surface of the nucleus to form the head cap. The acrosomic system is well developed in step 7 spermatids

when the Golgi apparatus detaches from it. Electron micrographs of spermatids in steps 1-7 are seen in Figures 25-31.

Nucleus

The chromatin of early spermatids appears as fine filaments and granules, with larger granules (250-400 A) interspersed among them. A thin, electron dense, granular layer is adjacent to a modified area of the nuclear envelope which will be described below.

The nuclear envelope of the early spermatids (1-7) is composed of undulating unit membranes separated by a variable space of 125-450 A. The nuclear envelope is modified in areas approximated by the acrosomic system as follows: 1) the membranes are close together with a narrow regular space between them forming an envelope of approximately 125 A in thickness; 2) there is a thin layer of electron dense material formed against the chromatin side of the inner membrane; and 3) obvious nuclear pores are absent in the modified nuclear envelope. Pores are seen infrequently in the other areas of the nuclear envelope.

The Golgi apparatus in the early spermatids is composed of several stacks of flattened saccules (Figs. 25-31). These stacks are arranged in a hemispherical shape with the inner or concave surface facing the nucleus in the step 2-7 spermatids (Figs. 27-31).

Acrosomic System

Small vesicles, which bud off from the innermost Golgi

saccules, presumably fuse in step 1 of spermiogenesis to form larger vesicles, the proacrosomic vesicles (Fig. 25). These proacrosomic vesicles contain an electron dense center, the proacrosomic granule. The granule is surrounded by material of lower electron density containing a reticulum of small thread-like filaments which radiate from the granule to the limiting membrane of the vesicle. By step 2, these small vesicles have apparently fused to form two to four larger proacrosomic vesicles containing larger proacrosomic granules, also formed by fusion (Fig. 27). In step 3, there is only one large acrosomic vesicle containing a large acrosomic granule (Fig. 26). Material formed in the Golgi apparatus is continually added to the vesicle during this phase.

In steps 4 through 7 of spermatid maturation (cap phase), the head cap is formed by the centrifugal growth of a thin layer from the edge of the acrosomic vesicle over the nuclear surface (Figs. 28-31). The head cap material is identical and continuous with that material surrounding the acrosomic granule. This material is composed of a fine thread-like network in a matrix of low electron density (Fig. 28). The granularity and electron density of the head cap material increases in steps 6 and 7 of this phase (Figs. 29-31), but it never becomes as dense as the acrosomic granule. Although secretory material from the Golgi apparatus is added continuously to the acrosomic system in this phase, the acrosomic granule does not appear to change in volume over that seen in step 3 spermatids.

Modification of the nuclear envelope occurs concurrently

with the growth of the acrosomic system over the nucleus. Small modified areas occur where the proacrosomic vesicles of steps 1 and 2 spermatids approach the nucleus (Fig. 25). This modified area then increases concomitantly with the increase in size of the acrosomic system.

Perinuclear Layer

A distinct layer of material is formed in the space between the acrosomic vesicle and the modified nuclear envelope of step 3 spermatids (Fig. 26). In steps 1 and 2 spermatids, a comparable space appears between the modified nuclear envelope and those acrosomic vesicles which approximate the nucleus. In these developmental steps, this space contains material similar in appearance to the background cytoplasmic matrix (Figs. 25 and 27), and it is only in step 3 and later steps that an obvious subacrosomic layer appears (Figs. 26, 28-31).

This subacrosomic layer forms concurrently with the growth of the head cap over the nucleus. The subacrosomic layer is composed of fine granular and flocculent material, and profiles of what appear to be fine filaments are seen occasionally. The thickness (approximately 250 A) and composition of this layer do not appear to change from the step 3 to the step 7 spermatid except for a small specialized area which becomes prominent in the step 7 spermatid. At this step of development, a furrow develops in the nucleus under the caudal edge or margin of the head cap (Fig. 31). This creates a widened marginal area in the subacrosomic layer.

The material in this marginal area of the subacrosomic layer is distinctly different from the rest of the layer. This distinction is still evident in later steps of spermiogenesis as will be pointed out in the subsequent discussion. Structures, which appear to be sections of large granules, are surrounded by granular material which is somewhat coarser than the rest of the subacrosomic layer (Figs. 32 and 33). These large coarse granules appear as short thick rods in oblique sections through the marginal area.

The subacrosomic layer ends abruptly at the caudal limit of the head cap. Vesicles of various sizes are seen occasionally in the cytoplasm close to the edge of the subacrosomic layer (Figs. 28 and 31).

Acrosome Phase (Steps 8-14)

Light Microscopic Observations

During the acrosome phase of development, steps 8-14 (Fig. 2), the spermatid nucleus changes from spherical to elongate and the chromatin begins to condense. The acrosomic system remains closely associated with the nucleus, and it changes in shape as the nucleus elongates. As the nucleus begins to elongate in step 9, the form of the mature spermatozoon begins to appear and surface designations used in the mature spermatozoon can now be employed. The fully developed head cap spreads over part of the lateral and dorsal nuclear surfaces and the acrosomic granule spreads along the dorsal surface.

In step 8, the orientation of the spermatid nuclei in the

seminiferous epithelium is no longer random; in all spermatids, the surface of the nucleus covered by acrosomic system now points toward the tubular wall. This orientation of the nuclei persists throughout the remainder of spermiogenesis. The spherical nucleus transforms into an oval shape and comes to lie with the acrosomic system close to the plasma membrane. At the same time, the bulk of the cytoplasm, including the Golgi apparatus, which became dissociated from the acrosomic system late in step 7, migrates toward the opposite pole of the cell.

The caudal tube, which began forming late in step 7, is clearly visible in the cytoplasm of acrosome phase spermatids stained with either iron hematoxylin or toluidine blue (Fig. 2). The caudal tube is shaped like a truncated cone with the apex surrounding the middle of the nucleus of the late step 7 and step 8 spermatid and with the base extending into the cytoplasm posterior to the nucleus. The apex of the cone actually surrounds the nucleus at the caudal margin of the head cap; this is seen clearly in the step 9 spermatid. In the subsequent developmental steps of the acrosome phase, the caudal tube changes its orientation to the elongating nucleus, while maintaining its relationship with the head cap as the acrosomic system is molded over the nucleus.

Electron Microscopic Observations of Steps 8 through 11

Nucleus

The chromatin of the acrosome phase spermatids has the same granulo-filamentous appearance as that of the earlier Golgi and

cap phase spermatids. The electron dense layer adjacent to the modified nuclear envelope, which is associated with the acrosome, is apparent during the early steps of the acrosome phase (steps 8-11). In step 8-10 spermatids, the larger coarse granules of chromatin accumulate in an irregular layer adjacent to that part of the nuclear envelope which is not covered by the acrosomic system (Figs. 32 and 33). Clumps of fused coarse granules of chromatin are spread throughout the nucleus of step 10 and 11 spermatids (Figs. 33 and 34). The remainder of the chromatin becomes more filamentous in step 11, and each filament also becomes thicker (Figs. 34 and 35).

The nuclear envelope is modified on that surface which approximates the caudal tube (Figs. 32, 33 and 35). This modified nuclear envelope has an appearance similar to the modified area under the acrosome. The two membranes have a regular space between them and form an envelope approximately 200 A in thickness, which is slightly wider than the modified area under the acrosome (approximately 150 A) (Figs. 32, 33 and 35). The electron dense layer, which lies against the inner membrane of the envelope under the acrosomic system, is not present on that part of the envelope covered by the caudal tube (Figs. 32, 33 and 35).

Only a small area of the nuclear envelope is not covered by acrosomic system or associated with the caudal tube. This small area is around the implantation fossa of the flagellum where the nuclear envelope is approximately 450 A in thickness. Pores are seen occasionally in this area of the nuclear envelope in step 8-10 spermatids.

Acrosomic System

The orientation of the head cap relative to the acrosomic granule changes in the acrosome phase. In the cap phase spermatid (steps 4-7), the head cap is symmetrically distributed around the acrosomic granule (Fig. 33). As the nucleus elongates in step 10, only part of the head cap elongates to cover the dorsal nuclear surface. The acrosome remains at the anterior tip of the nucleus, spreading along the dorsal surface later in the acrosome phase.

In the early acrosome phase (steps 8-11), the thickness of the head cap decreases and the electron density of the head cap increases over that of the step 7 spermatid (Figs. 32-35). The material of the acrosome is distinguishable from that of the head cap in step 10 spermatids (Fig. 33), although the distinction is not as clear as it is in the cap phase spermatids. In electron micrographs of step 11 spermatids, the head cap material appears very similar to that of the acrosome (Fig. 34).

Perinuclear Layer

The subacrosomic layer of the step 8-11 spermatids is similar in appearance to that of the cap phase spermatids. This granulo-filamentous layer has a prominent distinct region at the margin of the head cap (Figs. 32-35). The distinctive granularity of this marginal region is seen in the enlarged parts of Figures 32 and 33 and is also obvious in the more flattened spermatids (Figs. 34 and 35). A granular layer of material is beginning to form between the caudal tube and the nuclear envelope during

this phase of spermiogenesis (Figs. 32, 33 and 35).

The caudal tube appears as a collection of microtubules in electron micrographs (Figs. 32, 33 and 35). These microtubules insert in a specialized area of cytoplasm at the caudal margin of the head cap (Figs. 32 and 33). This area has been called the nuclear ring in light microscopic studies, but electron microscopic studies have shown that this is not a nuclear structure as the term implies. A more appropriate term, which will be used in this presentation, would be the caudal tube insertion ring. The caudal tube insertion ring becomes more prominent in step 11 and later steps of spermiogenesis (Figs. 34, 35, 37, 41).

After the cytoplasm migrates caudally in the step 8 spermatid, the plasma membrane of the spermatid covers the acrosomic system very closely. The structures in the Sertoli cell cytoplasm opposite the acrosomic system become modified in a characteristic manner. Cisternae of smooth endoplasmic reticulum form a layer a short distance from, and parallel to, the plasma membrane of the Sertoli cell. A dense layer of fine filaments develops between, and parallel to, the cisternae of smooth endoplasmic reticulum and the plasma membrane (Insert of Figs. 32 and 33). The area of Sertoli cell cytoplasm facing the acrosomic system of the spermatid always has this arrangement of smooth endoplasmic reticulum cisternae and filaments which is established in step 8 and persists until sperm release in step 19.

Electron Microscopic Observations of Steps 12 through 14

Nucleus

Chromatin condensation proceeds at a rapid rate in these steps of development. This is a continuation of the process begun in steps 10 and 11, in which the scattered granular chromatin areas act as foci around which fine chromatin fibers form. These granular areas become more numerous, and the fibers progressively larger, during development. Soon the fibers become very coarse and accumulate into irregular granular masses. Fine fibers curl between these masses giving the whole structure the appearance of lambs' wool (Figs. 36-38; 40-42). This condensation continues until a continuous granular mass is formed in the nuclei of step 14 spermatids (Fig. 39). These chromatin changes always begin in the apex of the nucleus and progress caudally to the posterior area (Figs. 37, 40). These changes also usually begin adjacent to the modified nuclear envelope under the acrosomic system and spread into other areas of the nucleus. Chromatin condensation always takes place in the same manner, but there is some variability in the degree of condensation amongst spermatids in any one step of development.

In the caudal part of the nucleus of step 12-14 spermatids, an area of low electron density, without chromatin filaments or granular chromatin material, is seen between the condensed chromatin and the nuclear envelope in that area of the nucleus not covered by the acrosomic system (Figs. 37, 38b, 39-42). On part of the future caudal surface of the head, i.e. that area of the nucleus which projects caudally over the insertion of the

flagellum, numerous nuclear pores are evident (Figs. 39-42). The fine granular and flocculent material, which forms the area of low electron density, is seen on both sides of the nuclear pores as well as within the pores (Figs. 37, 39-42). Chromatin condensation takes place adjacent to the nuclear envelope in the implantation fossa in an identical manner to the condensation under the acrosomic system (Figs. 39 and 40).

The nuclear volume decreases as a result of the chromatin condensation. As there is no concomitant decrease in the surface area of the nuclear envelope, an extensive fold of superfluous envelope appears in the anterior and middle portions of the head. This superfluous nuclear membrane is drawn out ventrally and is covered laterally by the head cap and subacrosomic material (Figs. 34, 36 and 38a). A thin layer of granular and flocculent material is seen between the apposed inner nuclear membranes of the ventral fold (Figs. 36 and 38a). This material is continuous with the condensing chromatin.

In the step 14 spermatid, a fold of nuclear envelope projects anteriorly from the nuclear tip. This fold of envelope is identical and continuous with the superfluous envelope on the ventral nuclear surface.

Acrosomic System

In the step 12 and 13 spermatids, the acrosome extends from the apex of the nucleus to about the middle of the nucleus. The acrosome forms a very prominent triangularly shaped ridge at the anterior tip of the nucleus, becoming dome-shaped in the mid-

portion of the nucleus. The head cap covers most of the dorsal surface in the middle and caudal parts of the nucleus and extends to its most posterior tip (Fig. 40). The head cap also covers most of the lateral surfaces of the nucleus as well as almost all of the superfluous nuclear envelope. The head cap covering of the superfluous nuclear envelope has a thickening on its ventral margin (Figs. 36 and 38a).

The acrosome of the step 14 spermatid covers most of the dorsal surface of the nucleus. The head cap covers the most anterior and posterior parts of the dorsal surface as well as most of the lateral surfaces of the nucleus. Late in step 14 and early in step 15, a longitudinal fissure on one of the two lateral surfaces of the head cap separates a small portion of the head cap from the remainder of the acrosomic system. This small part of the acrosomic system is destined to become the ventral component of the head cap. More details about this process will be discussed when the step 15 spermatid is described.

Perinuclear Layer

The subacrosomic layer is composed of granular and flocculent material with a few fine filaments, as in the previous steps of development. The distinct, marginal, coarse granular zone of the subacrosomic layer is evident in steps 12 through 14 (Figs. 36, 37a, 38a, 38b). Some of these coarse granules are in reality sections through short thick fibers. This can be shown by oblique sections through the marginal area of the subacrosomic layer (Fig. 37a). The layer is formed of two zones in the caudal portion of the head (Figs. 37b, 41). The part of the subacrosomic

layer adjacent to the nuclear envelope is more electron dense than that part of the layer adjacent to the acrosome.

The granular layer between the caudal tube and the nuclear envelope, which began to appear in sections of the early acrosome phase spermatids, is more prominent in the step 12-14 spermatids (Figs. 38b, 40, 42). The size and granularity of the caudal tube insertion ring have both increased (Figs. 37b, 38b, 41).

Many smooth-surfaced vesicles are seen in the cytoplasm surrounding the flagellum of the step 12-14 spermatids (Figs. 39-42). These vesicles are irregular in shape and contain a fine granular and flocculent material. The number of these vesicles and the porosity of the nuclear envelope in this area both increase as chromatin condensation progresses throughout the acrosome phase.

Maturation Phase (Steps 15-19)

During this final phase of spermiogenesis, the head of the spermatid acquires the definitive sickle shape of the mature spermatozoon. The acrosomic system shifts over the nucleus to occupy the same relative position to the nucleus that it has in the fully formed spermatozoon (Fig. 2).

The acrosomic system covers most of the nucleus in the step 15 and 16 spermatid, extending from the apex of the nucleus to the dorsal angle (Fig. 2). In the step 17 spermatid, the acrosomic system shifts anteriorly over the nucleus, leaving a space between it and the anterior tip of the nucleus. This shift in

position leaves part of the caudal nuclear surface devoid of a covering of acrosomic system. The structure called the perforatorium, which stains intensely with iron hematoxylin and toluidine blue, is formed in the space anterior to the tip of the nucleus. The perforatorium enlarges in the step 18 spermatid.

Electron Microscopic Observations of Steps 15 and 16

Nucleus

The chromatin of the step 15 and 16 nuclei has condensed to a coarse granularity. These coarse granules are usually more closely packed in the apical than in the caudal areas of the nucleus (Fig. 43). Dispersed throughout the chromatin are numerous small vacuoles, or areas where the coarse granules of chromatin are absent. Material of finer granularity, and less closely packed than the chromatin, is present in these vacuoles (Figs. 50-52). These vacuoles are more prevalent in the caudal area of the nucleus (Figs. 43, 50-52). Material of a similar fine granularity is present in an extensive fold of nuclear envelope, or nuclear protrusion, which forms around the implantation fossa in these developmental steps (Figs. 43, 48, 50-52). A small amount of fine granular material is also present in the fold of superfluous nuclear envelope of the anterior part of the nucleus (Figs. 43-47).

In the step 15 and 16 spermatids, the ventrally projecting superfluous nuclear envelope is still prominent in the anterior portion of the nucleus (Figs. 43-47). In addition to the superfluous nuclear envelope in this area, a wide fold of nuclear

envelope surrounds the implantation fossa in these spermatids (Figs. 43, 48, 50-52). This is the beginning of the formation of the perifossa collar seen in the mature spermatozoon. The nuclear envelope of this wide fold contains prominent nuclear pores (Figs. 49-52), and it is the only area of the nuclear envelope where pores are seen in these steps of development. Pores are no longer present in the nuclear envelope which covers the caudal surface of the nucleus projecting over the flagellum (Figs. 43 and 50).

Acrosomic System

The caudal displacement of the acrosome continues in the step 15 and 16 spermatids, causing the anterior tip of the nucleus to be covered by the head cap only (Figs. 44-46). The acrosome is prominent over the caudal part of the nucleus and at the dorsal angle (Figs. 43, 50, 52). In the middle portion of the head, the acrosome forms a triangularly shaped prominence on the dorsal surface of the nucleus (Figs. 48a and 48b).

The separate head cap portion, which was formed from the remainder of the head cap late in step 14, now lies as a flattened sac on the lateral surface of the head in early step 15 spermatids (Figs. 44 and 45). This flattened sac appears in cross section as a rounded structure late in step 16 (Fig. 46). The remainder of the head cap has a similar appearance to that of the acrosome phase spermatids, except that the prominence on the ventral edge is smaller or lacking entirely (Figs. 48a, 48b, and 52).

Perinuclear Layer

The relationship of the caudal tube to the nucleus changes in step 14 and early step 15. The caudal tube previously covered those lateral surfaces of the nucleus not covered by acrosomic system. A granular layer of material formed between the caudal tube and the nucleus during the acrosome phase of spermiogenesis. In step 14 and early 15, the caudal tube and the caudal tube insertion ring are disengaged from the nuclear surface, leaving the granular layer adjacent to the nuclear envelope covered by plasma membrane only (Figs. 48b, 49, 52). The density of the layer is greatest adjacent to the nuclear envelope and the plasma membrane.

This granular layer, which formed under the caudal tube, is continuous with the subacrosomic layer and the cytoplasm of the spermatid. This layer is also continuous with a granular layer which forms on the caudal surface of the nucleus projecting over the flagellum (Figs. 43 and 50). Therefore, a layer comparable to the perinuclear theca of the mature spermatozoon is first seen in steps 15 and 16 of development.

The subacrosomic layer contains the same elements as in the acrosome phase of development, but the arrangement and texture of the layer is somewhat changed. The layer has a slightly larger volume, and it is less tightly packed in the anterior portion of the head (Figs. 44-47). Coarse granules are more widely dispersed throughout the layer, and it also still contains fine granules and fine filamentous material (Figs. 44-46). The marginal region of the subacrosomic layer is obvious in

some, but not all, sections (Figs. 45, 48a, 48b, 52).

The spermatid cytoplasm in these steps contains many of the smooth-surfaced, irregularly shaped vesicles seen in the late acrosome phase spermatids. The microtubules of the caudal tube disintegrate into coarse granules in the cytoplasm around the connecting piece of the flagellum (Figs. 43, 50-52). The proximal centriolar adjunct disintegrates into the same type of granules (Figs. 43, 50-52).

Electron Microscopic Observations of Step 17

Any description of step 17 spermatid components has to be done in light of the major change in the shape of the anterior part of the head. This change is in addition to the formation of the space anterior to the tip of the nucleus. Electron micrographs of the anterior region of the head show that it has a triangular cross-sectional shape (Figs. 53-57). This change in shape, from the flattened oval appearance to a triangular one, results in a reorientation of the head components which will be described below.

Nucleus

The superfluous nuclear envelope undergoes a change in appearance in the step 17 spermatid. The ventral and anterior projection of the envelope is reduced in size, and the material between the opposed inner membranes has a hyaline rather than granular appearance (Figs. 55-57). Nodular material, apparently degenerating nuclear envelope, is seen on the ventral edge of

the superfluous membrane (Fig. 57).

The fold of nuclear envelope around the implantation fossa is larger in this step than in steps 15 and 16, and it forms long projections around the neck region of the flagellum (Figs. 49, 53, 60, 61). As in the previous steps (15 and 16), the nuclear envelope surrounding the implantation fossa has prominent nuclear pores. A small nuclear membrane fold is seen occasionally in the middle portion of the nucleus, but it does not contain nuclear pores (Fig. 58).

The chromatin granules have become closely packed in step 17 spermatids and, in some nuclei, they have fused to form a smooth homogeneous mass. Vacuoles are present throughout the chromatin. The chromatin material in the nuclear protrusion around the implantation fossa has a different appearance from that in the step 15 and 16 nuclei. A dense layer of fine granules lies adjacent to the condensed chromatin (Figs. 49, 59-61). Large coarse granules are sometimes present in this dense layer of fine granules (Figs. 60 and 61). The remainder of the nuclear fold contains loosely packed fine granules, similar to the material seen in this area of the step 15 and 16 spermatids.

Acrosomic System

Accompanying the change in shape of the anterior part of the head, the acrosomic system twists in such a way that both lateral surfaces of the head cap are again symmetrically placed on each side of the nucleus. The separated ventral flap of the head cap becomes centrally placed on the ventral head surface

(Figs. 53-57). The head cap forms a thin layer on the lateral head surfaces in the anterior one-third of the head, but in the other two-thirds of the head it is thicker with a thickening on its ventral margin (Fig. 53). The thickness of the head cap in the caudal two-thirds of the head is a distinguishing feature of step 17 spermatids.

The acrosome extends from a small distance caudal to the apex of the head to the posterior limit of the acrosomic system. The acrosome extends closer to the anterior tip of the head than it did in step 15 and 16 spermatids, and it now forms a small prominence along the dorsal surface in the anterior third of the head (Figs. 55-57). In the middle third of the head, the acrosome is a very prominent structure with its contents usually showing two different densities (Figs. 58-61). The size of the acrosome decreases in the caudal third of the nucleus (Figs. 49 and 62).

Perinuclear Layer

A perinuclear layer was described in the step 15 and 16 spermatids. This layer originated from three regions: the subacrosomic layer, the granular layer between the caudal tube and the nuclear envelope, and a small area which formed adjacent to that caudal surface of the nucleus facing the cytoplasm. This perinuclear layer in step 17 spermatids will be described as it is seen in these three regions.

The subacrosomic layer is considerably increased in size as the acrosomic system shifts over the nucleus and creates a

triangularly-shaped space around and anterior to the nuclear tip. The subacrosomic space in the anterior third of the head is filled with fine granular and flocculent material, with some coarse granules seen occasionally (Figs. 53-57). The granularity of the layer is slightly denser along the inner acrosomic membrane on the lateral and dorsal surfaces, on the inner surface of the ventral flap, and on the plasma membrane covering the ventral surface (Figs. 53-57). Some fine filaments are also seen in this layer. Myelin figures, which were never seen in this area in other steps of development, are frequently present in the step 17 spermatids (Figs. 55 and 56).

The material in the subacrosomic layer under the remainder of the acrosomic system is similar, and it contains granular, flocculent and some filamentous material. The marginal region at the ventral limit of the head cap is not recognized in this step of development.

The granular layer, which was between the caudal tube and the nuclear envelope in the acrosome phase spermatids, is clearly seen on the lateral and part of the ventral surface of the nuclei of step 17 spermatids. The granular layer is actually composed of two layers, one a dense granular layer adjacent to the plasma membrane and the other a less dense layer similar to the subacrosomic layer (Figs. 49, 58-62). Occasionally a thick layer forms against the nuclear envelope, opposite the thick layer adjacent to the plasma membrane (Figs. 58 and 59).

A dense, finely granular layer forms on that caudal surface of the nucleus projecting over the flagellum (Fig. 62). This

perifossa collar, as a relatively tightly fitting cover. The superfluous nuclear envelope is no longer present on the ventral surface of the nucleus. Neither remnants of the superfluous envelope, nor evidence of its site of attachment on the nuclear envelope, can be seen. The nuclear envelope in the perifossa collar contains pores, as it did in the previous steps of spermiogenesis (15-17), and does in the mature spermatozoon (Figs. 69 and 71).

Acrosomic System

The acrosomic system covers an identical area in the head of a step 18 or 19 spermatid that it does in the mature spermatozoon. The shape of the acrosomic system, or more specifically the shape of the acrosome, is the only major difference between late spermatids and mature spermatozoa. The limit of the acrosome, where it is attached to the head cap, is more clearly seen in the step 18-19 spermatids than in those of step 17 (Figs. 64-71, 73-75). The ventral flap portion of the head cap is now flattened on the ventral surface of the head and is about equal in thickness to the major part of the head cap (Figs. 65-67, 73). The contents of the acrosomic system are a homogeneous fine granular material similar in appearance to the contents of the acrosomic system of the mature spermatozoon.

Perinuclear Layer

The perinuclear layer takes on the appearance of a theca during step 19 of spermiogenesis. The layer has the appearance

layer directly faces the cytoplasm.

A few caudal tube microtubules and part of the caudal tube insertion ring are frequently seen in the spermatid cytoplasm (Figs. 49, 53, 60-62). The nuclear protrusion around the implantation fossa is always covered by a thin layer of cytoplasm during this step of development. The smooth-surfaced vesicles, which were previously present in the cytoplasm of this area, are seldom seen in step 17 spermatids.

Electron Microscopic Observations of Steps 18 and 19

The step 18 and 19 spermatids are very similar to the fully formed spermatozoa present in the head of the epididymis. The final form of the perinuclear theca and chromatin material is achieved in these steps. The shape of the spermatid head is now similar to the definitive head shape of spermatozoa of the caput epididymidis.

Nucleus

The chromatin of step 18 and 19 spermatids forms a dense homogeneous mass identical in appearance to that of a mature spermatozoon (Figs. 67-76). Vacuoles, or rarefactions, are present in this condensed chromatin. Usually these vacuoles are more prevalent in the caudal third of the nucleus (Figs. 68, 69 and 76). The fold of nuclear envelope in the perifossa collar contains granular and some flocculent material (Figs. 69 and 71).

The nuclear envelope covers the nucleus, except in the

of loosely packed granular and flocculent material containing fine filaments in both step 18 and early step 19 (Figs. 63-69). At the very end of step 19, this material condenses and takes on the electron dense granular appearance of the perinuclear theca of the mature spermatozoon (Figs. 73-76). The layer under the acrosome changes in shape in steps 18 and 19. A regular, fairly wide layer was present between the acrosome and dorsal area of the nucleus in the step 17 spermatid (Figs. 59-62). This layer becomes somewhat triangular in shape in steps 18 and 19 (Figs. 67-71, 73-75). The ventral spur is completely formed by late step 19, and the shape of the perinuclear theca of the mature spermatozoon is attained.

CHAPTER V

DISCUSSION

This study has shown for the first time the chronological development of the major structural components of the rat spermatid head. Most of the nuclear modifications occur independently of other changes in the spermatid head and therefore will be reviewed and discussed first. Structural modifications and spatial rearrangements of the acrosomic system are primarily dependent upon changes in nuclear shape and will be described second. The third major component, the perinuclear theca, forms in association with both the nucleus and acrosomic system.

Nucleus

Changes in the Chromatin during Spermiogenesis

The remarkable changes in nuclear morphology of rat spermatids, which result from a profound modification of the chromatin during spermiogenesis, will first be systematically reviewed.

The spermatid nucleus undergoes very few morphological changes during the Golgi and cap phases of spermiogenesis. However, modifications do take place in those parts of the nuclear envelope and karyoplasm which lie adjacent to the developing acrosomic system.

In step 3 of spermatid development, an electron dense layer of nuclear material develops against the inner membrane of the nuclear envelope which faces the covering acrosomic vesicle. This layer continues to spread as more of the nuclear envelope becomes modified during the growth of the acrosomic vesicle over

the nuclear surface. This entire process ceases in step 7 of development, but the electron dense layer remains an integral part of the modified nuclear envelope during nuclear elongation. The layer becomes obscured by condensing chromatin in step 12.

A modification or thickening of the nuclear envelope facing the acrosomic system had been noted by Horstmann (1961) in human spermatids and by Gardner (1966) in mouse spermatids. Brökelmann (1963) and Plöen (1971), studying rat and rabbit spermatids respectively, recognized that the thickening facing the acrosomic system was composed of both modified nuclear envelope and an associated electron dense layer of karyoplasm. As in many other mammalian species, the remainder of the karyoplasm in the Golgi and cap phases is composed of fine filaments and granules with clumps of coarse granules interspersed occasionally (Burgos and Fawcett, 1955; Fawcett and Burgos, 1956; Horstmann, 1961; Franklin, 1968; Plöen, 1971).

Recognizable changes in the chromatin, which may be considered as the beginning of condensation, take place in steps 8 through 10. In these steps of development, coarse chromatin clumps form a thin irregular layer adjacent to that area of nuclear envelope which is not covered by the acrosomic system. Similar chromatin clumps are dispersed throughout the nuclei of steps 10 and 11. The origin of the chromatin clumps has not been determined, but they may result from an accumulation of the coarse granules which are already present in the nucleus. The progressive thickening of filaments into coarse chromatin clumps, as will be described in later steps of spermiogenesis, was not

seen in steps 8 through 11.

In the step 11 nucleus, the remaining uncondensed chromatin becomes more filamentous and each of the filaments are thicker than in the previous steps. Therefore, the nucleus acquires a more dense overall appearance than in the step 8 and 9 spermatids. As the spermatid evolves, the filaments become coarse fibers which, in turn, appear to transform into coarse chromatin clumps. These chromatin clumps form the bulk of the nuclear material in the steps 12 and 13 nuclei. The karyoplasm between the clumps contains flocculent material and a network of fine fibers. This progressive modification of the chromatin can be observed in longitudinal sections of individual nuclei. The more advanced condensation or granular area is in the anterior part of the nucleus, while the least advanced or fibrous area is in the caudal part.

By the end of step 14, the chromatin clumps become more closely packed and this coarse granular chromatin now occupies most of the nucleus. However, there are relatively large nuclear areas of low electron density which contain filaments and fine granules. These low density areas are always present and can be considered to occur normally during chromatin condensation; it is unlikely that these areas are fixation artifacts, as stated by Brökelmann (1963).

Progressive packing of the chromatin granules continues in steps 15 and 16. The polarity of these changes is obvious as the anterior part of the nucleus contains more closely packed chromatin than the caudal area. Small areas of low electron

density are spread throughout the nucleus but are more numerous in the caudal third. These are vacuoles, or rarefactions, which are present in the nuclei of all the subsequent steps of development and in the mature spermatozoon. These areas of low electron density contain fine granular and flocculent material. A similar material is present in the nuclear protrusion which forms around the insertion point of the flagellum in these steps of development.

The chromatin granules are more closely packed in step 17 nuclei, and the density of the nucleus is more uniform than in the previous developmental steps. In some nuclei, the chromatin appears to have fused into a dense homogeneous mass. This process of condensation continues in steps 18 and 19 spermatids and, consequently, the nucleus at the time of sperm release has the same morphological appearance as that of a mature spermatozoon.

In most other mammalian species, the sequential chromatin changes taking place subsequently to the cap phase of development have been described as: fine granules of the karyoplasm being replaced by coarser granules, and the coarse granules becoming more closely packed with eventual coalescence into a homogeneous mass late in spermiogenesis (Burgos and Fawcett, 1955: Fawcett and Burgos, 1956; Fawcett, 1958; Horstmann, 1961; Franklin, 1968; DeKretser, 1969). Chromatin changes in steps 11 through 14 rat spermatids differ from the above descriptions in that most of the granular clumps seem to be formed by the fusion of coarse chromatin fibers. Plöen (1971) also has noted this fibrous step of chromatin condensation in the acrosome phase of rabbit spermatids.

It is uncertain whether this intermediate step of filament formation during chromatin condensation is a peculiarity of rat and rabbit spermatids, or whether it has been overlooked in other species.

A definite polarity of chromatin condensation is established in steps 10 and 11 after initial condensation has begun. Condensation begins in the apex and spreads caudally, independent of the irregular chromatin layer formed adjacent to the nuclear envelope in steps 8 through 10. There is a slight difference in the degree of chromatin condensation between spermatids in any one step of development, but the polarity is so constant that the levels of sections through the heads of steps 12 through 14 spermatids can be determined by the relative extent of chromatin condensation.

Brökelmann (1963) claimed that chromatin condensation in rat spermatids spreads from the periphery to the center of the nucleus and from the region below the acrosomic system to the distal part of the spermatid nucleus. In the preceding discussion, it was pointed out that an irregular layer of condensed chromatin first forms adjacent to some areas of the nuclear envelope in steps 8 through 11; some chromatin clumps also are dispersed throughout the karyoplasm. These areas do not necessarily act as foci for continued chromatin condensation, as Brökelmann implied.

Fawcett et al. (1971) have indicated from a study of many animal species that the shape of the spermatozoon head is not a consequence of external modeling brought about by cytoplasmic elements such as the caudal tube. They believe that shape is

largely determined from within the nucleus, by a genetically controlled pattern of aggregation of the molecular subunits of DNA and protein during chromatin condensation. This view contrasts with that of Kessel and Spaziani (1969) who concluded that both the caudal tube and the Sertoli cell complex, which lies adjacent to the spermatid head, determined nuclear shape. In the present study, there was no evidence that the caudal tube or any other cytoplasmic structure influenced the progressive modification of the chromatin and shaping of the nucleus.

During the rapid chromatin condensation in steps 12 through 14, a large space is formed between the condensed chromatin and the nuclear membrane in the caudal region of the nucleus not covered by the acrosomic system. This space contains granular and flocculent material similar in appearance to the material in the low electron density areas dispersed throughout the condensing chromatin. Brökelmann (1963) and Andre (1963) also described a space containing material of low electron density in the caudal area of rat spermatid nuclei. Franklin (1968) studied the development of this space in maturation phase monkey spermatids. His description of the evolution of this space and its associated nuclear envelope is similar to the following description in rat spermatids.

The nuclear envelope forms a doughnut-shaped bulge, or nuclear protrusion, around the insertion point of the flagellum of the step 15 and 16 spermatids. This area contains granular and flocculent material of low electron density which is similar to the material present between the condensing chromatin and the

nuclear envelope in the caudal region of step 12-14 spermatids. The nuclear protrusion of the step 17 spermatid also contains large coarse granules and fibers of what appears to be chromatin material. Some granular and flocculent material is present as well in the nuclear protrusion area of the step 18-19 spermatid and in the mature spermatozoon.

The nature of this material of low electron density, which is present in steps 12 through 19 spermatids and mature spermatozoa, is not known. This material may be histones resulting from the replacement of lysine-rich histone by arginine-rich histone in the last phases of spermiogenesis (Lison, 1955; Monesi, 1964, 1965; Vaughn, 1966).

In summary, the first morphological evidence of chromatin condensation is seen in steps 8-10 when coarse chromatin clumps appear in the nucleus. Chromatin filaments form in step 11; these filaments become thicker in steps 12 and 13 and begin to accumulate into coarse granular masses. The coarse granular masses gradually fuse, so that by steps 18 and 19 the chromatin forms a dense homogeneous mass. Chromatin condensation is a highly ordered process which takes place with an anterior to caudal polarity.

Nuclear Envelope

The nuclear envelope undergoes changes and rearrangements which parallel, although with some delay, the changes taking place within the nucleus. These modifications will now be discussed.

The wavy membranes of the early spermatid nuclear envelope become regularly spaced where they lie adjacent to the developing acrosomic system. A component of this modified nuclear envelope was referred to above as the electron dense karyoplasm layer adjacent to the inner nuclear membrane. This modified area of the nuclear envelope always corresponds to the area covered by the acrosomic system. Sandoz (1970) has said that the modification of the mouse spermatid nuclear envelope precedes the approach of acrosomal vesicles during the early spermiogenesis steps. The morphological evidence from the present study indicates that, in the early steps of spermiogenesis (steps 1 and 2), the nuclear envelope is modified simultaneously with the attachment of acrosomic and proacrosomic vesicles. The present observations on the rat agree with those of Franklin (1968) who has pointed out that the modification of the nuclear envelope in monkey spermatids always corresponds to the area covered by the forming acrosomic system.

A somewhat similar regular-spacing of the nuclear envelope membranes occurs adjacent to the caudal tube and the basal plate of the implantation fossa. The electron dense layer does not form against the inner membrane in these areas, although the area adjacent to the implantation fossa acts as a minor focus for chromatin condensation in steps 12 and 13.

In the discussion on chromatin condensation, the formation of a nuclear protrusion around the implantation fossa in steps 15 and 16 was mentioned. The nuclear protrusion increases in size up to early step 17. This is probably due to the reduction

in size of the nucleus resulting from chromatin condensation without concomitant loss of nuclear envelope.

The nuclear protrusion becomes reduced in size during late step 17 due to a loss of nuclear membrane, vide infra. It is, therefore, of reduced size in steps 18 and 19, but it still contains granular and flocculent material. The nuclear protrusion is obviously the precursor of the folded nuclear envelope seen in the perifossa collar of the mature spermatozoon. This agrees with the conclusion of Franklin (1968) on the origin of the redundant nuclear envelope in the neck region of the monkey spermatozoon.

Nuclear pores are present in that area of the nuclear envelope not modified by acrosomic system, caudal tube or basal plate. The pores are inconspicuous until the step 10 and 11 spermatids. In the nuclei of step 12 through 14 spermatids, the future caudal surface of the nucleus contains a large number of pores. These disappear from this area between steps 14 and 15, and pores now appear in the nuclear protrusion. There is no indication of a shift in the nuclear envelope over the nucleus; therefore, the character of the envelope must change, with pores forming in one area and disappearing in another. Similar changes have not been reported in spermatids of other species, although similar nuclear pores have been recognized in the caudal regions of spermatid nuclei in many mammals (Horstmann, 1961; DeKretser, 1969; Sandoz, 1970; Rattner and Brinkley, 1971). Nuclear pores are present in the region of the membrane which will form the redundant nuclear envelope in the mature spermatozoon (Franklin,

1968; Rattner and Brinkley, 1971). Nuclear membrane folds or redundant nuclear envelope in the mature spermatozoon always contain pores (Nicander and Bane, 1962, 1966; Franklin, 1968; Pedersen, 1969a; Koehler, 1970; Rattner and Brinkley, 1971; Zamboni et al., 1971). These findings agree very well with the observations on rat spermatids and spermatozoa in this study.

The striking features of the nuclear pores in rat spermatids are that they become prominent during chromatin condensation and are always associated with a nuclear area containing material of low electron density. The likely possibility is that this nuclear material of low electron density is being expelled through pores, possibly accounting for the reduction in nuclear volume during these steps of spermiogenesis. There was no morphological evidence in this study which would support this hypothesis. Franklin (1968) also believed that there was only indirect evidence that material was being expelled from monkey spermatid nuclei. Histone synthesis and turnover take place during these steps of spermiogenesis (Lison, 1955; Monesi, 1964, 1965; Vaughn, 1966), and it is possible that the prominent nuclear pores are involved with the transport of this material across the nuclear envelope.

Many smooth-surfaced vesicles become prominent in the cytoplasm around the caudal surface of the nucleus in steps 12 through 16. The material in these vesicles is very similar to the low electron density nuclear material facing the nuclear pores. These vesicles are similar to those described by Horstmann (1961) in a comparable area of the maturation phase

human spermatid. He believed that the material in these vesicles was nuclear material which was being transported from the nucleus to the cytoplasm. None of the observations in the present study can substantiate this claim, although it is an attractive hypothesis because of the similarity of vesicular material with the low electron density nuclear material.

In the preceding discussion, the formation of the nuclear protrusion during reduction of the nuclear volume was mentioned. There is a simultaneous formation of superfluous nuclear envelope in the anterior and ventral part of the condensing nucleus. This begins in steps 10 and 11 and becomes obvious in steps 12 and 13. In nuclei of steps 12 and 13, the anterior superfluous envelope forms a ventrally projecting plate of two opposed layers of nuclear envelope separated by a thin layer of electron dense material. A small anterior component, which is continuous with the ventral projecting superfluous envelope, forms in step 14. Brökelmann (1963) also reported the presence of a ventral nuclear component in the rat, but the formation of superfluous nuclear envelope on such a large scale has not been reported in other species.

The superfluous nuclear envelope in the anterior part of the spermatid nucleus, and also a part of the envelope in the nuclear protrusion, degenerate in step 17. The superfluous envelope appears to degenerate into myelin figures. Consequently, after step 17 the nuclear protrusions are reduced in size and now appear similar to the nuclear protrusions found in mature spermatozoa. Brökelmann (1963) reported that the nuclear

protrusion budded-off into the cytoplasm of the late spermatid, carrying nuclear contents along. It appears that Brökelmann mistakenly identified sections through irregular elongating nuclear protrusions as separate vesicle-like structures. An analysis of the present material did not show loss of nuclear membrane or nuclear material by a budding-off process. However, Rattner and Brinkley (1971) have also described the loss of nuclear envelope in marmoset spermatids by a pinching-off process.

In summary, chromatin condensation and the reduction of nuclear size up to step 17 is not accompanied by a concomitant reduction in surface area of the nuclear envelope. This results in the formation of a large area of superfluous nuclear envelope in the anterior and ventral parts of the nucleus and a nuclear protrusion around the implantation fossa. All the superfluous nuclear envelope and part of the envelope of the nuclear protrusion disintegrate in step 17. Porous nuclear envelope is always adjacent to nuclear material of low electron density.

Acrosomic System

Electron microscopic studies have revealed that early formation of the acrosomic system is similar in all mammals so far studied. Burgos and Fawcett (1955) and Fawcett and Burgos (1956) first described the general process of acrosomic system formation in cat and human spermatids, respectively. They observed that proacrosomic vesicles, each containing an electron dense proacrosomic granule, first coalesced to form a large

acrosomic vesicle containing an acrosomic granule. This acrosomic vesicle attached to the nuclear envelope. Vesicles from the Golgi apparatus eventually fused with the acrosomic vesicle as it continued to grow over the nuclear surface. This process has also been described recently by Sandoz (1970) and Susi et al. (1971).

In rat spermatids, the process of acrosomic system formation takes place during steps 1 through 7. The size of the acrosomic granule does not appear to increase after step 3, although the less electron dense head cap material increases in volume as the acrosomic system enlarges. Fawcett and Hollenberg (1963) referred to the acrosomic granule and head cap as two distinct areas, or zones, of the developing guinea pig acrosomic system. They suggested that these two areas developed during two temporally distinct phase of Golgi apparatus activity.

The morphological differences between the acrosomic granule and head cap have also been investigated by histochemical techniques. In a light microscopic study, Clermont and Leblond (1955) demonstrated a difference in PAS staining of the outer and inner zones of the developing rat acrosomic system. Differential staining of the two acrosomic system components was also demonstrated by Susi et al. (1971), using PA-silver and electron microscopy. In their study, the acrosomic granule stained weakly with PA-silver, while the head cap material was heavily stained. They attributed this staining differential to possible differences in the concentration or nature of the glycoprotein contained in the two structures.

Both the morphological and histochemical evidence indicate that the acrosomic system may be composed of at least two substances or two forms of the same substance. This is probably not due to two temporally distinct phases of Golgi activity as proposed by Fawcett and Hollenberg (1963), but rather to a brief production of acrosomic granule material through step 3 and a continuous production of head cap material through step 7.

The displacement of the acrosomic system over the falciform rat spermatid nucleus is considerably different than it is in those animals with spatulate or ensiform-shaped spermatozoa. In addition to the flattening and elongation which take place in the developing spermatids of the latter animals, the rat spermatid nucleus becomes curved so that the acrosomic system lies over the long axis of the nucleus. Also, the entire acrosomic system shifts over the nucleus in step 17 of development. During the shaping of the spermatid head, the definitive acrosome changes its position relative to that of the head cap.

The acrosome material is morphologically distinct from the head cap material through step 11 of development. In later steps, the electron density of the head cap material is similar to that of the acrosome. In this study, the acrosome material has been identified in steps 12 through 19 spermatids and in mature spermatozoa by following chronologically the location of the material derived from the acrosomic granule. The acrosome material is located over the apex of the nucleus in step 11. The bulk of this material appears to migrate to the middle area of the nucleus in steps 12 and 13, and by steps 14 and 15 some

of this material forms a prominence close to the dorsal angle of the nucleus. Then some of this acrosome material flows anteriorly so that, in step 17, the acrosome occupies the same relative position in the acrosomic system as it does in the mature spermatozoon. This redistribution of the acrosome material was first demonstrated in the developing rat spermatid by Leblond and Clermont (1952a, b). Forces causing this change in acrosome position were not determined in the present study. Change in nuclear shape which, in turn, could cause rearrangement of acrosomic structures does not seem to be a factor. That is, in steps 13 to 14, the bulk of the acrosome material flows approximately one-half the length of the nucleus, while the change in nuclear shape is barely perceptible.

The head cap accommodates to the change in nuclear shape in steps 8 through 11. Beginning in step 12, the anterior part of the nucleus condenses and forms the ventral plate of superfluous nuclear envelope. The head cap does not decrease in size and continues to cover the lateral surfaces of the redundant nuclear envelope. In step 14, a part of the head cap covering one of these lateral surfaces becomes separated from the remainder of the head cap. This separated structure will form the ventral flap. In steps 15 and 16, the future ventral flap lies on the lateral nuclear surface and moves toward the ventral surface as development proceeds through step 16. In step 17, the acrosomic system undergoes a spatial change over the nucleus; this results in the ventral flap rotating to the ventral nuclear surface, the anterior part of the head becoming triangular in

shape, and the head cap again symmetrically covering the lateral head surfaces. These changes take place as the entire acrosomic system is shifted forward over the nucleus, thus creating a space under the acrosomic system anterior to the tip of the nucleus.

The head cap and ventral flap both flatten and their contents become slightly more electron dense during steps 18 and 19. At the time of sperm release, these components are identical in appearance to those of the mature spermatozoon.

Pikó (1969) reported that rat and mouse spermatozoa have a small separate vesicle, located on the ventral nuclear surface, which is similar to the thin lateral portion of the head cap. Brökelmann (1963) was the first to recognize this structure in rat spermatids. He thought that it resulted from the proliferation of one of the lower edges of the head cap ("acrosome cap") and thus was part of the acrosomic system. The present study also shows that the ventral flap is part of the acrosomic system, being derived from the head cap by a splitting rather than by a proliferation of one of its edges.

A specialized area of the acrosomic system, called the equatorial segment, has been described in electron microscopic studies of the spermatozoa of a number of mammals (Nicander and Bane, 1962, 1966). The equatorial segment is located on the ventral edge of the head cap area; it is slightly narrower and more electron dense than the head cap (Nicander and Bane, 1966; Fawcett and Phillips, 1969a; Franklin et al., 1970a; Yanagimachi and Noda, 1970a). The equatorial segment remains morphologically

intact after the acrosome reaction (Barros et al., 1967), and it is the most stable part of the acrosomic system during sperm degeneration (Franklin et al., 1970a; Yanagimachi and Noda, 1970c).

It might be assumed that the equatorial segment and ventral flap are homologous structures because both are derived from, or are modifications of, the head cap. The information available is not adequate to test this assumption, although some comparisons can be made between the two structures. The fate of the ventral flap has not been followed during the acrosome reaction, or during any part of the fertilization process; thus it can not be compared with the equatorial segment which remains intact after the acrosome reaction. Unlike the equatorial segment, both the width of the ventral flap and the density of its enclosed material are similar to those of the remainder of the head cap. Finally, the ventral flap formation occurs at a different time and in a different manner during spermiogenesis than the formation of the equatorial segment. The equatorial segment is formed at the end of spermiogenesis, at about the time of sperm release, by a process of attenuation and condensation (Fawcett and Phillips, 1969a).

The final shaping of the acrosome takes place in the epididymis. As in the guinea pig (Fawcett and Hollenberg, 1963), chinchilla (Fawcett and Phillips, 1969a) and rabbit (Bedford, 1965), the rat acrosome undergoes a diminution in size during transit through the epididymis. This change in size changes the shape of the spermatozoon by reducing the dorsal ridge formed

by the acrosome. The spatial relationships of the spermatozoon components remain constant during passage through the epididymis. The size of the acrosome changes independently of the other components, except for the change in fit of the plasma membrane.

In the rat, as in the guinea pig (Fawcett and Hollenberg, 1963), the size of the acrosome changes during a short distance of travel in the epididymis. The area of the epididymis in which the morphological change takes place is restricted, and the spermatozoon population is morphologically homogeneous in any one area of the epididymis. This contrasts with the situation in the epididymis of the rabbit, in which morphologically mature and immature spermatozoa may be seen at the same level (Bedford, 1965).

Therefore, the change in shape of the spermatozoon head during transit through the epididymis is the result of a change in shape of one component of the head, the acrosome. The change in acrosome size does not affect the morphological appearance of the other head components, which do not change after release from the seminiferous epithelium.

Leblond and Clermont (1952a, b) used the term acrosomic system to describe a group of structures produced by the spermatid Golgi apparatus. These structures included the proacrosomic granules, acrosomic granule, head cap, and acrosome. According to this description, the acrosomic system consisted only of head cap and acrosome in the maturing spermatids and in spermatozoa. The use of this terminology was challenged by Burgos and Fawcett (1955), Fawcett (1958, 1965), Fawcett and Ito (1965) and Fawcett

and Phillips (1969a). They argued that the acrosome and head cap material was morphologically similar in electron micrographs of mature spermatozoa, and that both structures were enclosed in a single continuous membrane. Thus, they proposed that the structures called the acrosome and head cap by Leblond and Clermont (1952a, b) be collectively designated the acrosome or acrosomal cap. Most recent authors have adopted this terminology.

This simplification of terminology is not justified and has not been followed in the present work. At the time this simplified terminology was proposed, there were already electron microscopic investigations indicating the complexity of the acrosomic system. Fawcett and Hollenberg (1963) had indicated the presence of an inner and outer zone in the developing acrosomic vesicle. They further demonstrated that the part of the acrosome derived from the outer zone underwent a dramatic modification during epididymal transit. The demonstration of Nicander and Bane (1962) that the narrowed equatorial segment of the head cap was an area of increased electron density, and thus differed from the remainder of the head cap material, also was not considered.

In the present study, there is morphological evidence to support the use of the term acrosomic system to designate a complex structure. In the developing acrosomic system of the early spermatid, the separate components that become the head cap and acrosome are clearly distinguishable. The acrosome undergoes a change in size during transit through the epididymis, and this change is completely independent of the other stable acrosomic system components. In the rat, the use of the term acrosomic

system would be justified, if for no other reason than to indicate a collective term which includes the ventral flap, a part of the acrosomic system.

Perinuclear Layer

The presence of varying amounts of material between the inner acrosomic membrane and the nuclear envelope (subacrosomal space) has been reported in the spermatozoa and spermatids of a variety of mammals (Nicander and Bane, 1962; 1966; Bane and Nicander, 1963). These authors equated the subacrosomal material with the perforatorium of rat spermatozoa. Hadek (1963) and Bedford (1964) reported the presence of subacrosomal material in rabbit spermatozoa and implied that it was homologous with the rat perforatorium. The homology of subacrosomal material in most mammals and the perforatorium in rodents was questioned by Fawcett and Phillips (1969a).

A number of recent investigations have conclusively demonstrated the presence of subacrosomal material in mature spermatozoa of a number of species (Stefanini et al., 1969; Franklin et al., 1970a; Sandoz, 1970; Yanagimachi and Noda, 1970a; Bedford and Nicander, 1971; Zamboni et al., 1971). These studies, plus the present study, have also demonstrated the continuity of this subacrosomic layer with the layer over the caudal area of the nucleus, commonly referred to as the postnuclear cap.

Observations in the present study indicate that the formation of a subacrosomic layer begins in step 3 and continues as the head cap spreads over the nucleus in steps 4 through 7. This

subacrosomic layer forms in the same manner in mouse spermatids (Sandoz, 1970). Bedford and Nicander (1971) have observed subacrosomal material in cap phase monkey and rabbit spermatids. The subacrosomic layer is heterogeneous in the rat and contains fine filaments, granules of varying sizes, and flocculent material. In step 7 of development, a widened area forms in the subacrosomic layer under the marginal region of the head cap. Coarse granules and small rods develop in this area and remain in the spermatid until step 17. Similar material has been observed in this area of developing mouse spermatids (Sandoz, 1970).

During the acrosome phase (steps 8-14) as the spermatid head elongates and the nucleus condenses, the subacrosomic layer appears to increase in thickness. The composition of the layer remains the same as in earlier steps. Brökelmann (1963) and Sandoz (1970) reported a widening of the subacrosomic layer in the spermatids of rats and mice, respectively, during comparable steps of development. According to the drawings and electron micrographs of Plöen (1971), rabbit spermatids also have a subacrosomic layer comparable to the one described above in the rat.

During maturation phase (steps 15-19), distinctive changes take place in the subacrosomic layer of rat spermatids, and probably those of other myomorphs, which do not occur in mammalian spermatids without a perforatorium. As judged from previously published electron micrographs, the subacrosomic layer appears to change very little in maturation phase spermatids of the rabbit (Plöen, 1971), guinea pig and chinchilla (Fawcett and Phillips, 1969a), and monkey (Franklin, 1968). There appears to

be only a meager amount of subacrosomic material, which does not increase during the maturation phase of spermiogenesis, in these animals which lack a conspicuous perforatorium.

In steps 15 and 16, the subacrosomic layer begins to enlarge around the anterior tip of the nucleus, and it appears to be of a lower electron density than in the previous steps (8-14). In order to discuss the further development of this part of the subacrosomic layer, the formation of the postnuclear cap, which is continuous with this layer, will be described first.

The postnuclear cap (postacrosomal dense lamina) material is first seen in steps 8-11 of development, when a granular layer of material is deposited between the caudal tube and the nuclear envelope. This layer becomes more prominent in steps 11-14. Fawcett et al. (1971) observed the presence of similar material in the spermatids of a number of mammalian species. This electron dense layer appears to become entrapped between the plasma membrane and the nuclear envelope as the caudal tube insertion ring and the caudal tube move caudally over the nucleus in steps 14 and 15. Other authors have associated the formation of the postnuclear cap with the migration of the caudal tube in spermatids of dogs (Gresson and Zlotnik, 1945), mice (Sandoz, 1970), and rabbits (Plöen, 1971).

The postnuclear cap is not homogeneous during the maturation phase of spermiogenesis but shows an area of increased electron density against both the plasma membrane and the nuclear envelope. These areas of increased density were also noted in mouse spermatids (Sandoz, 1970). In the rat, the area of increased electron

density against the nuclear envelope is not prominent in the mature spermatozoon, but the area adjacent to the plasma membrane remains obvious in some areas of the head. A periodic organization, such as that described by Fawcett and Ito (1965) in bat, Koehler (1970) in rabbit and Zamboni et al. (1971) in monkey and human spermatozoa, was not observed in the caudal area of the perinuclear layer of rat spermatids or spermatozoa.

An additional area of the nucleus becomes covered with granular material in steps 14 and 15. This is the caudal surface of the nucleus overlying the flagellum. This area of the nucleus was never covered with acrosomic system or caudal tube and therefore is not covered by a layer formed in association with these structures. The nuclear envelope on this surface contained numerous pores prior to step 14, but these pores disappear during step 14 and the envelope becomes continuous. An electron dense layer then forms against this surface in steps 14 and 15.

Therefore, the nuclei of the steps 15-16 spermatids are covered by a continuous layer of material. This layer can be divided into three regions, differing on the basis of which structure they were associated with during formation. The layer under the acrosomic system becomes continuous with the layer developing over the caudal region of the nucleus as the caudal tube becomes disassociated from the nucleus. This caudal region also becomes continuous with the layer which forms over the caudal surface adjacent to the spermatid cytoplasm.

The origins of the various regions of the perinuclear layer were not determined. It is unlikely that the subacrosomic region

results from simple trapping of cytoplasm between the acrosomic system and the nucleus, for its density is far greater than the surrounding cytoplasm. There is no morphological evidence, such as nuclear pores, to indicate transfer of material to the subacrosomic layer from either the nucleus or the acrosomic system. That part of the layer which forms in the area adjacent to the caudal tube appears to be formed in two steps. Firstly, as described above, a layer of material forms between the microtubules of the caudal tube and the nuclear envelope in steps 8-14. The origin of the material is probably cytoplasmic, as there are no nuclear pores present adjacent to this region during its development. Secondly, material appears to be added to this layer from the caudal tube insertion ring, as the ring moves caudally over the nucleus. The small part of the layer on the caudal surface of the nucleus appears to form by the deposition of material directly from the surrounding spermatid cytoplasm.

In step 17, the position of the acrosomic system changes relative to the nucleus, and a large triangular space is created under the acrosome, around and anterior to the nuclear tip. This is an enlargement of part of the subacrosomic layer. A similar enlargement of the subacrosomic layer in the late, hamster spermatid was noted by Franklin et al. (1970b).

The contents of this space decrease in electron density as the space is created (steps 16 and 17), and then rapidly increase in density so that a dense homogeneous appearance is acquired by step 18. As the volume of the space appears to remain constant during these steps, this increase in density must be due to

addition of material to this space anterior to the nuclear tip. The addition of material to the perinuclear layer in step 17 of development is probably different than it was during steps 3-15. The orientation of the head structures now is different for, as described above, the various regions are continuous and the whole perinuclear layer is connected to the spermatid cytoplasm over the caudal limit of the nucleus. Nuclear material now has direct access to the perinuclear layer through those pores of the nuclear protrusion which face the perinuclear layer and the cytoplasm.

Based upon this morphological arrangement of head structures, the source of perinuclear material formed in step 17 could be of either nuclear or cytoplasmic origin, or both. In addition to these sources, the degenerating superfluous nuclear envelope may also contribute material to the perinuclear layer. Nuclear membrane whorls, comparable to the superfluous nuclear membrane, have been seen in the anterior part of the forming head in spermatids of rabbits (Hadek, 1963), lemmings (Hopsu and Arstila, 1965) and mice (Sandoz, 1970). Franklin et al. (1970b) have reported that the subacrosomic space of hamster spermatids contains elements of nuclear envelope as well as cytoplasmic material.

A chronological analysis of the development of the perinuclear layer has not been done in other mammalian species but, in the electron micrographs of Franklin (1968), the continuity of the perinuclear layer with the cytoplasm can clearly be seen in maturation phase monkey spermatids. The nuclear protrusion also is closely associated with the perinuclear layer at the

junction of the layer and the cytoplasm. As pointed out above, an increase in volume of the perinuclear layer comparable to that in the rat does not occur in maturation phase spermatids of mammals other than mice and hamsters. With the exception of this increase in volume of the perinuclear layer, the development of this layer in other species appears to be similar to that of myomorph rodents.

The perinuclear layer condenses into an electron dense granular theca and acquires its mature morphology late in step 19 prior to sperm release. The theca has a homogeneous granular appearance except in an area of increased electron density against the plasma membrane in the caudal region. That part of the theca usually referred to as the perforatorium differs in hamster spermatids in that it has two distinct electron densities (Franklin et al., 1970a). The rat perinuclear theca covers all of the nucleus except in the implantation fossa and a small area immediately surrounding it. A small ventral prominence, the ventral spur, forms late in spermiogenesis due to a localized accumulation of perinuclear layer material.

In summary, the nucleus of the rat spermatozoon is covered by a perinuclear theca except for a small area in and around the implantation fossa. The theca develops from a perinuclear layer which, in turn, is formed in three separate nuclear regions. After these regions become continuous, the perinuclear layer enlarges anterior to the tip of the nulceus. This anterior enlargement is a distinctive feature of myomorph spermatozoa.

SUMMARY

The following major developmental steps in the formation of spermatozoa head components were elucidated by the use of electron microscopy.

Nucleus

The chromatin appears as fine filaments and granules with a few clumps of coarse granules in the nuclei of Golgi and cap phase spermatids. The first morphological evidence of chromatin condensation appears in steps 8 through 10 when coarse chromatin clumps form along that part of the nuclear envelope which is not covered by the acrosomic system. Clumps of fused chromatin granules are dispersed throughout the nuclei of steps 10 and 11 spermatids. The chromatin becomes more filamentous in step 11. In steps 12 and 13, these filaments become very thick and accumulate into irregular granular clumps. The chromatin clumps become progressively more closely packed in steps 14 through 16. Fusion of the clumps begins in step 17, and by steps 18 and 19 the chromatin has a dense homogeneous appearance except for a few rarefactions or vacuoles which form between the fusing clumps. The formation of large chromatin fibers, as an intermediate step in chromatin condensation, is unusual in mammals. During chromatin condensation, nuclear material of low electron density forms in the caudal region of the nucleus between the condensing chromatin and the nuclear envelope. This material is seen, although in lesser quantities, in the nuclear protrusions of late

spermatids and in the nuclear folds of mature spermatozoa.

As a result of nuclear condensation, superfluous nuclear envelope is formed in the anterior and ventral parts of the nucleus and a nuclear protrusion appears around the implantation fossa. The superfluous envelope and part of the nuclear protrusion disintegrate in step 17. The nuclear envelope of the remainder of the nuclear protrusion becomes the nuclear membrane folds which are seen in the perifossa collar and neck region of mature spermatozoa. Nuclear pores are prominent in steps 12 through 19 spermatids and in mature spermatozoa. These pores are always associated, during chromatin condensation, with the nuclear material of low electron density in the caudal region of the nucleus. Nuclear pores form in the envelope of the nuclear protrusion and remain in the nuclear membrane folds of the mature spermatozoon.

Acrosomic System

The formation of the acrosomic system in the rat is similar to that described in other mammals. The forming acrosomic system is composed of two morphologically distinct components, the acrosomic granule and the head cap. The acrosomic granule is formed by the Golgi apparatus material produced in steps 1 through 3 and the head cap by Golgi material formed in steps 1 through 7. The acrosomic granule becomes the acrosome which forms a prominent dorsal ridge in the late spermatid and in the spermatozoon. The acrosome is the only head structure that undergoes morphological modification during epididymal transit. This

change is a reduction in acrosome volume independent of the remainder of the acrosomic system. During step 14 of spermiogenesis part of the head cap is split off to form the ventral flap of the acrosomic system. The ventral flap comes to lie in the ventral midline of the anterior part of the head during a change in spermatid shape in steps 16 and 17.

Perinuclear theca

The perinuclear theca forms from the condensation of the perinuclear layer material late in spermiogenesis. The perinuclear layer is formed in three regions of the nucleus: the area between the nuclear envelope and the forming acrosomic system; the area between the caudal tube and the nuclear envelope; and a small area on the caudal surface of the nucleus which was covered by neither the acrosomic system nor the caudal tube. These areas become continuous over the nucleus and connect directly to the spermatid cytoplasm in steps 15 and 16. The large porous nuclear protrusion lies in the area of the connection of this layer with the cytoplasm. In step 17, that part of the perinuclear layer under the acrosomic system and anterior to the nuclear tip enlarges. That part of the perinuclear layer which has been referred to in the past as the perforatorium forms in this enlarged area during step 17. The addition of material to the perinuclear layer during the maturation phase of spermiogenesis probably occurs only in myomorph rodents. When the perinuclear layer undergoes condensation late in spermiogenesis, the layer between the nuclear protrusion and the plasma membrane

disappears, Therefore, the nuclear folds of the perifossa collar, which form from the nuclear protrusion, are not covered with perinuclear theca in the mature spermatozoon.

ORIGINAL CONTRIBUTIONS

This study is a detailed chronological analysis of the ultrastructural formation, development and structural transformation of three head components of the rat spermatozoon, i.e. nucleus, acrosomic system and perinuclear theca, during spermiogenesis and passage through the epididymis. The following observations provide new insight into this process in the rat and indicate some features which may be found to occur generally in mammalian spermiogenesis.

1) Nucleus and Nuclear Envelope

As in other species, the early rat spermatid nucleus (steps 1 through 10 of spermiogenesis) contains fine filamentous and granular material. In steps 11 through 13, distinctive changes take place in chromatin condensation; the chromatin first becomes coarsely filamentous, then these filaments aggregate to form electron dense granular clumps. During steps 14 through 16, the granular clumps become closely packed, and in steps 17 through 19 the clumps fuse into a dense homogeneous mass. Thus, nuclear condensation is clearly an elaborate and stepwise process.

Nuclear condensation results in an accumulation of excess nuclear envelope in the anterior and ventral parts of the nucleus and in the formation of a nuclear protrusion around the implantation fossa of the flagellum. All the excess nuclear envelope in the anterior and ventral areas of the nucleus and part of the envelope in the nuclear protrusion degenerate in step 17 of spermiogenesis. The remainder of the nuclear envelope in the

nuclear protrusion, which shows characteristic nuclear pores, persists as the so-called nuclear folds seen around the implantation fossa of the mature spermatozoon.

2) Acrosomic System

The formation and chronological development of the acrosome appears to be independent of the head cap. The material produced from the acrosomic granule, forming the acrosome, flows along the dorsal edge of the nucleus during spermiogenesis and is selectively condensed and remodeled during passage through the epididymis.

A portion of the head cap seen on one lateral surface of the nucleus is split off in step 14 of spermiogenesis. This split-off portion of the head cap was followed chronologically and was seen to form the distinct structure called the ventral flap of the head cap. The ventral flap lies in the antero-ventral portion of the spermatozoon head.

3) Perinuclear Theca

It was demonstrated that a well developed, densely packed layer, tentatively called the perinuclear theca, covers the nucleus of the mature spermatozoon except for a small area in and around the implantation fossa. The theca includes those structures, which have been called by other authors the perforatorium located in the subacrosomal space and the postnuclear cap seen caudal to the acrosomic system. The formation of this perinuclear layer was studied chronologically from the beginning of

the formation of the subacrosomic layer in step 3. The subacrosomic layer becomes continuous with a layer of material formed betwen the caudal tube and the nuclear envelope, so that by steps 16 and 17 there is a continuous layer of material covering the nucleus. This layer of material condenses at the very end of spermiogenesis (steps 18-19) to form a compact, seemingly rigid layer referred to as the perinuclear theca.

LITERATURE CITED

André, J. 1963. Some aspects of specialization in sperm. In: General physiology of cell specialization. D. Mazia and A. Tyler (Eds.). McGraw-Hill: New York. Pp. 91-115.

Austin, C.R. 1968. Ultrastructure of fertilization. Holt, Rinehart, and Winston: New York. 196 pp.

Austin, C.R. and M.W.H. Bishop. 1958a. Some features of the acrosome and perforatorium in mammalian spermatozoa. Proc. R. Soc. B. 148: 234-240.

Austin, C.R. and M.W.H. Bishop. 1958b. Role of the rodent acrosome and perforatorium in fertilization. Proc. R. Soc. B. 148: 241-248.

Austin, C.R. and C.S. Sapsford. 1952. The development of the rat spermatid. Jl R. microsc. Soc. 71: 397-406.

Bane, A. and L. Nicander. 1963. The structure and formation of the perforatorium in mammalian sperm. Int. J. Fert. 8: 865-866.

Barros, C., J.M. Bedford, L.E. Franklin and C.R. Austin. 1967. Membrane vesiculation as a feature of the mammalian acrosome reaction. J. Cell Biol. 34: C1-C5.

Barros, C. and L.E. Franklin. 1968. Behavior of the gamete membranes during sperm entry into the mammalian egg. J. Cell Biol. 37: C13-C18.

Bedford, J.M. 1964. Fine structure of the sperm head in ejaculate and uterine spermatozoa of the rabbit. J. Reprod. Fert. 7: 221-228.

Bedford, J.M. 1965. Changes in fine structure of the rabbit sperm head during passage through the epididymis. J. Anat. 99: 891-906.

Bedford, J.M. 1967a. Observations of the fine structure of spermatozoa of the bush baby (Galago senegalensis), the African green monkey (Cercopithecus aethiops) and man. Am. J. Anat. 121: 443-460.

Bedford, J.M. 1967b. Experimental requirement for capacitation and observations on the ultra-structural changes in rabbit spermatozoa during fertilization. J. Reprod. Fert. Suppl. 2: 35-48.

Bedford, J.M. 1968. Ultrastructural changes in the sperm head during fertilization in the rabbit. Am. J. Anat. 123: 329-358.

Bedford, J.M. 1970. Sperm capacitation and fertilization in mammals. Biol. Reprod. Suppl. 2: 128-158.

Bedford, J.M. and L. Nicander. 1971. Ultrastructural changes in the acrosome and sperm membranes during maturation of spermatozoa in the testis and epididymis of the rabbit and monkey. J. Anat. 108: 527-543.

Bennett, H.S. and J.H. Luft. 1959. S-collidine as a basis for buffering fixatives. J. biophys. biochem. Cytol. 6: 113-114.

Bishop, M.W.H. and A. Walton. 1960. Spermatogenesis and the structure of mammalian spermatozoa. In: Marshall's physiology of reproduction. A.S. Parkes (Ed.). Longmans: London. Vol. 1, Part II, pp. 1-129.

Blandau, R.J. 1951. Observations on the morphology of rat spermatozoa mounted in media of different refractive indices and examined with the phase microscope. Anat. Rec. 109: 271. (Abstract).

Blandau, R.J. and R.E. Rumery. 1961. Fertilizing capacity of rat spermatozoa recovered from various segments of the epididymis. Anat. Rec. 139: 209. (Abstract).

Blandau, R.J. and R.E. Rumery. 1964. The relationship of swimming movements of epididymal spermatozoa to their fertilizing capacity. Fert. Steril. 15: 571-579.

Blom, E. and A. Birch-Andersen. 1965. The ultrastructure of the bull sperm. II. The sperm head. Nord. Vet-Med. 17: 193-212.

Bowen, R.H. 1924. On the acrosome of the animal sperm. Anat. Rec. 28: 1-13.

Brökelmann, J. 1963. Fine structure of germ cells and Sertoli cells during the cycle of the seminiferous epithelium in the rat. Z. Zellforsch. 59: 820-850.

Brown, H.H. 1885. On spermatogenesis in the rat. Q. Jl microsc. Sci. 25: 343-370.

Burgos, M.H. and D.W. Fawcett. 1955. Studies on the fine structure of mammalian testis. I. Differentiation of the spermatids in the cat. J. biophys. biochem. Cytol. 1: 287-300.

Burgos, M.H. and D.W. Fawcett. 1956. An electron microscopic study of spermatid differentiation in the toad, Bufo arenarum Hensel. J. biophys. biochem. Cytol. 2: 223-240.

Challice, C.E. 1953. Electron microscope studies of spermiogenesis in some rodents. Jl R. microsc. Soc. 73: 115-127.

Christensen, A.K. 1965. The fine structure of testicular interstitial cells in guinea pigs. J. Cell Biol. 26: 911-935.

Clermont, Y. 1956. The Golgi zone of the rat spermatid and its role in the formation of cytoplasmic vesicles. J. biophys. biochem. Cytol. 2 (Suppl. 4): 119-122.

Clermont, Y. and C.P. Leblond. 1955. Spermiogenesis of man, monkey, ram and other mammals as shown by the "periodic acid"-Schiff technique. Am. J. Anat. 96: 229-250.

Clermont, Y., E. Einberg, C.P. Leblond and S. Wagner. 1955. The perforatorium - An extension of the nuclear membrane of the rat spermatozoon. Anat. Rec. 121: 1-12.

Courot, M. and J. Fléchon. 1966. Ultrastructure de la manchette de la spermatide chez le bélier et le taureau. Annls Biol. anim. Biochim. Biophys. 6: 479-482.

Dan, J.C. 1967. Acrosome reaction and lysins. In: Fertilization. C.B. Metz and A. Monroy (Eds.). Academic Press: New York. Pp. 237-293.

Daoust, R. and Y. Clermont. 1955. Distribution of nucleic acids in germ cells during the cycle of the seminiferous epithelium in the rat. Am. J. Anat. 96: 255-283.

Das, C.M.S. 1962. Ultrastructure of postnuclear cap in the developing sperms of Microtus pennsylvanicus (Ord.). Proc. zool. Soc., Calcutta. 15: 75-81.

DeKretser, D.M. 1969. Ultrastructural features of human spermiogenesis. Z. Zellforsch. 98: 477-505.

Duesberg, J. 1908. La spermiogénèse chez le rat. Arch. Zellforsch. 2: 137-180.

Fawcett, D.W. 1958. The structure of mammalian sperm. Int. Rev. Cytology. 7: 195-234.

Fawcett, D.W. 1965. The anatomy of the mammalian spermatozoon with particular reference to the guinea pig. Z. Zellforsch. 67: 279-296.

Fawcett, D.W. 1970. A comparative view of sperm ultrastructure. Biol. Reprod. Suppl. 2: 90-127.

Fawcett, D.W. and M.H. Burgos. 1956. Observations on the cytomorphosis of the germinal and interstitial cells of the human testis. In: Ciba Foundation Colloquia on Ageing. Vol. 2. Ageing in transient tissues. Little Brown and Co.: Boston. Pp. 86-99.

Fawcett, D.W. and R.D. Hollenberg. 1963. Changes in the acrosome of guinea pig spermatozoa during passage through the epididymis. Z. Zellforsch. 60: 276-292.

Fawcett, D.W. and S. Ito. 1965. The fine structure of bat spermatozoa. Am. J. Anat. 116: 567-610.

Fawcett, D.W. and D.M. Phillips. 1967. Further observations on mammalian spermiogenesis. J. Cell Biol. 35: 152A. (Abstract).

Fawcett, D.W. and D.M. Phillips. 1969a. Observations on the release of spermatozoa and on the changes in the head during passage through the epididymis. J. Reprod. Fert. Suppl. 6: 405-418.

Fawcett, D.W. and D.M. Phillips. 1969b. The fine structure and development of the neck region of the mammalian spermatozoon. Anat. Rec. 165: 153-184.

Fawcett, D.W. and D.M. Phillips. 1970. Recent observations on the ultrastructure and development of the mammalian spermatozoon. In: Comparative spermatology. B. Baccetti (Ed.). Academic Press: New York. Pp. 13-28.

Fawcett, D.W., W.A. Anderson and D.M. Phillips. 1971. Morphogenetic factors influencing the shape of the sperm head. Developmental Biol. 26: 220-251.

Franklin, L.E. 1968. Formation of the redundant nuclear envelope in monkey spermatids. Anat. Rec. 161: 149-162.

Franklin, L.E. 1970. Fertilization and the role of the acrosomal region in non-mammals. Biol. Reprod. Suppl. 2: 159-176.

Franklin, L.E., C. Barros and E.N. Fussell. 1970a. The acrosomal region and the acrosome reaction in sperm of the golden hamster. Biol. Reprod. 3: 180-200.

Franklin, L.E., C. Barros and E.N. Fussell. 1970b. The perforatorium of golden hamster sperm. Anat. Rec. 166: 305. (Abstract).

Friend, G.F. 1936. The sperms of British Muridae. Q. Jl microsc. Sci. 78: 419-443.

Gardner, P.J. 1966. Fine structure of the seminiferous tubule of the Swiss mouse. The spermatid. Anat. Rec. 155: 235-250.

Gatenby, J.B. and S.B. Wigoder. 1929. The post-nuclear body in the spermatogenesis of Cavia cobaya and other animals. Proc. R. Soc. B. 104: 471-480.

Gordon, M. 1969. Localization of the 'apical body' in guinea-pig and human spermatozoa with phosphotungstic acid. J. Reprod. Fert. 19: 367-369.

Gresson, R.A.R. and I. Zlotnik. 1945. A comparative study of the cytoplasmic components of the male germ cells of certain mammals. Proc. R. Soc. Edinb. B. 62: 137-170.

Hadek, R. 1963. Study on the fine structure of the sperm head. J. Ultrastruct. Res. 9: 110-122.

Hadek, R. 1969. Mammalian fertilization. Academic Press: New York. 295 pp.

Hancock, J.L. 1966. The ultrastructure of mammalian spermatozoa. In: Advances in reproductive physiology. A. McLaren (Ed.). Academic Press: New York. Pp. 125-154.

Harrison, R.G. 1949. The comparative anatomy of the blood-supply of the mammalian testis. Proc. zool. Soc. Lond. 119: 325-344.

Hopsu, V.K. and A.W. Arstila. 1965. Development of the acrosomic system of the spermatozoon in the Norwegian lemming (Lemmus lemmus). Z. Zellforsch. 65: 562-572.

Horstmann, E. 1961. Elektronenmikroskopische Untersuchungen zur Spermiohistogenese beim Menschen. Z. Zellforsch. 54: 68-89.

Karnovsky, M.J. 1965. A formaldehyde-glutaraldehyde fixative of high osmolality for use in electron microscopy. J. Cell Biol. 27: 137A-138A.

Kessel, R.G. and P. Spaziani. 1969. Nuclear morphogenesis in rat spermatid. J. Cell Biol. 43: 67a. (Abstract).

Koehler, J.K. 1969. The acrosome-postnuclear cap junction. A characteristic landmark in rabbit spermatozoa revealed by freeze-etching. J. Cell Biol. 43: 70a. (Abstract).

Koehler, J.K. 1970. A freeze-etching study of rabbit spermatozoa with particular reference to head structures. J. Ultrastruct. Res. 33: 598-614.

Kopečný, V. 1970. Labelling of mouse spermatozoa with L-arginine-^{14}C (U)monohydrochloride. Z. Zellforsch. 109: 414-419.

Leblond, C.P. and Y. Clermont. 1952a. Spermiogenesis of rat, mouse, hamster and guinea pig as revealed by the "periodic acid-fuchsin sulfurous acid" technique. Am. J. Anat. 90: 167-215.

Leblond, C.P. and Y. Clermont. 1952b.. Definition of the stages of the cycle of the seminiferous epithelium in the rat. Annls N.Y. Acad. Sci. 55: 548-573.

Lenhossék, M. 1898. Untersuchungen über Spermatogenesse. Arch. mikrosk. Anat. EntwMech. 51: 215-318.

Lillie, R.D. 1965. Histopathologic technic and practical histochemistry. Blakiston: New York. 716 pp.

Lison, L. 1955. Variation de la basophilie pendant la maturation du spermatozoïde chez le rat et sa signification histochimique. Acta Histochem. 2: 47-67.

Monesi, V. 1964. Autoradiographic evidence of a nuclear histone synthesis during mouse spermiogenesis in the absence of detectable quantities of nuclear RNA. Expl Cell Res. 36: 683-688.

Monesi, V. 1965. Synthetic activities during spermatogenesis in the mouse. RNA and protein. Expl Cell Res. 39: 197-224.

Moricard, R. 1961. Des structures de l'acrosome des spermatozoïdes contenus dans l'utérus chez la lapine. C. r. Séanc. Soc. Biol. 155: 2243-2245.

Nicander, L. and A. Bane. 1962. Fine structure of boar spermatozoa. Z. Zellforsch. 57: 390-405.

Nicander, L. and A. Bane. 1966. Fine structure of the sperm head in some mammals with particular reference to the acrosome and sub-acrosomal substance. Z. Zellforsch. 72: 496-515.

Niessing, G. 1897. Die Betheiligung von Centralköper und Sphäre am Aufbau des Samenfädens bei Saugethieren. Arch. mikrosk. Anat. EntwMech. 48: 111-142.

Odor, D.L. and R.J. Blandau. 1951. Observations on fertilization and the first segmentation division in rat ova. Am. J. Anat. 89: 29-48.

Oliver, J.R. 1913. The spermiogenesis of the Pribilof fur seal (Callorhinus alascanus J. & C.). Am. J. Anat. 14: 473-499.

Pedersen, H. 1969a. Ultrastructure of the ejaculated human sperm. Z. Zellforsch. 94: 542-554.

Pedersen, H. 1969b. Microtubules in the spermatid of the rabbit. Z. Zellforsch. 98: 148-156.

Pikō, L. 1964. Mechanism of sperm penetration in the rat and Chinese hamster based on fine structure studies. Proc. V Int. Congr. Anim. Reprod. 7: 301-302.

Pikō, L. 1969. Gamete structure and sperm entry in mammals. In: Fertilization. C.B. Metz and A. Monroy (Eds.). Academic Press: New York. Pp. 325-403.

Pikō, L. and A. Tyler. 1964a. Fine structural studies of sperm penetration in the rat. Proc. V Int. Congr. Anim. Reprod. 2: 372-377.

Pikó, L. and A. Tyler. 1964b. Ultrastructure of the acrosome and the early events of sperm penetration in the rat. Am. Zoologist. 4: 287. (Abstract).

Plöen, L. 1971. A scheme of rabbit spermateleosis based upon electron microscopical observations. Z. Zellforsch. 115: 553-564.

Prokof'Yeva-Bel'Govskaya, A.A. and C. Chun-He. 1961. Electron microscopic investigation of spermiogenesis in the mouse. Biophysics. 6: 764-776.

Rattner, J.B. and B.R. Brinkley. 1971. Ultrastructure of mammalian spermiogenesis. II. Elimination of nuclear membrane. J. Ultrastruct. Res. 36: 1-7.

Retzius, G. 1909. Die Spermien der Nagetiere. Biol. Unters., N.F. 14: 133-162.

Reynolds, E.S. 1963. The use of lead citrate at high pH as an electron-opaque stain in electron microscopy. J. Cell Biol. 17: 208-212.

Sandoz, D. 1970. Evolution des ultrastructures au cours de la formation de l'acrosome du spermatozoïde chez la souris. J. Microscopie. 9: 535-558.

Stefanini, M., C. ŌUra and L. Zamboni. 1969. Ultrastructure of fertilization in mouse. 2. Penetration of sperm into the ovum. J. Submicr. Cytol. 1: 1-23.

Susi, F.R., C.P. Leblond and Y. Clermont. 1971. Changes in the Golgi apparatus during spermiogenesis in the rat. Am. J. Anat. 130: 251-268.

Vaughn, J.C. 1966. The relationship of the "sphere chromatophile" to the fate of displaced histones following histone transition in rat spermiogenesis. J. Cell Biol. 31: 257-278.

Venable, J.H. and R. Coggeshall. 1965. A simplified lead citrate stain for use in electron microscopy. J. Cell Biol. 25: 407-408.

Waldeyer, W. 1906. Die Geschlechtzellen. Handbuch der Vergleichenden und Experimentellen Entwicklungslehre der Wirbeltiere. 1: 86-476.

Watson, M.L. 1952. Spermatogenesis in the albino rat revealed by electron microscopy. Biochim. biophys. Acta. 8: 369-374.

Watson, M.L. 1958. Staining of tissue sections for electron microscopy with heavy metals. J. biophys. biochem. Cytol. 4: 475-478.

Wimsatt, W.A., P.H. Krutzsch and L. Napolitano. 1966. Studies on sperm survival mechanisms in the female reproductive tract of hibernating bats. I. Cytology and ultrastructure of uterine spermatozoa in Myotis lucifugus. Am. J. Anat. 119: 25-60.

Wu, S.H. and J.D. Newstead. 1966. Electron microscope study of bovine epididymal spermatozoa. J. Anim. Sci. 25: 1186-1196.

Yanagimachi, R. and Y.D. Noda. 1970a. Fine structure of the hamster sperm head. Am. J. Anat. 128: 367-388.

Yanagimachi, R. and Y.D. Noda. 1970b. Electron microscope studies of sperm incorporation into the golden hamster egg. Am. J. Anat. 128: 429-462.

Yanagimachi, R. and Y.D. Noda. 1970c. Ultrastructural changes in the hamster sperm head during fertilization. J. Ultrastruct. Res. 31: 465-485.

Yanagimachi, R. and Y.D. Noda. 1970d. Physiological changes in the postnuclear cap region of mammalian spermatozoa: A necessary preliminary to the membrane fusion between sperm and egg cells. J. Ultrastruct. Res. 31: 486-493.

Young, W.C. 1931. A study of the function of the epididymis. III. Functional changes undergone by spermatozoa during their passage through the epididymis and vas deferens in the guinea pig. J. exp. Biol. 8: 151-162.

Zamboni, L. 1971. Acrosome loss in fertilizing mammalian spermatozoa: A clarification. J. Ultrastruct. Res. 34: 401-405.

Zamboni, L. and M. Stefanini. 1968. On the configuration of the plasma membrane of the mature spermatozoon. Fert. Steril. 19: 570-579.

Zamboni, L. and M. Stefanini. 1971. The structure of the neck of mammalian spermatozoa. Anat. Rec. 169: 155-172.

Zamboni, L., R. Zemjanis and M. Stefanini. 1971. The fine structure of monkey and human spermatozoa. Anat. Rec. 169: 129-154.

Fig. 1 A diagrammatic representation of the 14 stages of the cycle of the rat seminiferous epithelium. The cellular components of each stage are shown in the vertical columns designated by roman numerals. The 19 steps of spermiogenesis are designated by arabic numerals. Note that the first 14 steps of spermiogenesis can be used to identify the 14 stages of the cycle.
A_1-A_4, type A spermatogonia; Im, intermediate spermatogonia; B, type B spermatogonia; A_M, I_M, B_M, spermatogonia mitoses; Pl, preleptotene spermatocytes; L, leptotene spermatocytes; Z, zygotene spermatocytes; P, pachytene spermatocytes; Di, diplotene; II, secondary spermatocytes.

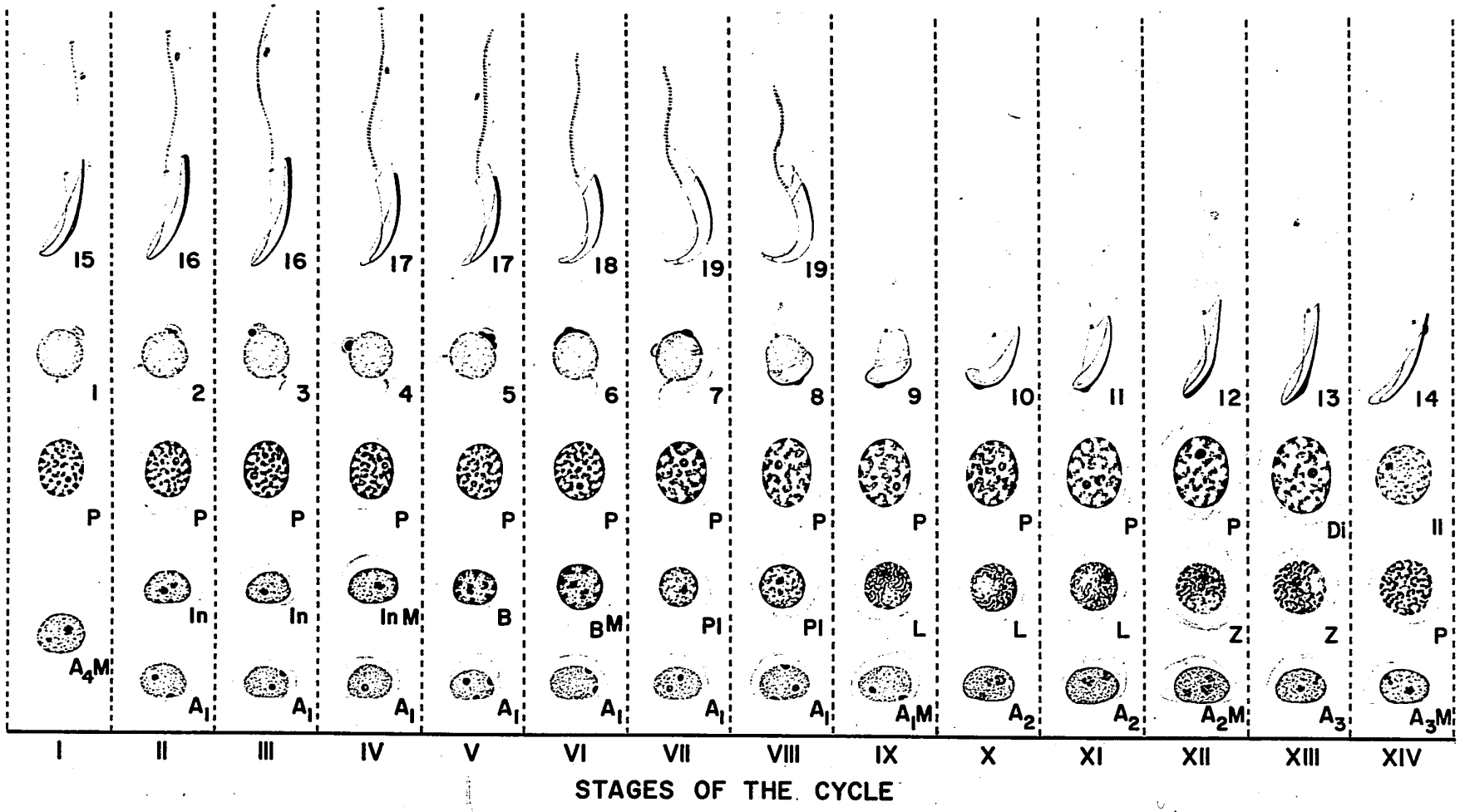
15
16
16
17
17
18
19
19
1
2
3
4
5
6
7
8
9
10
11
12
13
14
P
P
P
P
P
P
P
P
P
P
P
P
Di
II
In
In
In M
B
BM
PI
PI
L
L
L
Z
Z
P
A4M
A1
A1
A1
A1
A1
A1
A1
A1M
A2
A2
A2M
A3
A3M
I
II
III
IV
V
VI
VII
VIII
IX
X
XI
XII
XIII
XIV
STAGES OF THE CYCLE

Fig. 2 Light microscopic drawings of spermatids in the 19 steps of spermiogenesis as seen in paraffin sections fixed in Flemming's fluid and stained with iron hematoxylin (from unpublished work of Dr. Y. Clermont). There is a great similarity of this material to that of Epon embedded material fixed in glutaraldehyde and stained with either iron hematoxylin or toluidine blue. A detailed description of the spermatid is given in the text.

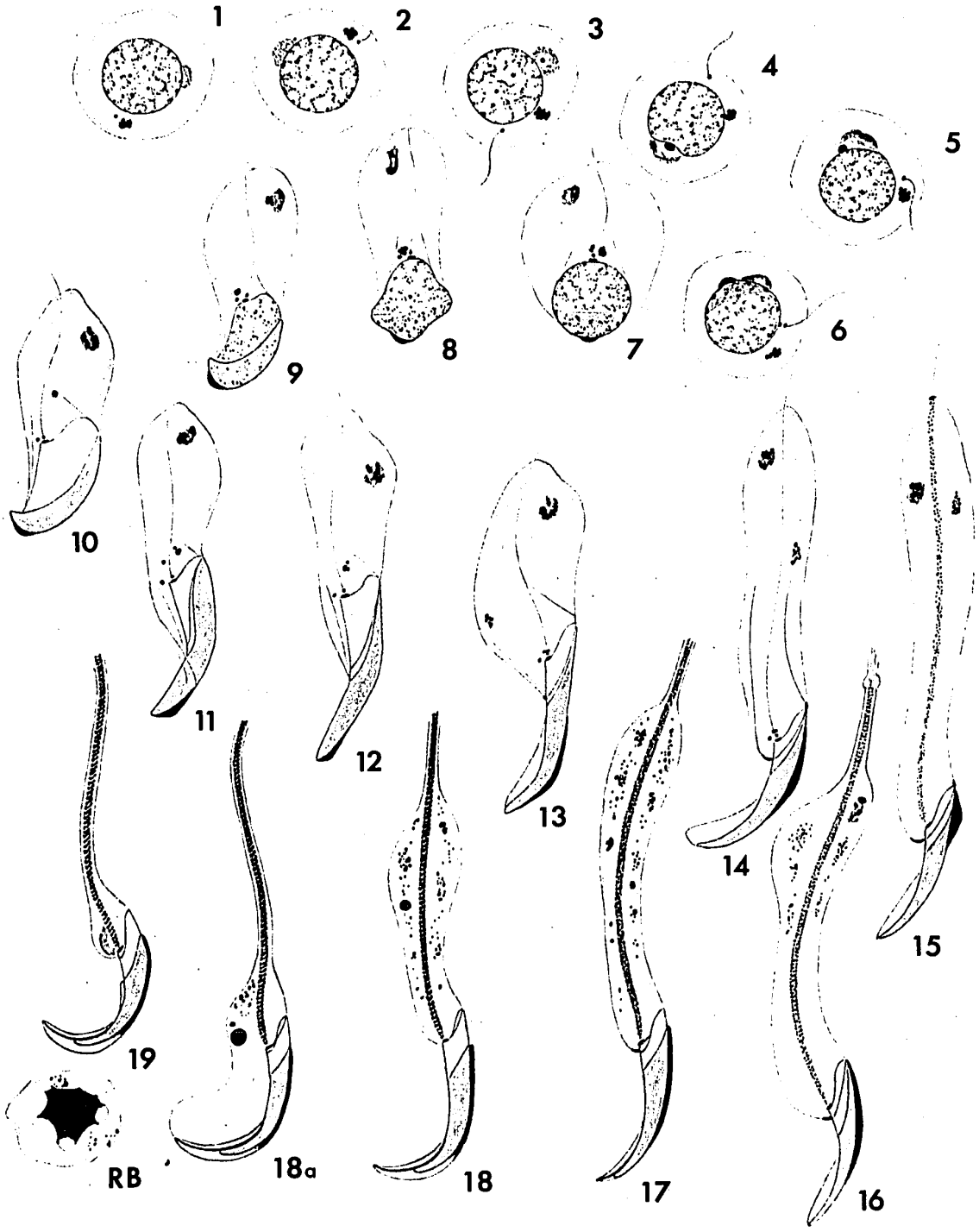
1
2
3
4
5
6
7
8
9
10
11
12
13
14
15
16
17
18
18a
19
RB

Fig. 3 A lateral view of a mature spermatozoon cut at two different levels of the head to show the regional differences in cross-sectional shape and the general arrangement of the head components. A, acrosome; Fl, flagellum; FC, perifossa collar; HC, head cap; N, nucleus; PM, plasma membrane; PT, perinuclear theca.

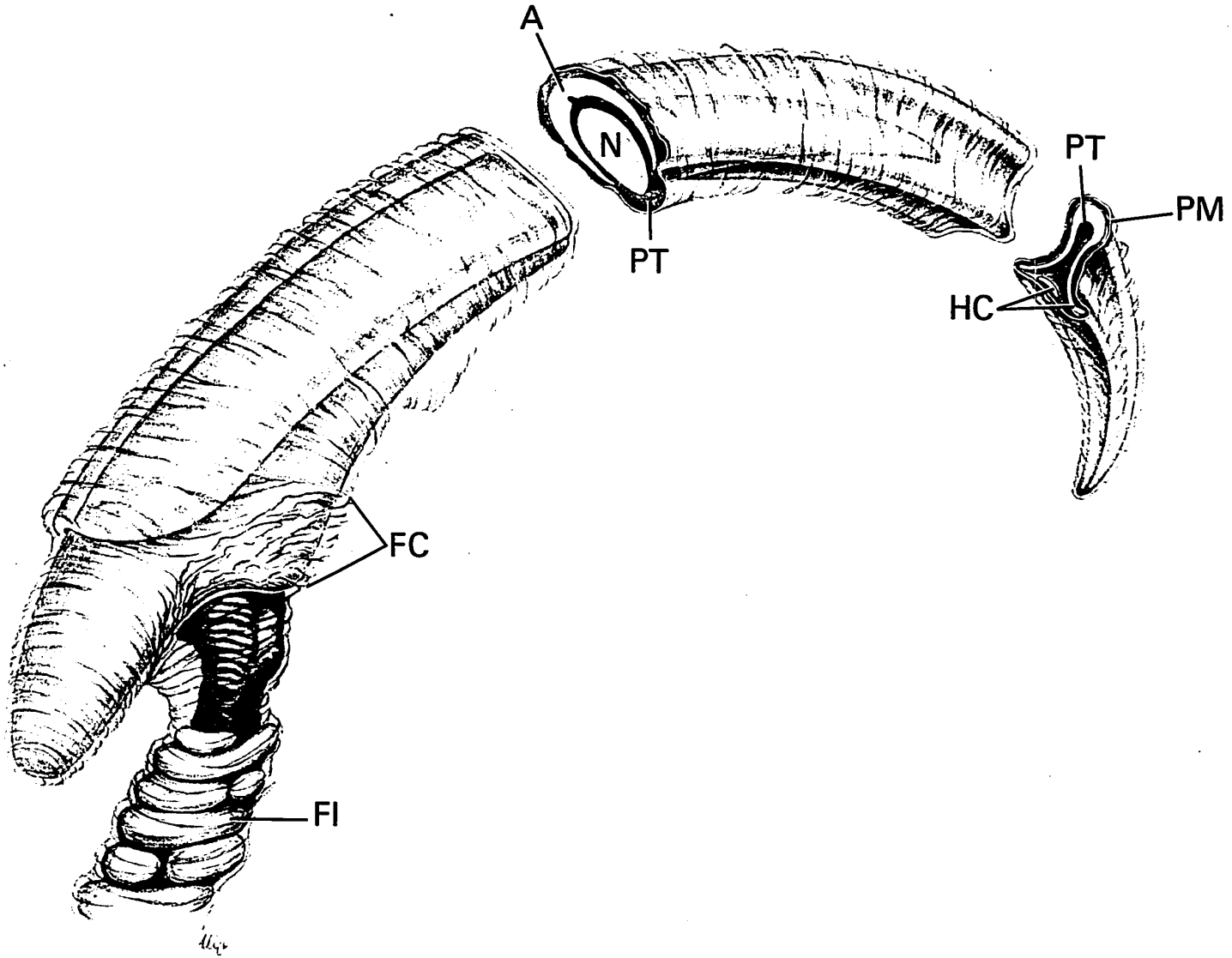
A
N
PT
PT
PM
HC
FC
FI

Fig. 4 A longitudinal section through a fully formed spermatozoon at the time of sperm release from the seminiferous epithelium. Part of the head structures, at the apex, have been drawn on the electron micrograph to complete the falciform shape of the head. The dorsal and ventral surfaces are indicated. A, acrosome; DA, dorsal angle; Fl, flagellum; N, nucleus; P, perforatorium; R.Cyto., residual spermatid cytoplasm; VA, ventral angle; VS, ventral spur.

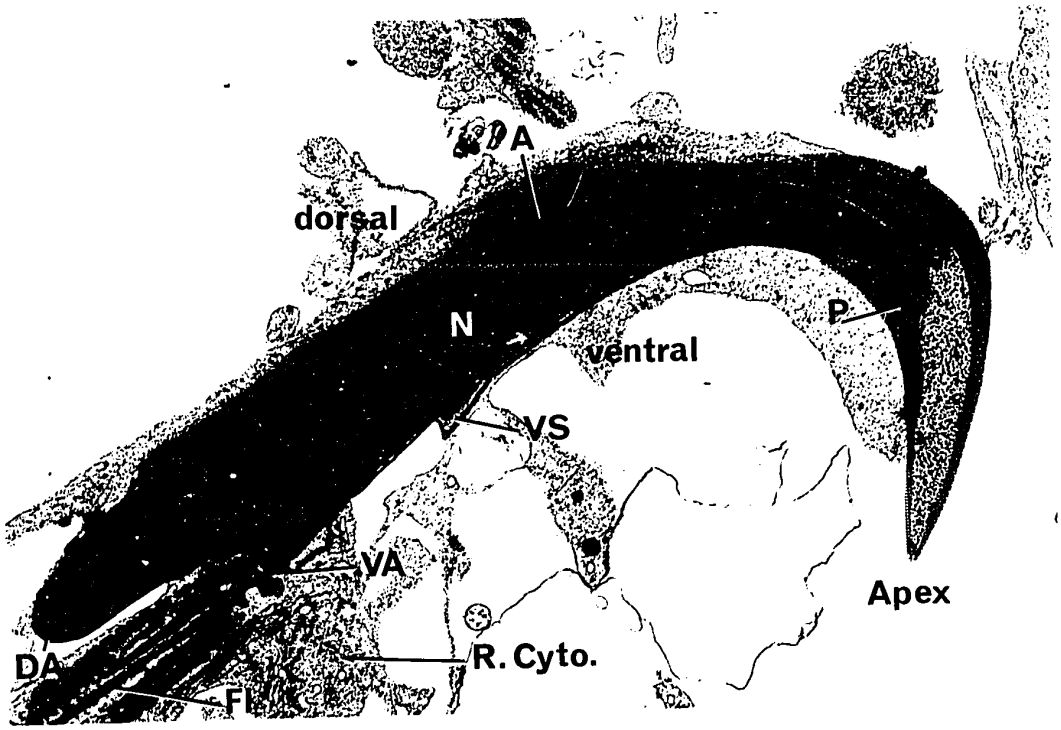

4

For orientation of the plane of section shown in Figures 5-17 a fold-out orientation drawing is provided in Figure 23.

Fig. 5 A section through the anterior tip of the spermatozoon head. HC, head cap; PT, perinuclear theca. (50,000 X)

Fig. 6 Two sections of the anterior part of the head (see Figure 23). In section (b) the three components of the acrosomic system can be seen: LHC, the lateral head cap component; VHC, the ventral head cap component; A, the acrosome proper; PT, perinuclear theca. (50,000 X)

Fig. 7 A section through the anterior tip of the nucleus (N). Note that the plasma membrane (PM) loosely covers the acrosomic system and is tightly adherent to the perinuclear theca (PT) on the ventral surface. (50,000 X)

Fig. 8 At this level of the head the nucleus (N) has a definite oval cross-sectional shape. The arrowheads designate the limit between the acrosome and lateral component of the head cap. The nucleus is encased in a triangular layer of electron dense material, the perinuclear theca (PT). (50,000 X)

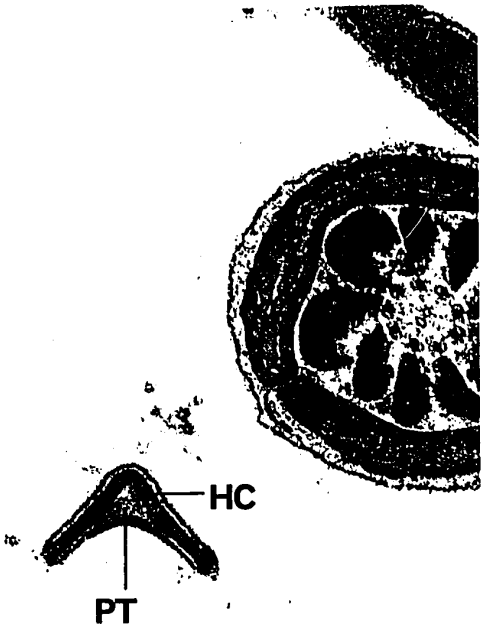

5

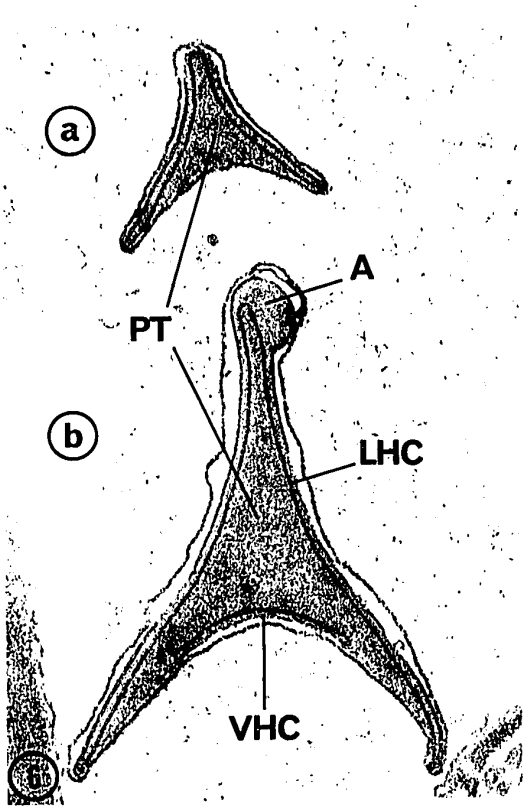

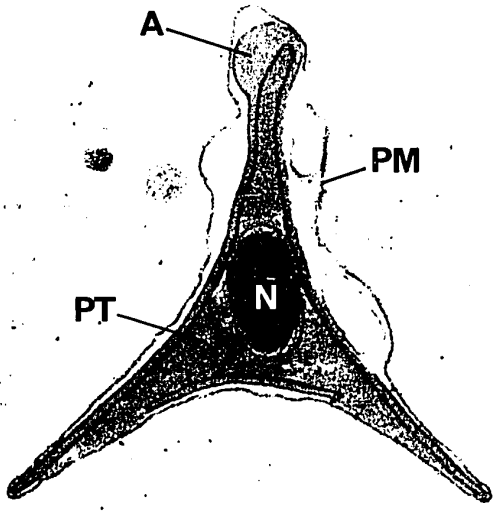

7

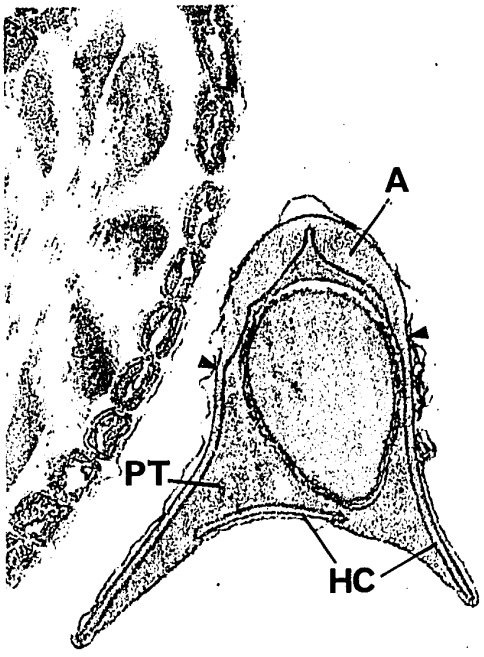

8

Fig. 9 A section through the spermatozoon head where the cross-sectional configuration changes from a triangular to an oval outline. HC, head cap; N, nucleus; PM, plasma membrane; PT, perinuclear theca. Note the rarefaction or vacuole in the nucleus. (50,000 X)

Fig. 10 This section is from the middle region of the head where the cross-sectional shape is oval. The arrowheads point out the boundary between acrosome (A) and head cap (HC). The perinuclear theca (PT) forms a thick layer on the ventral surface. The volume of the perinuclear theca is reduced on the dorsal and lateral surfaces of the nucleus (N) compared to that seen in the section in Figure 9. Note that the ventral portion of the head cap is not present in this section. (50,000 X)

Fig. 11 An enlarged portion of Figure 8 showing the trilaminar membranes delimiting the acrosomic system, the plasma membrane and the double membranes of the nuclear envelope. N, nucleus; PT, perinuclear theca; VHC, ventral head cap. (100,000 X)

Fig. 12 An enlarged section of Figure 10. A thin layer of perinuclear theca (PT) lies between the inner acrosomic membrane and the outer membrane of the nuclear envelope. Note that the plasma membrane (PM) is closely bound to the perinuclear theca on the ventral surface. (100,000 X)

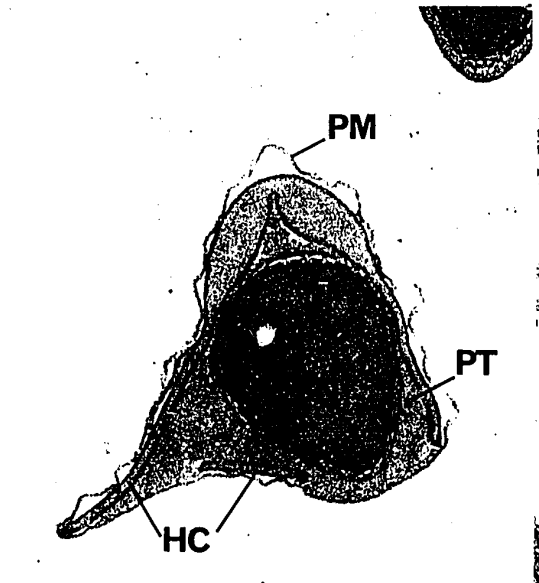

9

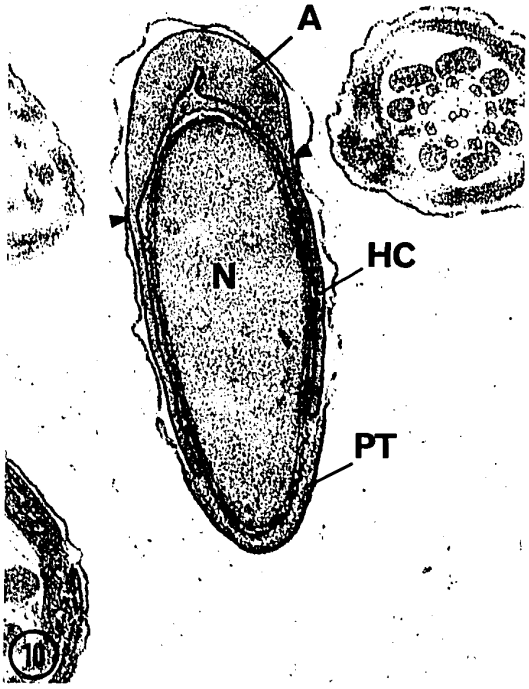

10

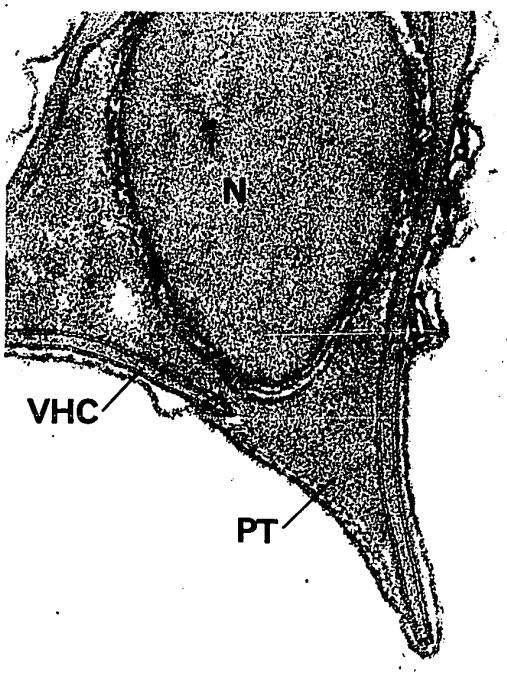

11

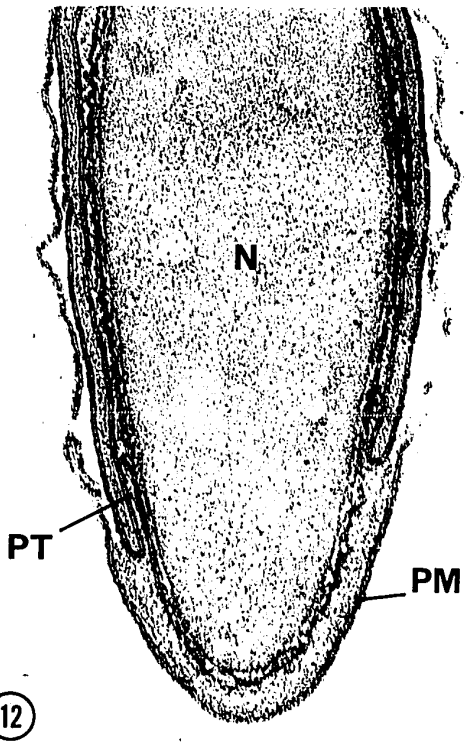

12

Fig. 13 A section through the ventral spur (VS) region of the head. Note that the perinuclear theca (arrow) is bilaminated with an electron dense layer adjacent to the plasma membrane on the lateral surface and a less dense layer close to the nucleus. Note also that the head cap (HC) covers less of the lateral surface of the head than it does in the anterior part of the head. (50,000 X)

Fig. 14 This section passes through the perifossa collar region just anterior to the insertion of the flagellum. The asterisks, which face an indentation of the plasma membrane, mark the dorsal limit of the perifossa collar. The perinuclear theca (PT) is present dorsal to the asterisks, but is absent ventrally where the plasma membrane loosely covers the porous nuclear envelope across the ventral surface forming the perifossa collar. N, nucleus; NP, nuclear pores. (50,000 X)

Fig. 15 (a) A section similar to Figure 14. Asterisks show the indentation of plasma membrane delimiting the perifossa collar.

(b) A section similar to Figure 8. Note the similar electron density of the perinuclear theca (PT) at these two levels of the head. The arrowheads designate the limit between the acrosome (A) and lateral component of the head cap (HC). (50,000 X)

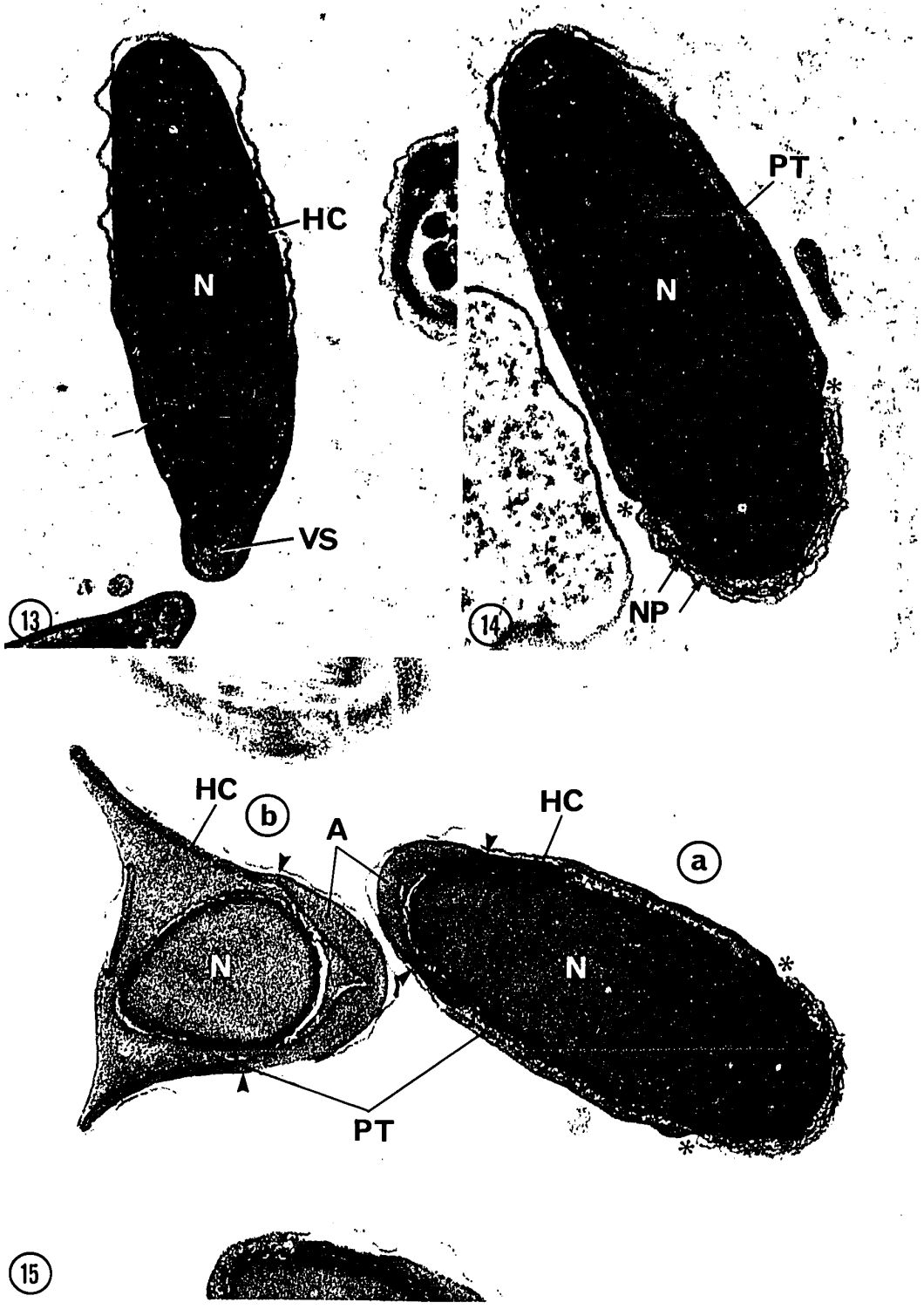
HC
N
VS
13
PT
N
NP
14
HC
b
A
HC
a
N
N
PT
15

Fig. 16 An oblique cut through the spermatozoon head and connecting piece of the flagellum (Fl). Porous nuclear protrusions (P) extend into the connecting piece of the flagellum. The basal plate (BP) lies against the outer nuclear membrane in the implantation fossa. The asterisks mark the dorsal limit of the perifossa collar. N, nucleus; NP, nuclear pore; PT, perinuclear theca. (50,000 X)

Fig. 17 A section through the posterior tip of the head and flagellum (Fl). This is posterior to the limit of the acrosomic system and the nucleus (N) is covered only by perinuclear theca (PT) and plasma membrane (PM). (50,000 X)

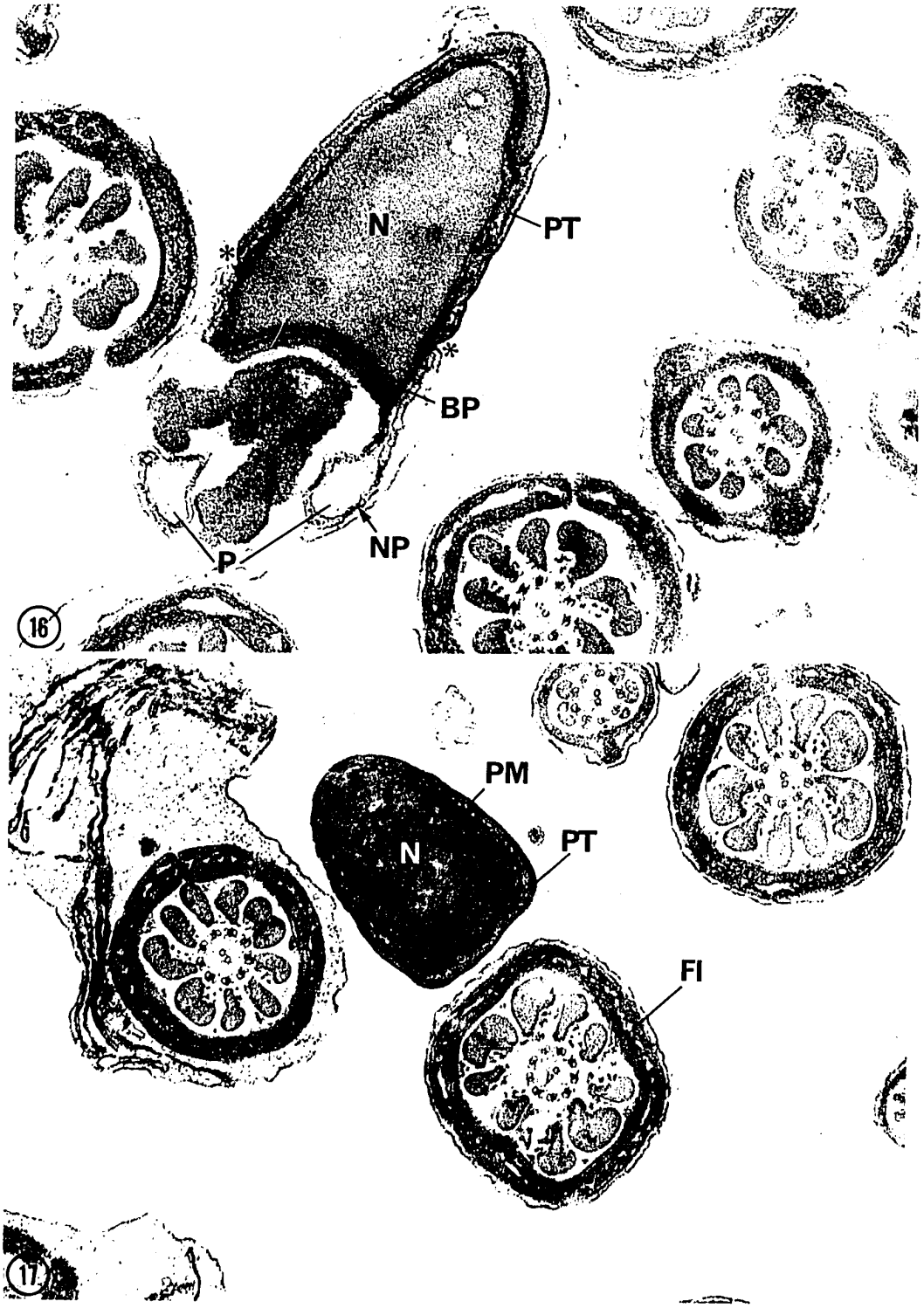
N
PT
BP
P
NP
16
PM
N
PT
FI
17

Fig. 18 A section through the spermatozoon head where the cross-sectional shape changes from triangular to oval. It illustrates the continuity of the perinuclear theca (PT) around the nucleus (N), even in the area where the inner acrosomic membrane closely approximates the outer nuclear membrane (arrows). A, acrosome; HC, head cap; PM, plasma membrane. (120,000 X)

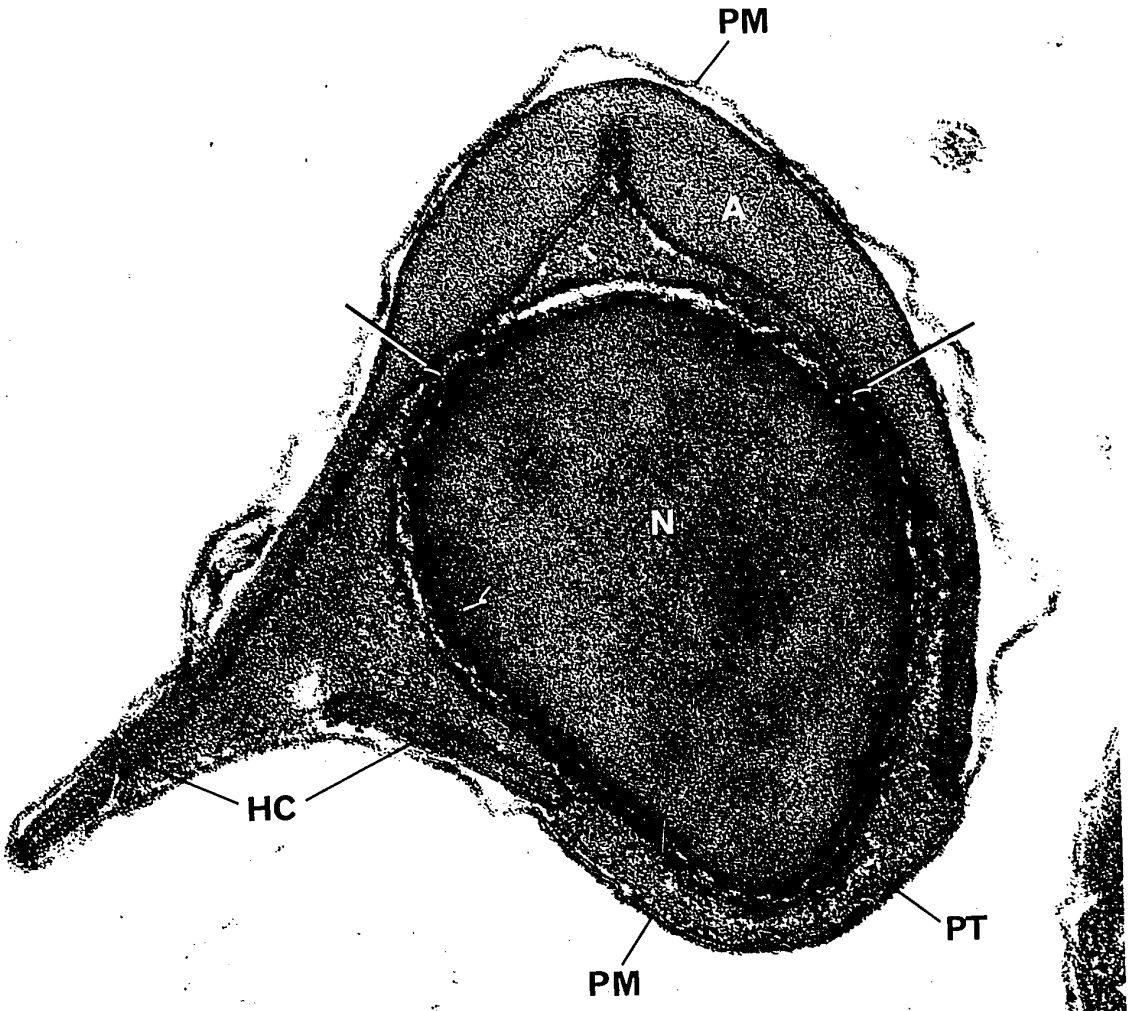
PM
A
N
HC
PT
PM

Fig. 19 A longitudinal section through the posterior part of the head and the flagellum (Fl). The basal plate (BP) of the implantation fossa can be seen. The anterior and posterior limits of the perifossa collar are marked by asterisks. The perinuclear theca (PT) ends abruptly at these points. A comma-shaped curve connecting these two points would give the dorsal boundary of the fossa collar. (50,000 X)

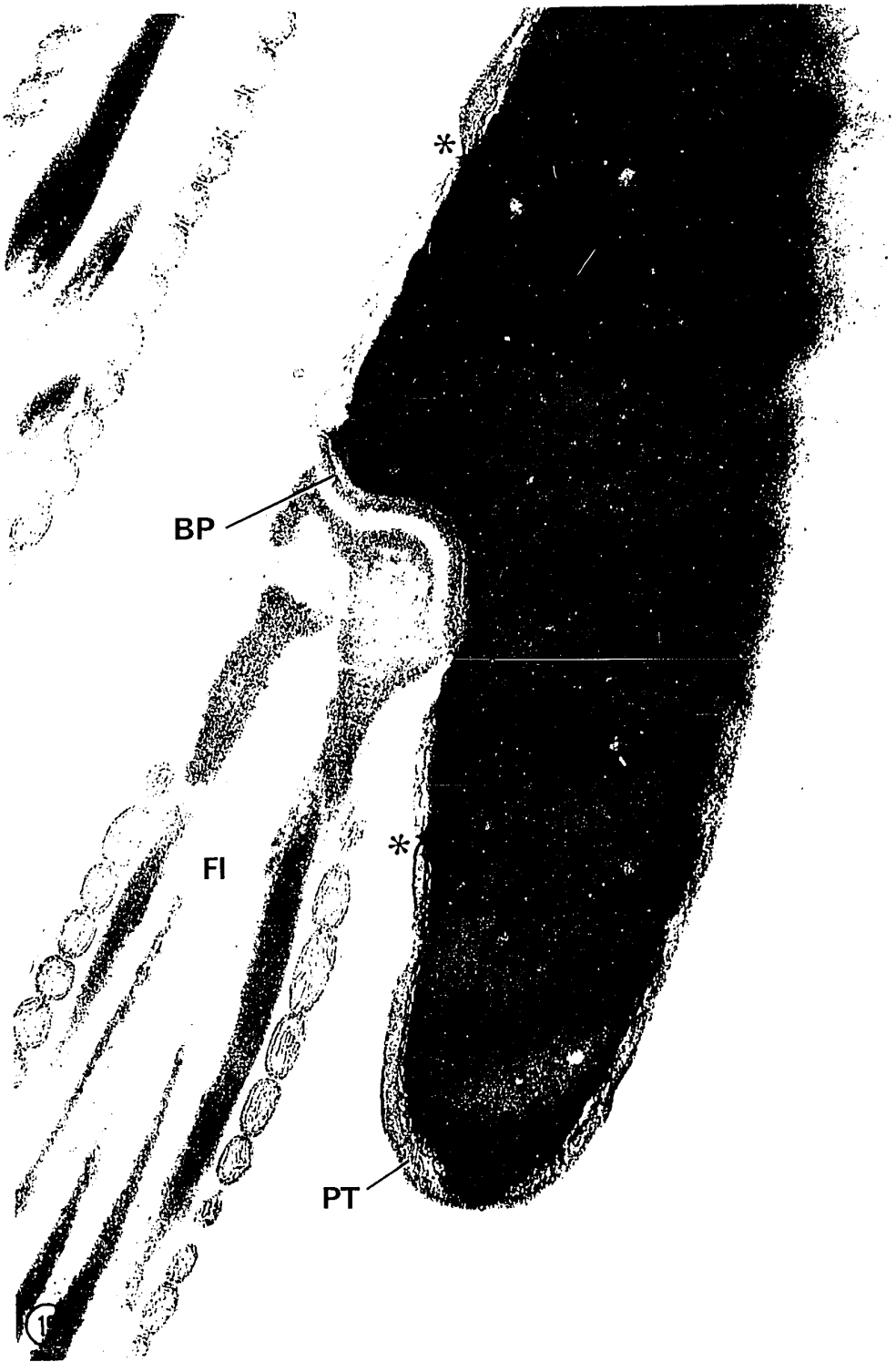
*
BP
Fl
*
PT

Figs. 20, 21, 22 These sections illustrate the appearance of the caput epididymal spermatozoa. Notice that the plasma membrane (PM) is more regular and closely applied to the acrosomic system than it is in the more mature spermatozoon. The large size of the acrosome (A) is also striking in these spermatozoa. The electron density of the perinuclear theca (PT) is similar to that of spermatozoa from the cauda epididymis. (50,000 X)

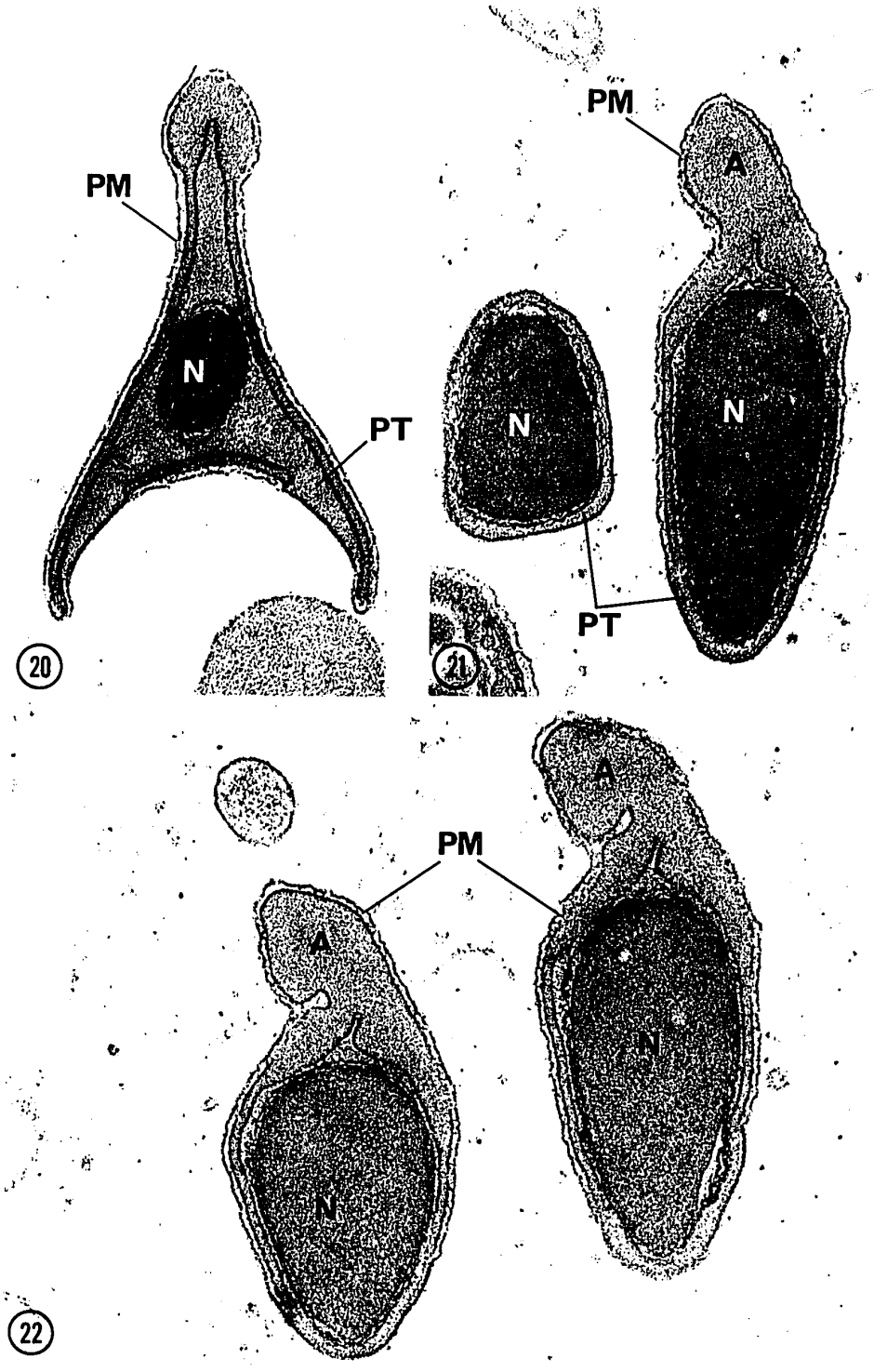
PM
N
PT
20
PM
A
N
N
PT
21
A
PM
A
N
N
22

Fig. 23 A diagrammatic lateral view of the head and part of the flagellum of a rat spermatozoon illustrating the planes of sections which appear in Figures 5 through 17.

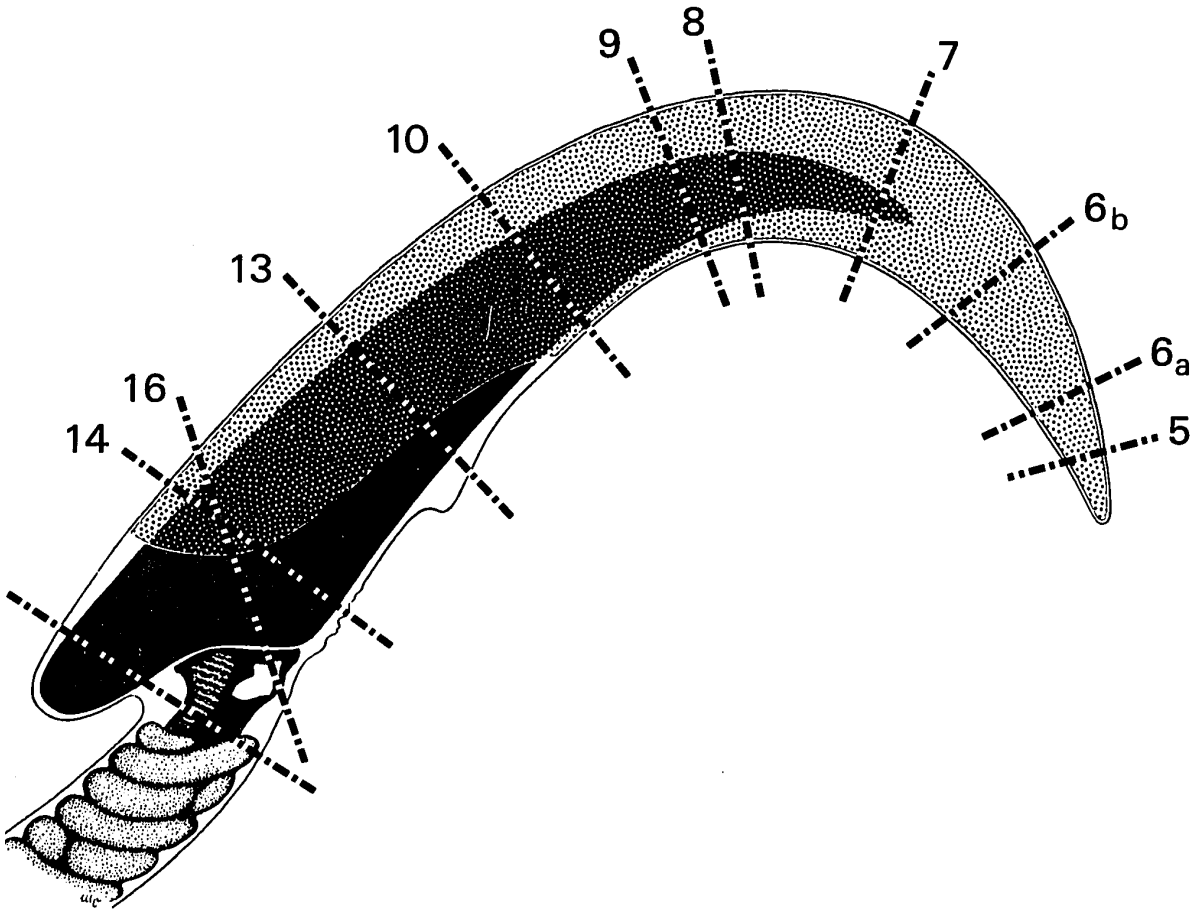
9
8
7
10
6b
13
6a
16
14
5

Fig. 24 A drawing of longitudinal and cross sections through the head and part of the flagellum of a caudal epididymal rat spermatozoon. The shape of the nucleus and the disposition of the perinuclear theca and acrosomic system around the nucleus can be followed in this summary drawing.

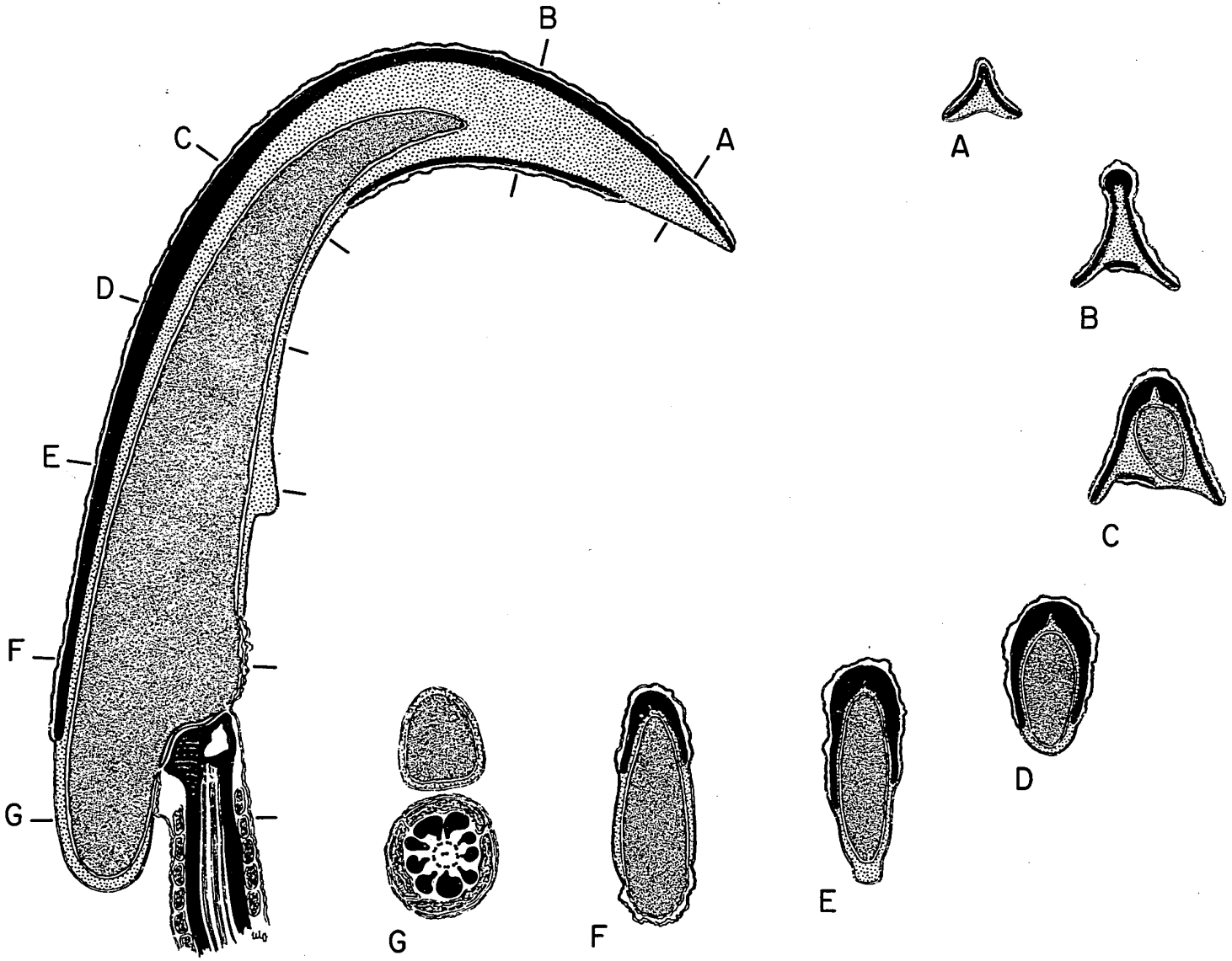
B
C
A
D
E
F
G
A
B
C
D
E
F
G

Fig. 25 The Golgi area of a step 1 spermatid. The undulating nuclear membrane is modified at the points indicated by arrows. G, Golgi apparatus; N, nucleus; PAG, pro-acrosomic granules. (45,000 X)

Fig. 26 A step 3 spermatid. The nuclear envelope is modified between the arrows. Note the condensation of electron dense material against the inner nuclear membrane. The subacrosomic layer can be seen between the outer nuclear membrane and the acrosomic vesicle (AV). AG, acrosomic granule; G, Golgi apparatus; N, nucleus. (30,000 X)

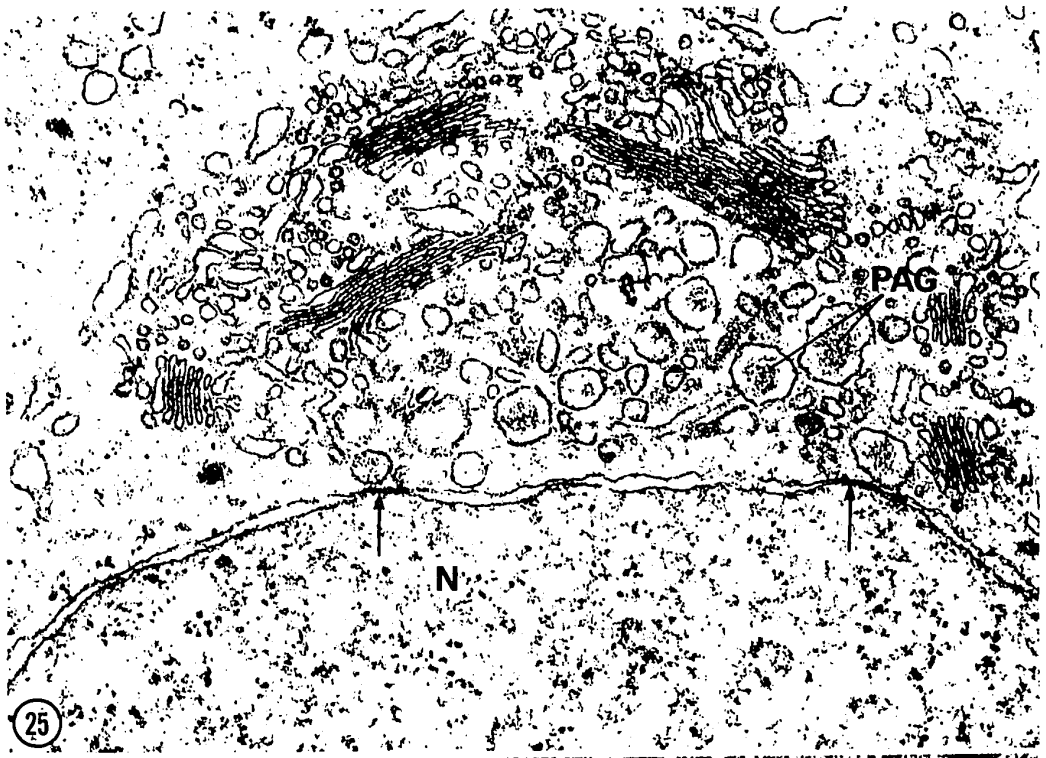

25

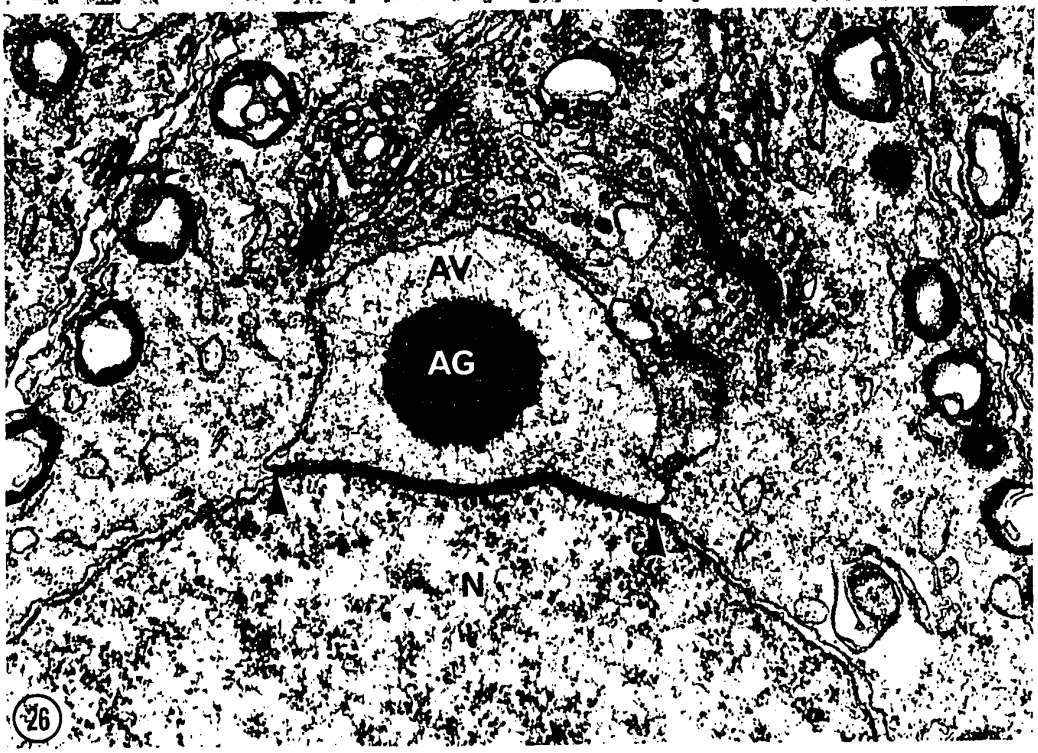

26

Fig. 27 A step 2 spermatid sectioned through the Golgi apparatus (G) and two acrosomic vesicles (AV), one of which contains an acrosomic granule (AG). Between the two arrows is a modified area of nuclear envelope adjacent to an acrosomic vesicle. N, nucleus. (45,000 X)

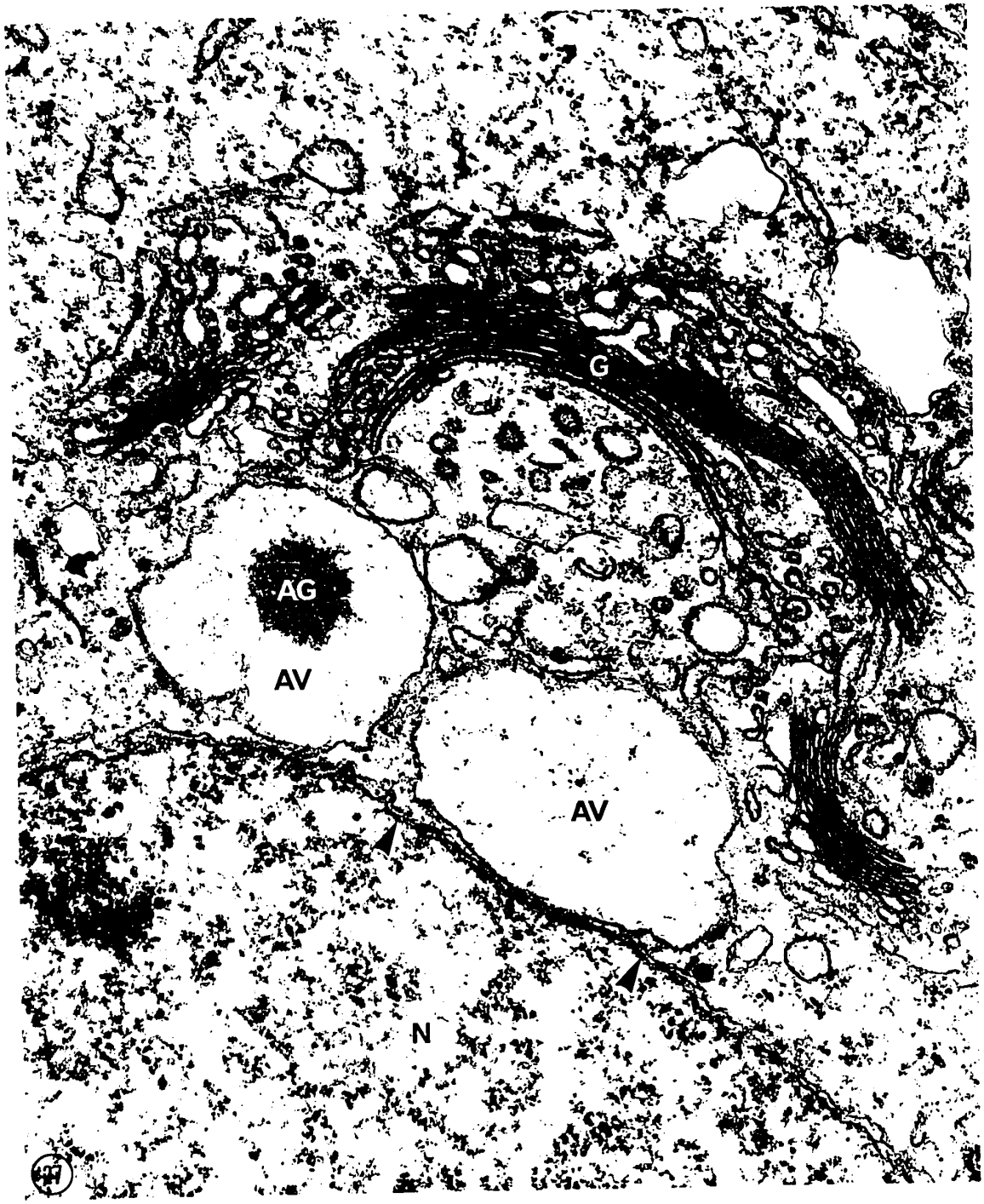
G
AG
AV
AV
N

Fig. 28 A step 5 spermatid. AG, acrosomic granule; G, Golgi apparatus; HC, head cap; N, nucleus. Note that the narrow space between the nuclear envelope and the inner acrosomic membrane contains a finely granular material (arrows). (25,000 X)

Fig. 29 A step 6 spermatid. Abbreviations as in Figure 28. Note the increased density of the head cap material compared with that of the previous step. An electron dense layer can be seen adjacent to the inner nuclear membrane in the modified portion of the nuclear envelope which is covered by the acrosomic system. (30,000 X)

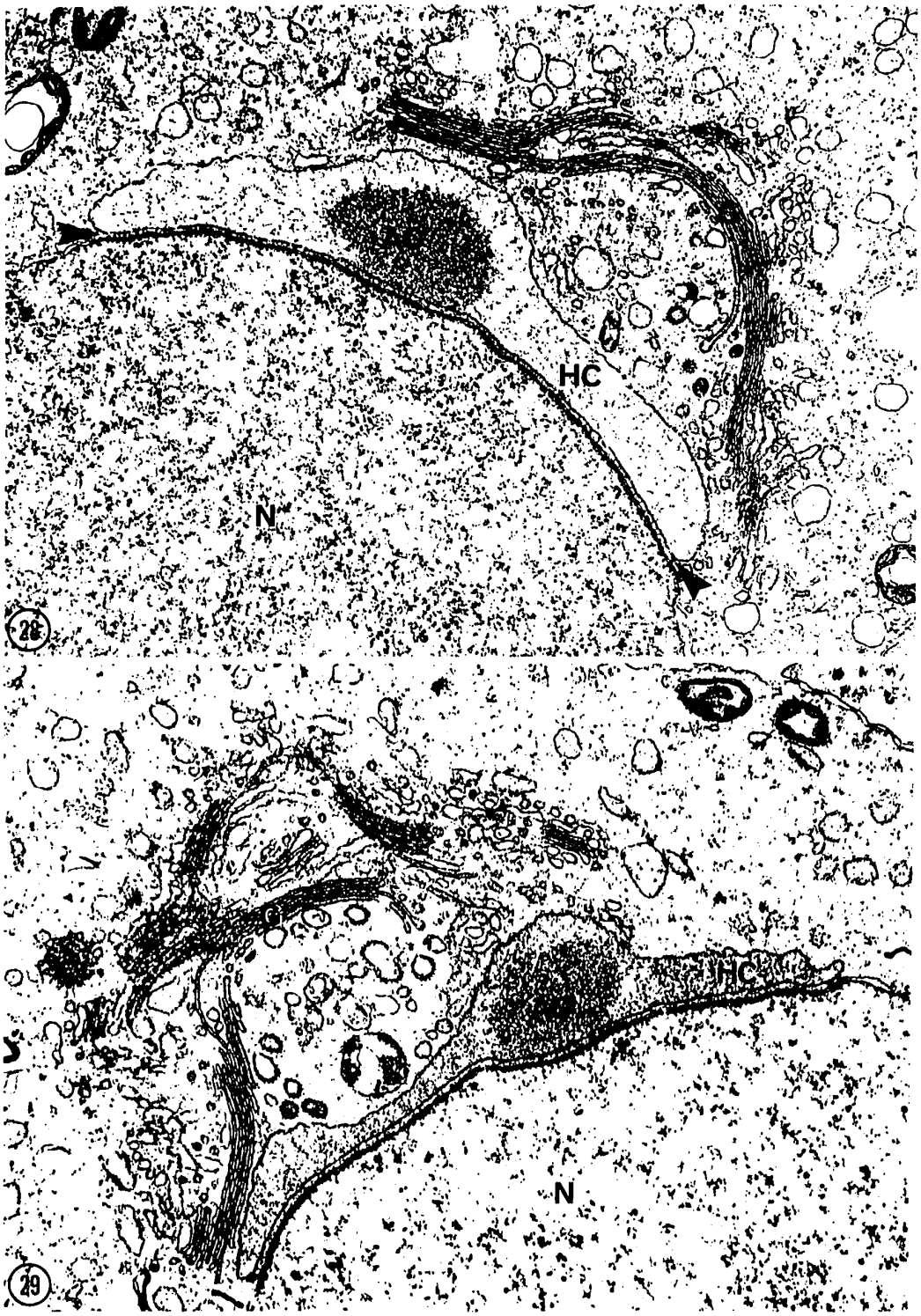
HC
N
28
HC
N
29

Fig. 30 A step 6 spermatid. Note the relationship of the Golgi saccules (G) to the edge of the head cap (HC). The interface between the electron dense subacrosomic layer and the surrounding cytoplasm is marked by the arrow. AG, acrosomic granule; N, nucleus. (40,000 X)

Fig. 31 An early step 7 spermatid. The arrow points out the forming marginal fossa. Note the marked difference in the configuration of the nuclear envelope under the acrosomic system (to the left of the arrow) and facing the cytoplasm (to the right of the arrow). G, Golgi apparatus; HC, head cap; N, nucleus. (45,000 X)

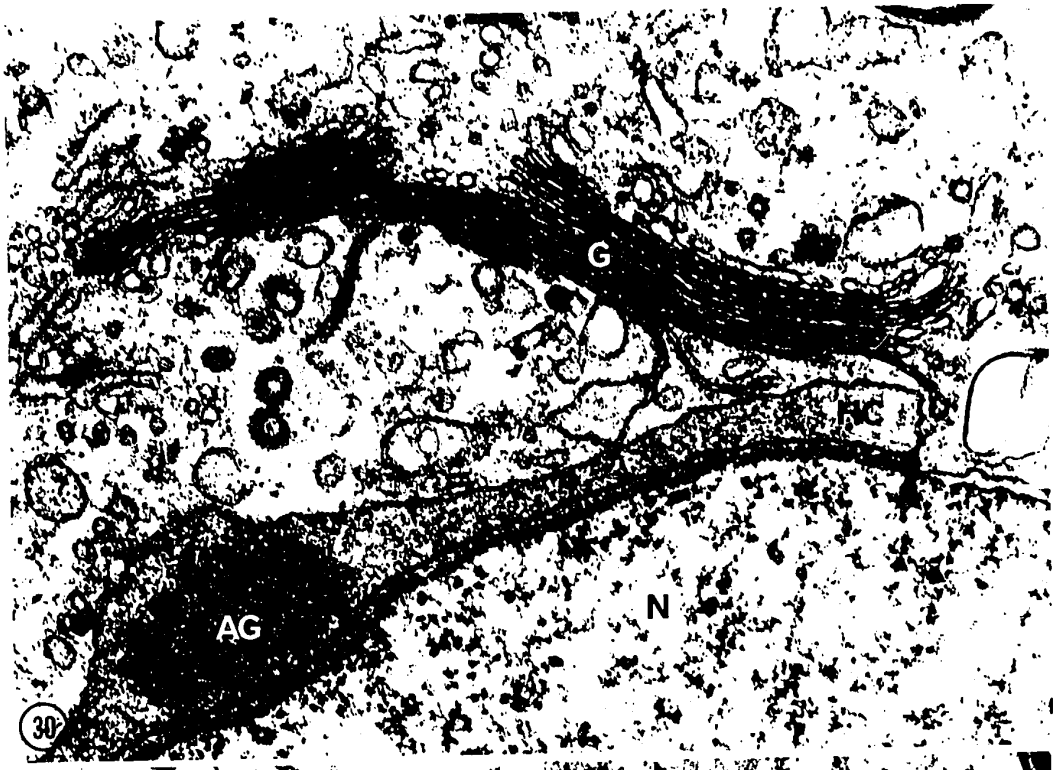

30

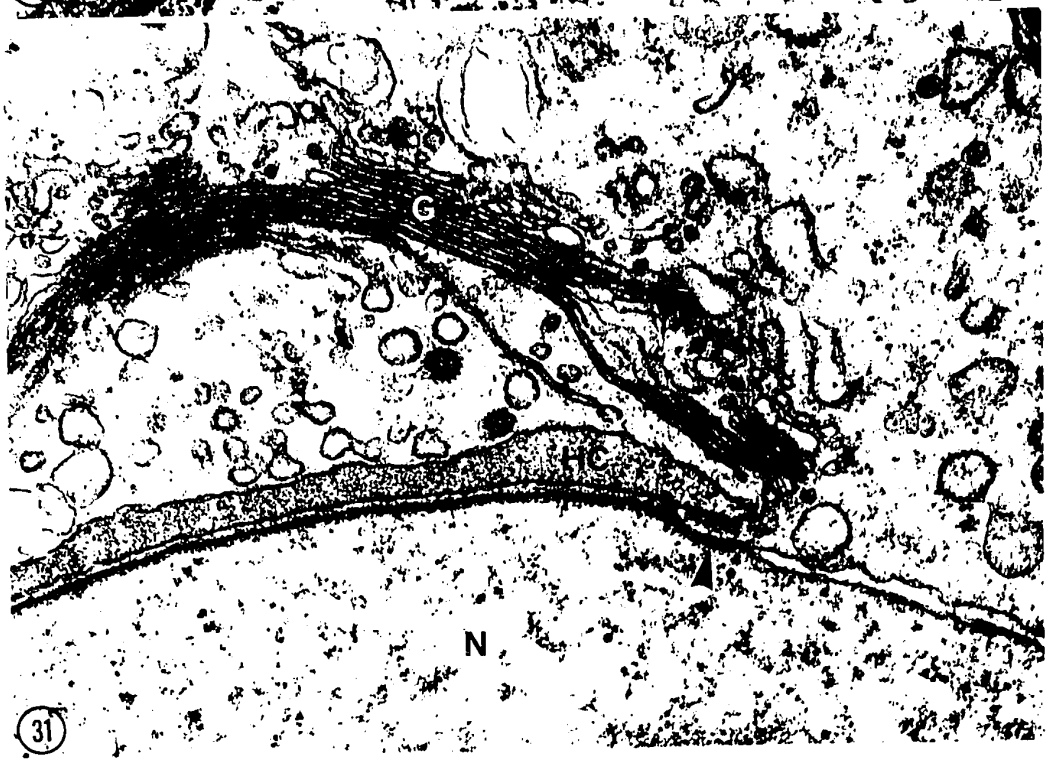

31

Fig. 32 A step 9 spermatid sectioned to the side of the acrosome so that only the head cap (HC) part of the acrosomic system appears in the section. CT, caudal tube; N, nucleus. Note the fine granular material between the nuclear envelope and the caudal tubee (arrows). (30,000 X)

The inset of Figure 32 is an enlargement of the marginal fossa region. The arrowhead points out the inner limit of the marginal fossa. Note that the material of the marginal fossa has a different appearance than that of the remainder of the sub-acrosomic layer. ER, endoplasmic reticulum of Sertoli cell; F, filaments; SC, Sertoli cell cytoplasm; SF, Sertoli cell filaments. (45,000 X)

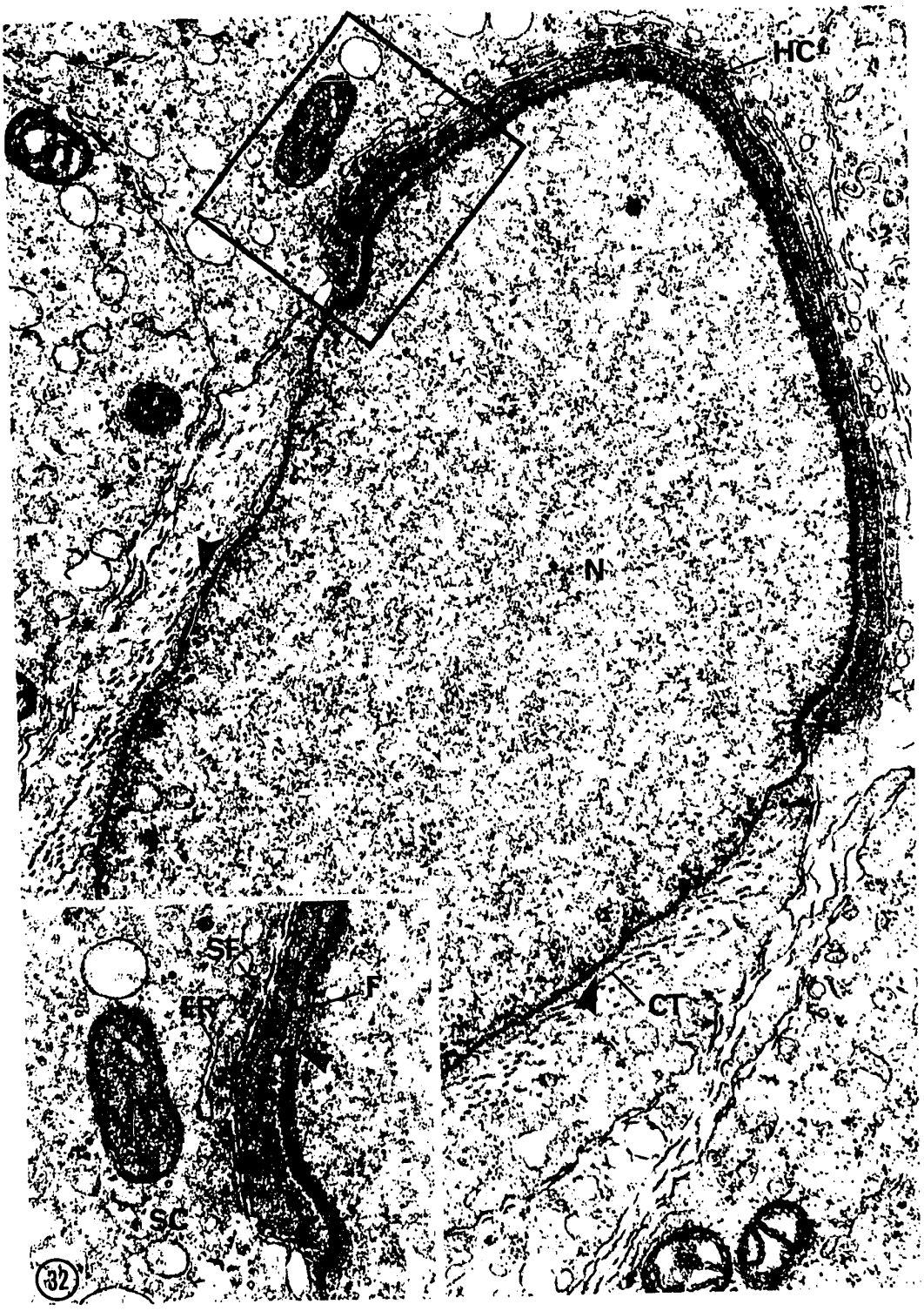
HC
N
CT
SE
F
ER
SC
32

Fig. 33 A longitudinal section of a step 10 spermatid. The anterior-dorsal limits of the acrosome (A) are pointed out by arrows. CB, chromatoid body; CT, caudal tube; HC, head cap; IF, implantation fossa; N, nucleus. (15,000 X)

The marginal fossa area of the subacrosomic layer is enlarged in the inset. The Sertoli cell filaments are indicated with an asterisk. (30,000 X)

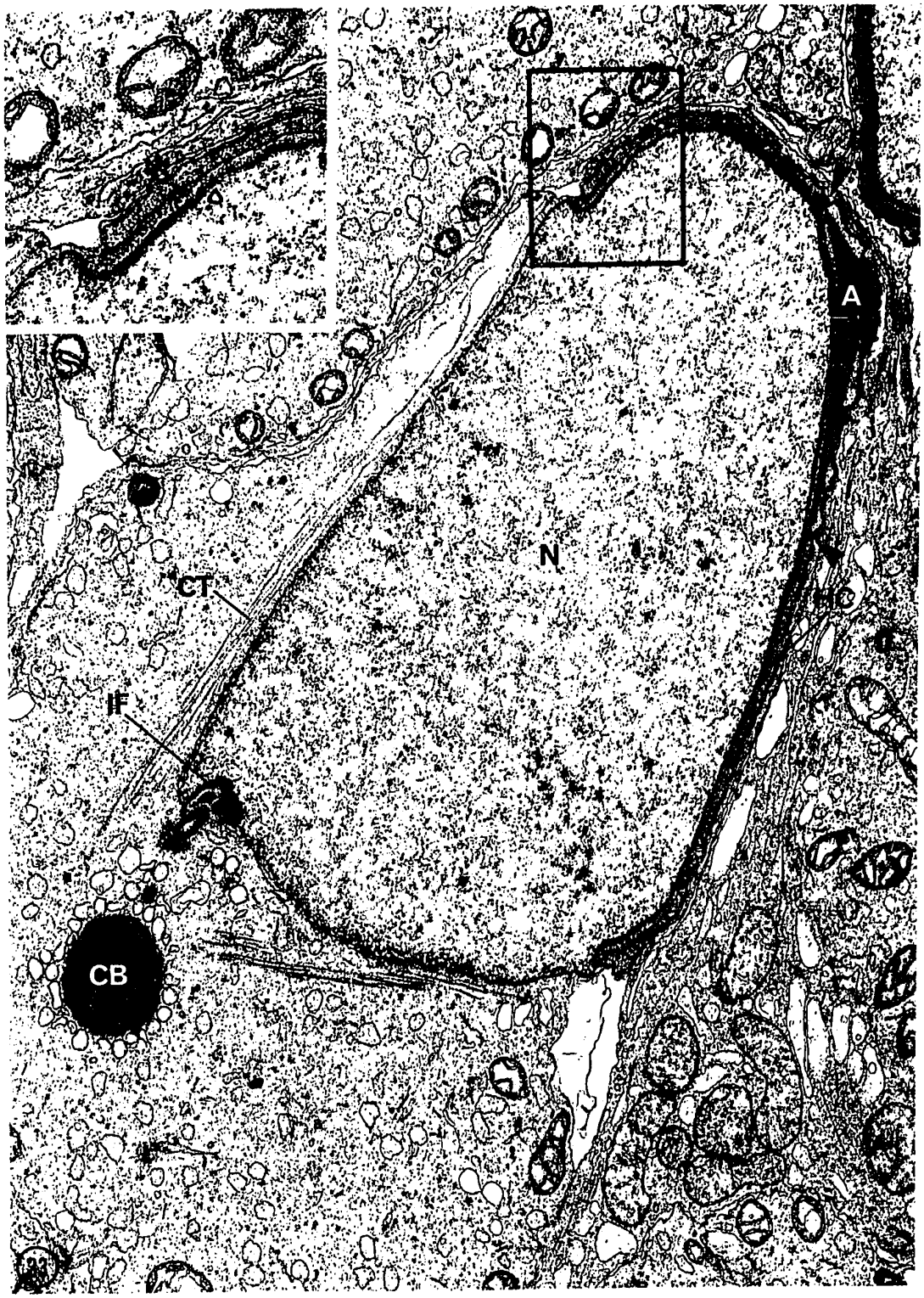
A
N
CT
IF
CB

Fig. 34 A section through the anterior third and a small part of the caudal area of step 11 spermatids. A, acrosome; CIR, caudal tube insertion ring; CT, caudal tube; HC, head cap; SL, subacrosomic layer. The asterisk indicates a small ventral fold on the nuclear envelope. The dorsal limit of the marginal fossa is marked by the two lines. (40,000 X)

Fig. 35 The caudal portion of a step 11 spermatid. CIR, caudal tube insertion ring; CT, caudal tube; Fl, flagellum; HC, head cap. Note that the head cap is the only part of the acrosomic system present at this level of the head in step 11. (30,000 X)

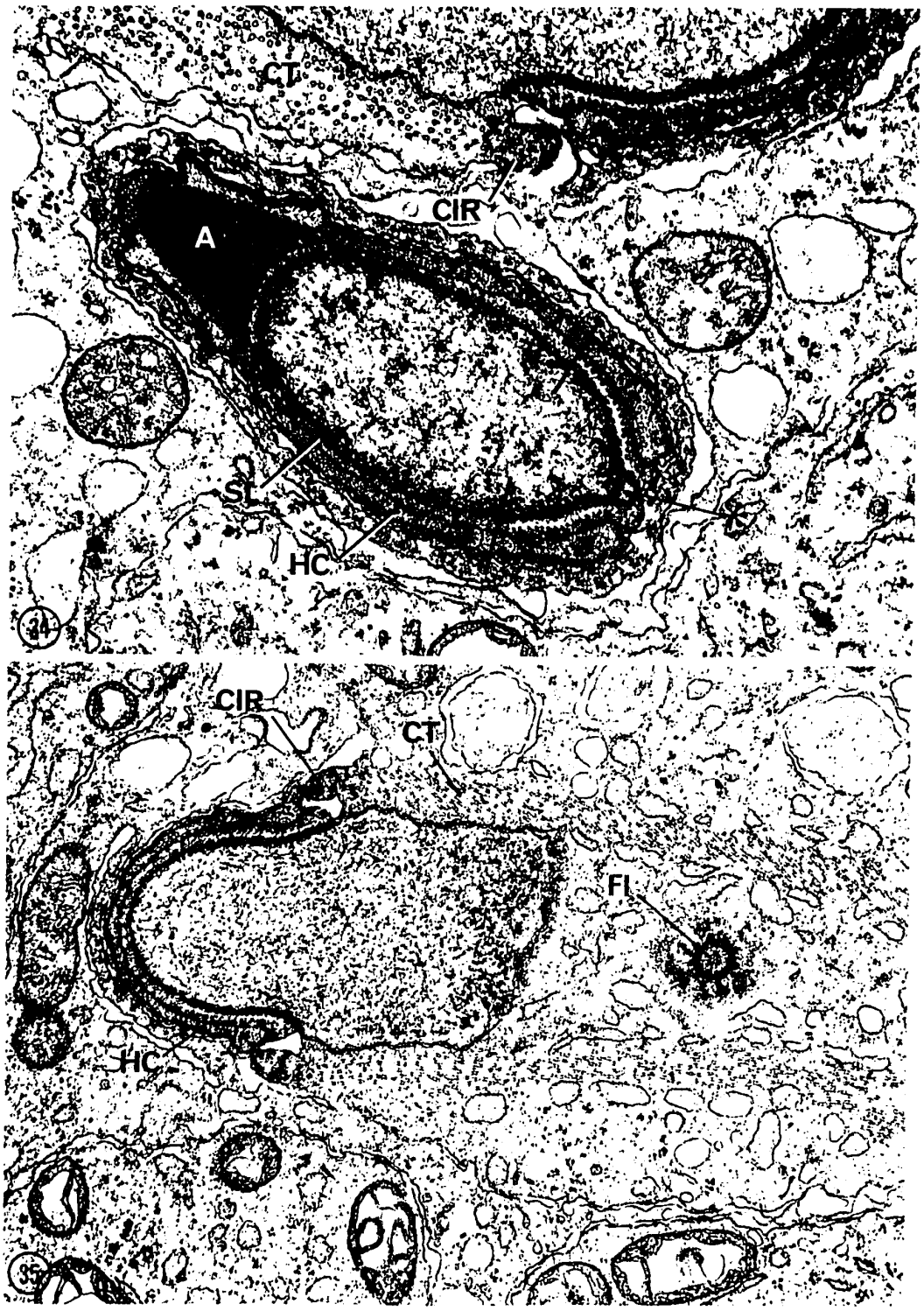
CT
CIR
A
SL
HC
34
CIR
CT
FL
HC
35

Fig. 36 A section through the anterior portion of a step 12-13 spermatid. A, acrosome; ER, endoplasmic reticulum of Sertoli cell; N, nucleus with partly condensed chromatin; NE, nuclear envelope; SF, Sertoli cell filaments; SL, subacrosomic layer. The dorsal limit of the marginal fossa is indicated by two vertical lines. (40,000 X)

Fig. 37 This section through two levels of the head of step 12-13 spermatids illustrates that chromatin condensation is more advanced in the anterior part of the nucleus (a) than in the caudal part (b). The image of the chromatin in figure (b) changes to that of figure (a) as chromatin condensation takes place. The asterisk points out the appearance of the coarse material in the marginal fossa when it is cut tangentially. CIR, caudal tube insertion ring; CT, caudal tube. (30,000 X)

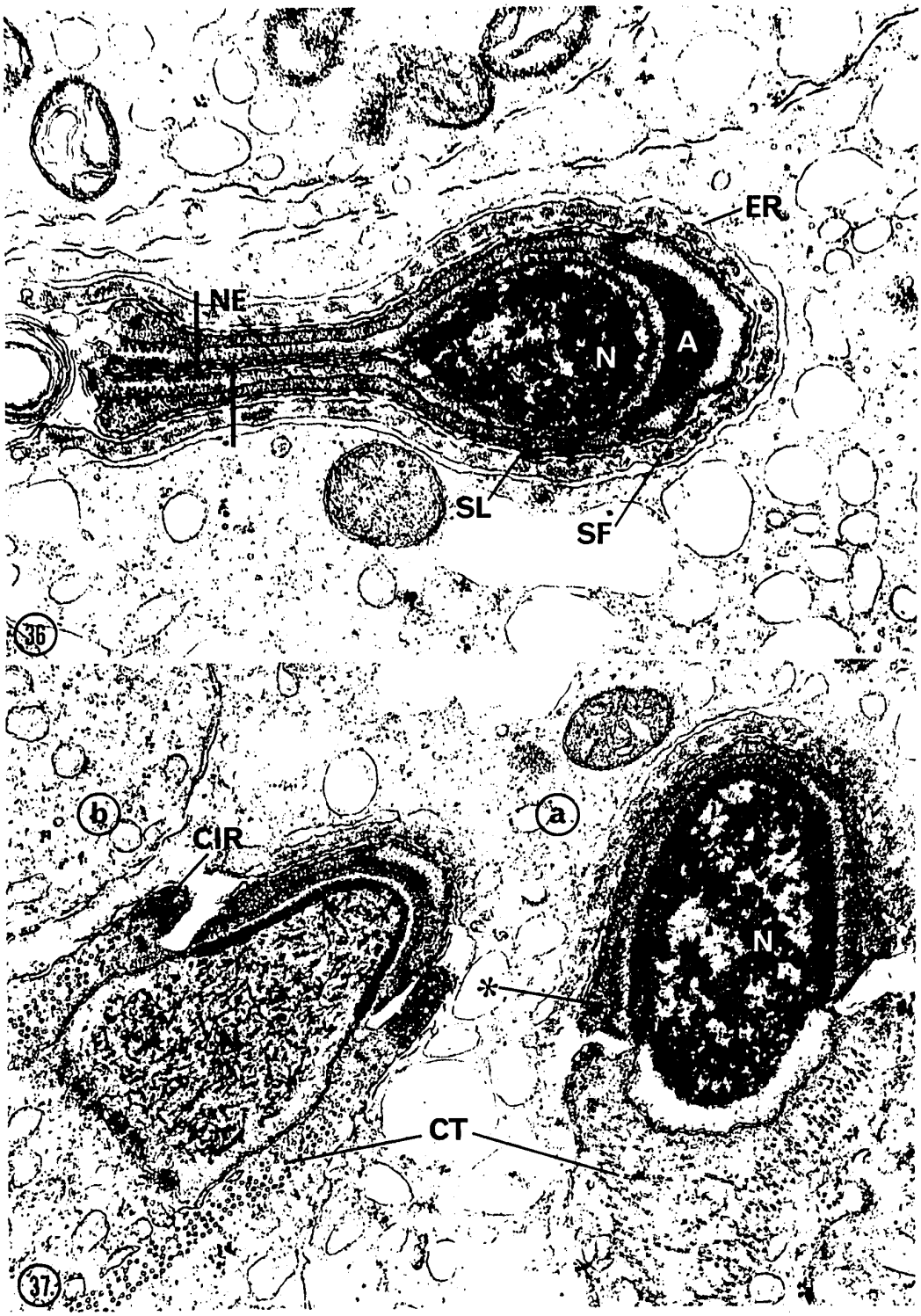
ER
NE
N
A
SL
SF
36
b
CIR
a
N
*
CT
37

Fig. 38 Sections through two spermatids in steps 12-13. Figure (a) is more anterior in the head than figure (b) and the chromatin is slightly more condensed. The arrows point to a finely granular dense layer between the nuclear envelope and the caudal tube. The asterisks indicate an area of low density in the nucleus between the condensing chromatin and the nuclear membrane. Compare with Figure 40. A, acrosome; CIR, caudal tube insertion ring. (30,000 X)

Fig. 39 A section through the implantation fossa and the caudal tube (CT) of a step 14 spermatid. An, annulus; Fl, flagellum; PC, proximal centriole. The nuclear pores (NP) are on the caudal surface of the head which projects over the flagellum. The asterisk indicates the area of low electron density in the nucleus adjacent to the nuclear pores. (30,000 X)

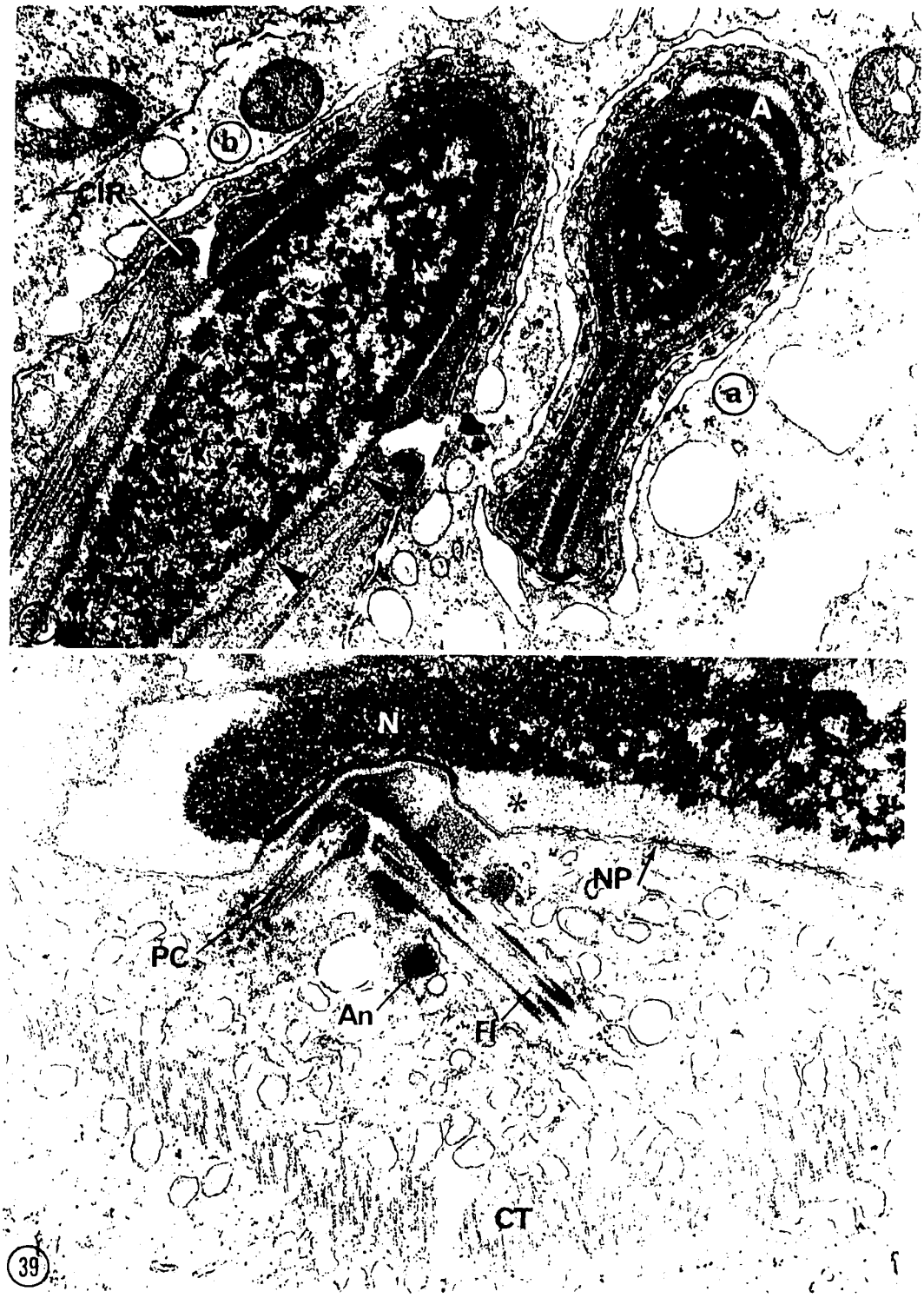
b
CIR
A
a
N
*
NP
PC
An
Fl
CT
39

Fig. 40 A longitudinal section through the caudal half of the head of a step 12-13 spermatid. Chromatin condensation is more advanced in the anterior part of the nucleus than it is in the caudal region of the nucleus. The asterisk is over an area of the nucleus of low electron density adjacent to the caudal tube (CT) (see Figure 38b). A similar area adjacent to the nuclear pores on the caudal surface is not as prominent as it is in the comparable area of the step 14 spermatid (compare with Figure 39). An, annulus; Fl, flagellum; HC, head cap; PC, proximal centriole with centriolar adjunct; SL, subacrosomic layer. (19,500 X)

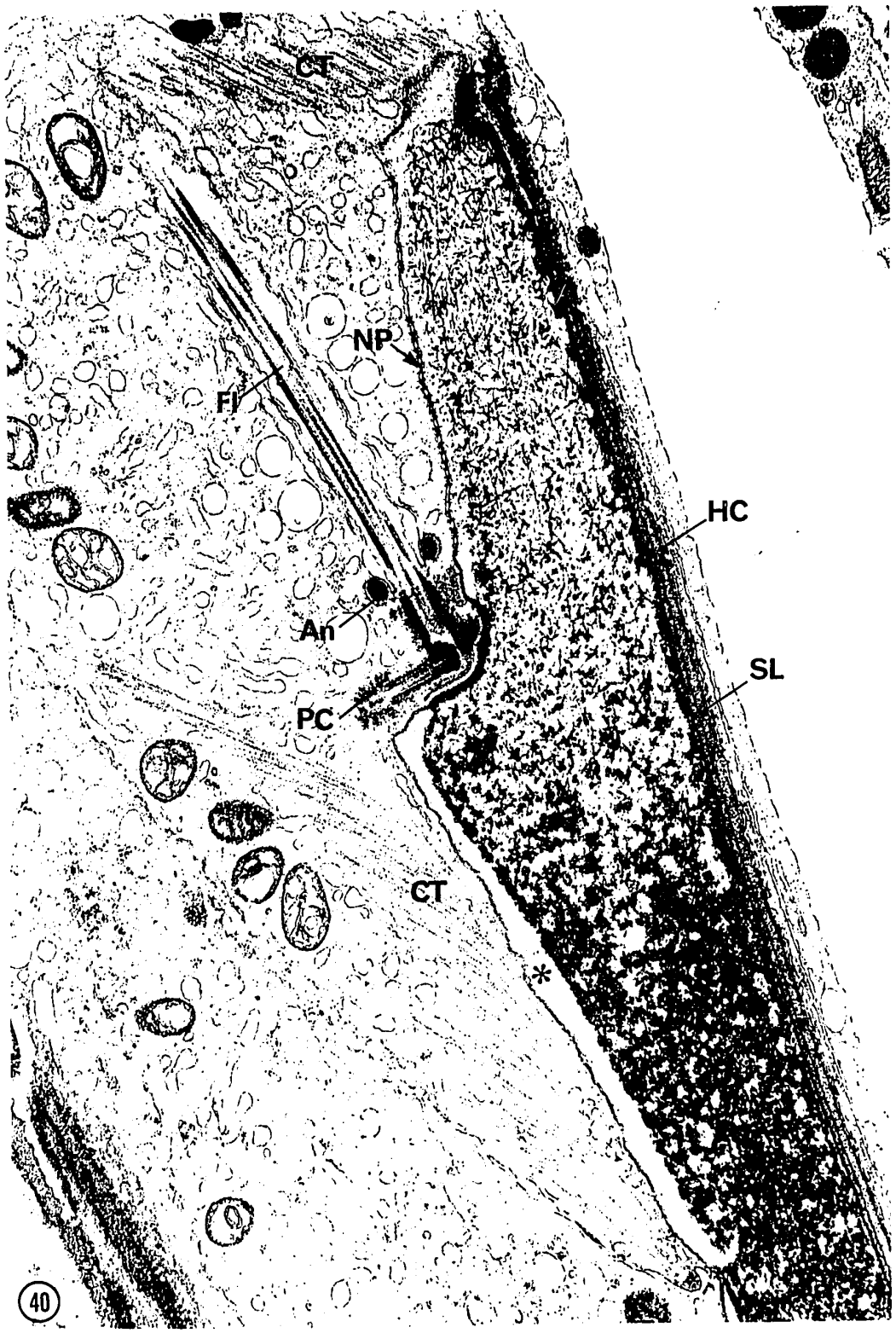
CT
NP
Fl
HC
An
SL
PC
CT
*
40

Figs. 41, 42 Cross sections through the caudal part of the head of step 12-13 spermatids. Figure 41 is a little more anterior than Figure 42 and shows a portion of head cap (HC). Note the abundance of smooth-surfaced vesicles around the flagellum (Fl) within the caudal tube (CT). CIR, caudal tube insertion ring; N, nucleus; NP, nuclear pore. (30,000 X)

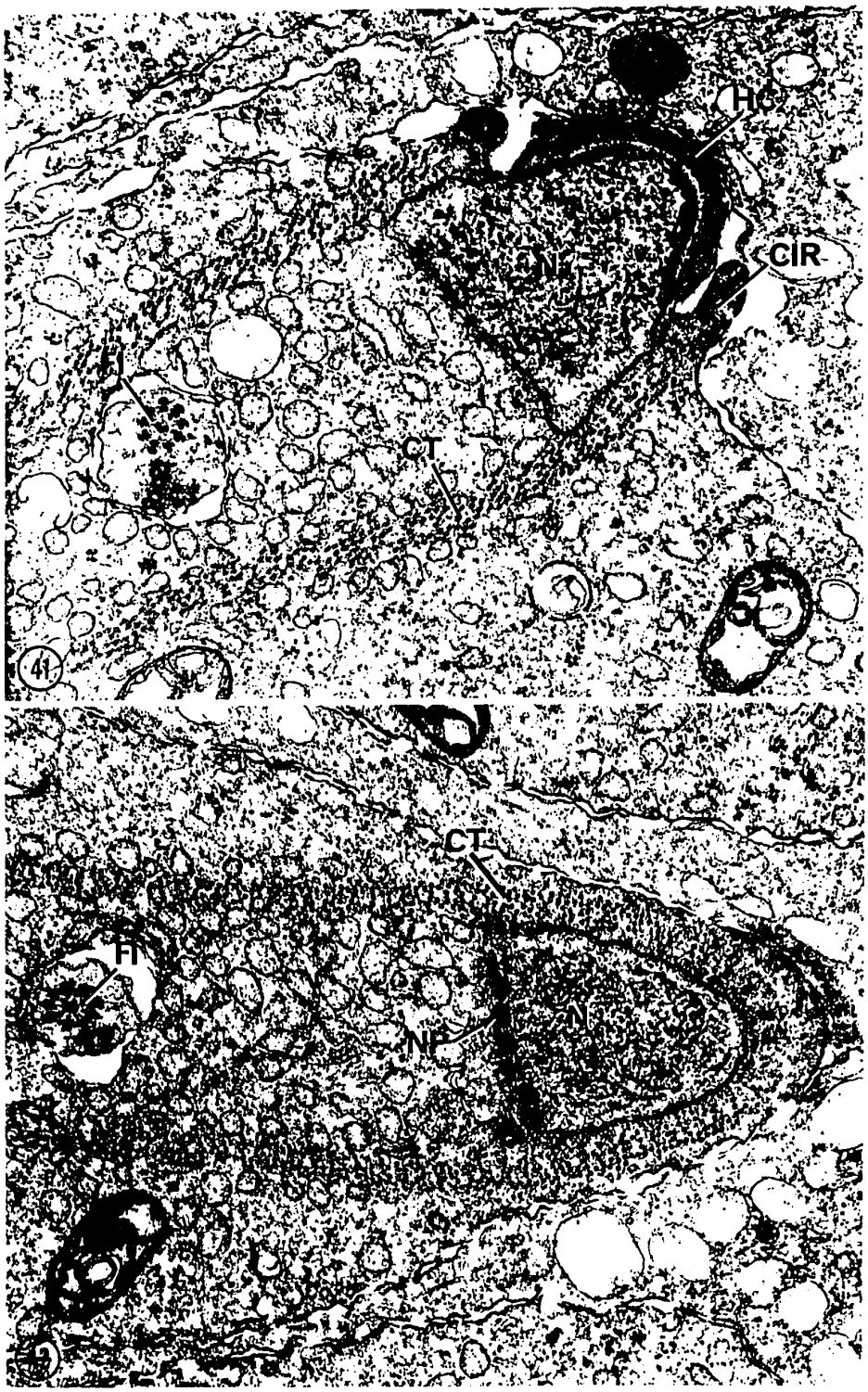
HC
CIR
NF
CT
41
CT
FI
NF
N

Fig. 43 A longitudinal section through the head of a step 15 spermatid. The superfluous nuclear envelope (NE) in the anterior part of the head projects ventrally. The caudal tube is less prominent at this step of development and only the anterior region of the caudal tube insertion ring (CIR) appears in this section. Note the numerous nuclear vacuoles in the chromatin. Coarse electron dense granules are seen in the neck region of the flagellum (arrow). A, acrosome; P, nuclear protrusion; PC, proximal centriole; SF, Sertoli cell filaments. (15,000 X)

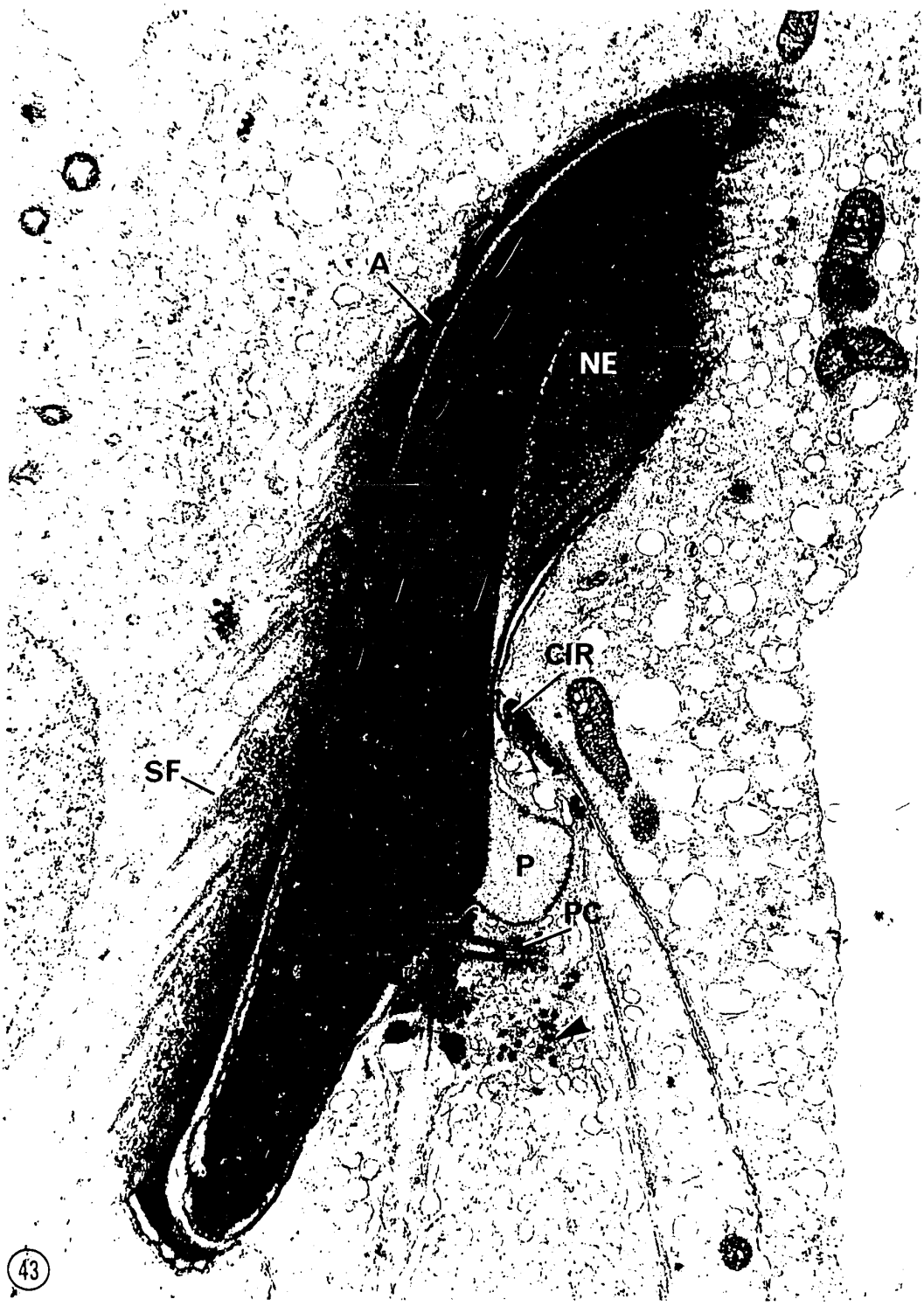

43

Figs. 44-47 Cross sections through the anterior portion of the head of step 15 (Figures 44, 45, 47) and step 16 (Figure 46) spermatids. Figure 44 is slightly more anterior in the head than Figure 45 which, in turn, is anterior to Figure 47. Figure 46 is at the same level of the head as Figure 45 but at a later step of development. Figure 47 is at the anterior limit of the acrosome just posterior to the fissure which separates the ventral head cap from the remainder of the head cap. A, acrosome; F, filaments; HC, head cap; NE, superfluous nuclear envelope; SL, subacrosomic layer; VHC, ventral head cap. (40,000 X)

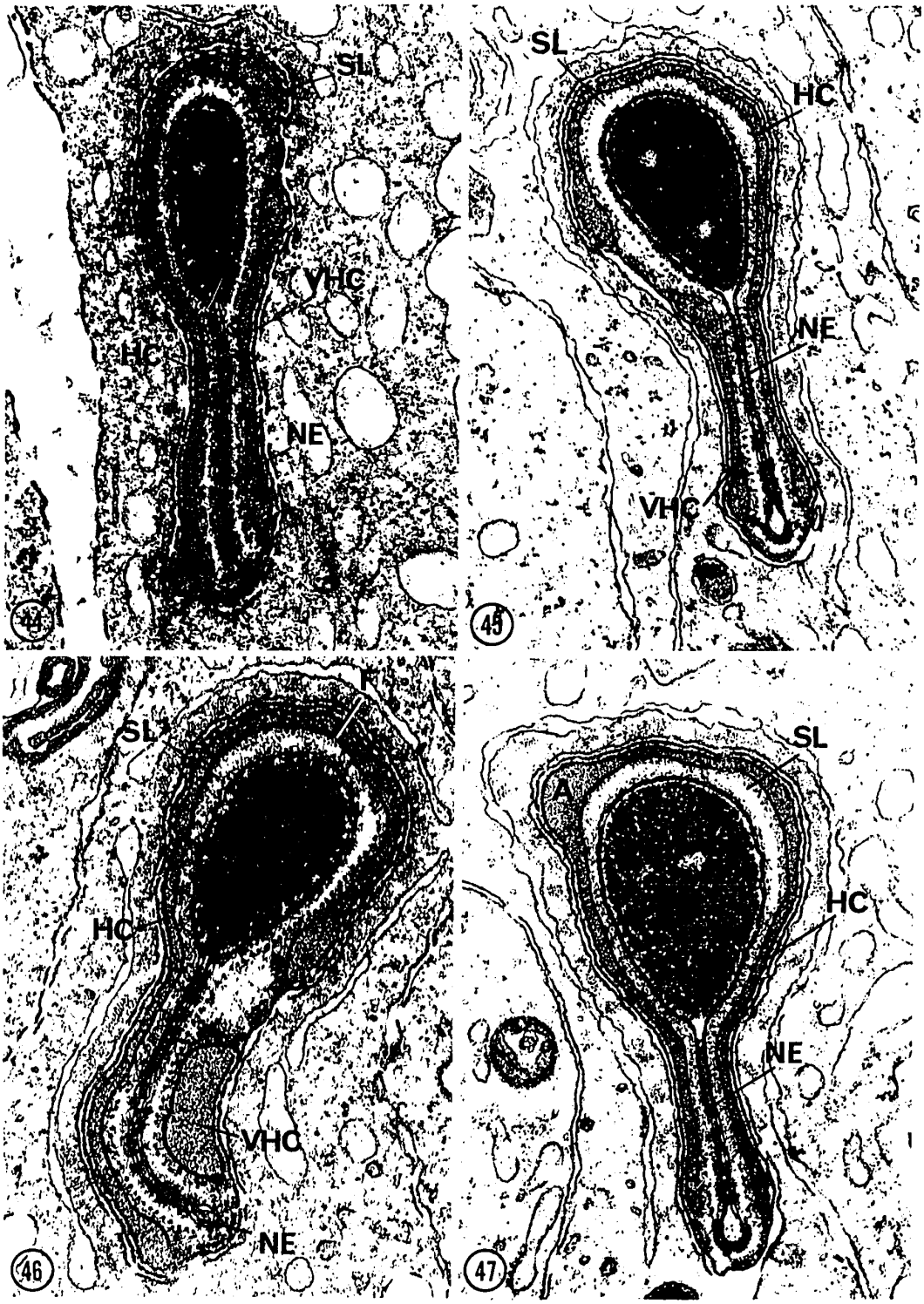
SL
VHC
HC
NE
44
SL
HC
NE
VHC
45
SL
HC
VHC
NE
46
SL
HC
NE
47

Fig. 48 Step 15 spermatids cut atvtwo levels of the head: (a) immediately posterior to the level of the head shown in Figure 47 and (b) immediately anterior to the implantation fossa. The arrows point out areas of increased electron density in the layer on the ventral and lateral surfaces of the head which is continuous with the subacrosomic layer (SL). The caudal tube insertion ring (CIR) is becoming detached from the head and is more spongy and granular than in the previous steps. A, acrosome; HC, head cap; P, nuclear protrusion. (30,000 X)

Fig. 49 A section of a step 17 spermatid through the connecting piece of the flagellum showing the arrangement of the nuclear protrusions(P) in this area. There are materials of different densities in the protrusions. Note the large granules around the flagellum. A, acrosome; CIR, caudal tube insertion ring; HC, head cap; SL, subacrosomic layer. (30,000 X)

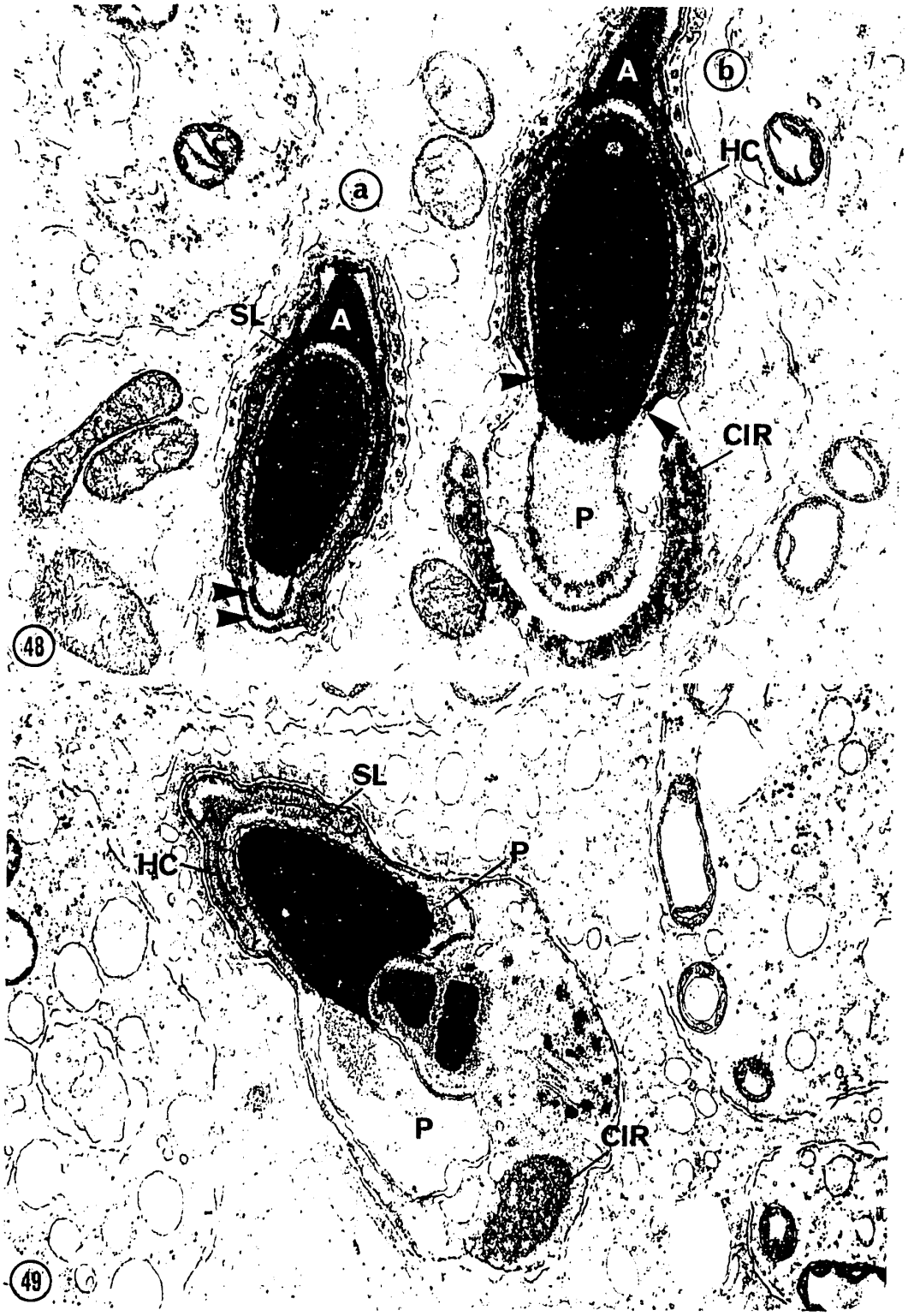
a
b
A
HC
SL
A
CIR
P
48
SL
HC
P
P
CIR
49

Fig. 50 A longitudinal section of the caudal part of the step 15 spermatid head. The porous caudal surface of the nucleus of the step 14 spermatid seen in Figure 39 is no longer present. The arrows point to a dense granular layer against the nuclear envelope of the caudal surface. The subacrosomic layer (SL) has a fibrous appearance in this section. Many areas of low electron density are present in the condensing chromatin. An, annulus; CIR, caudal tube insertion ring; Fl, flagellum; NP, nuclear pore; P, nuclear protrusion; SF, Sertoli cell filaments. (30,000 X)

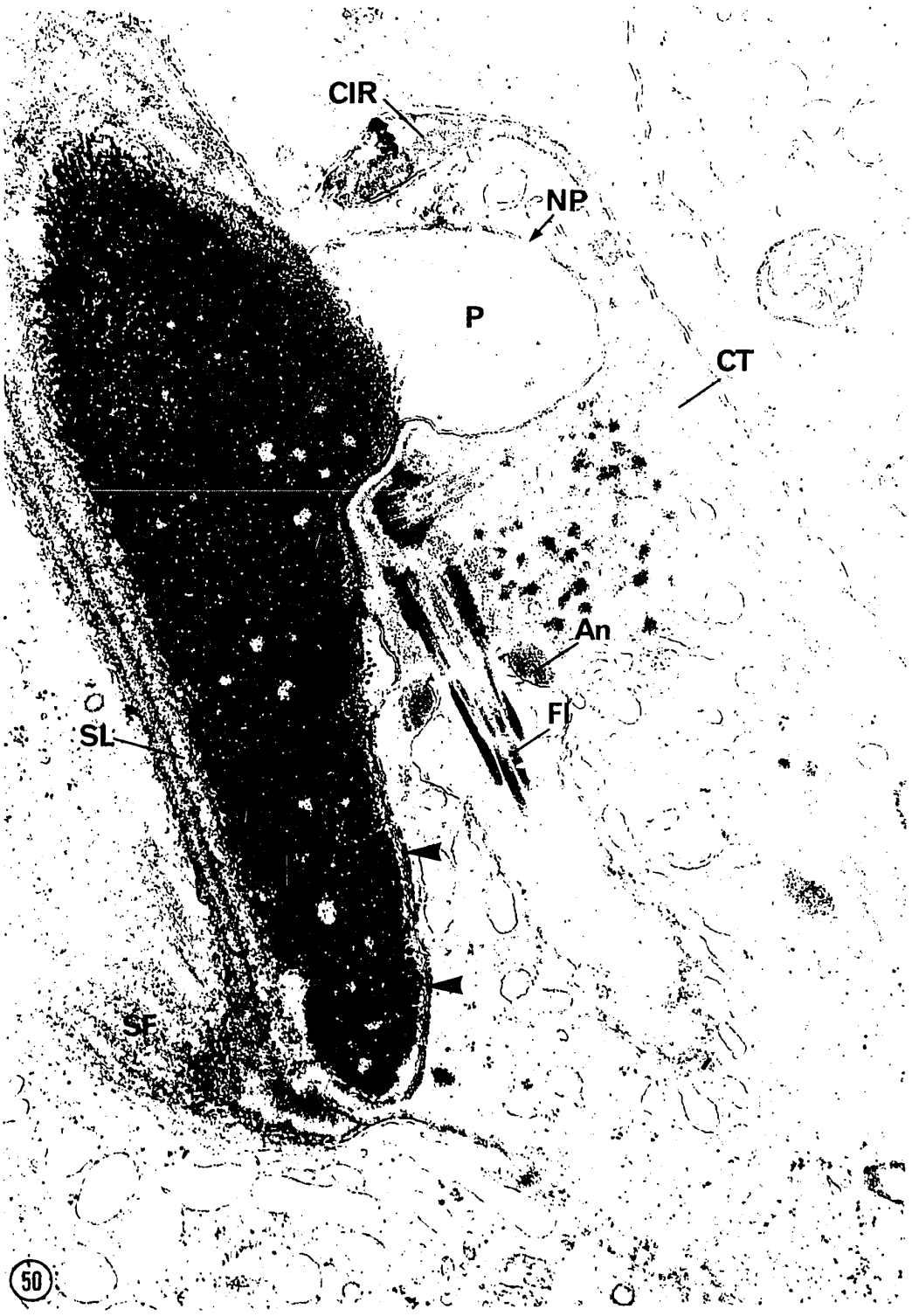
CIR
NP
P
CT
An
Fl
SL
SF
50

Fig. 51 The implantation fossa region of a step 15 spermatid showing two sections through the nuclear protrusion (P). Note the fibrous appearance of the subacrosomic layer (SL). BP, basal plate; CT, caudal tube; PC, proximal centriole. (45,000 X)

Fig. 52 A cross section at the implantation fossa of a step 15 spermatid. The arrows point to the dense layers of granular material against the nuclear envelope and the plasma membrane. The increased height of the acrosome (A) in this section is normal for this region of a step 15 spermatid (see drawing in Figure 2). P, nuclear protrusion; SL, subacrosomic layer. (45,000 X)

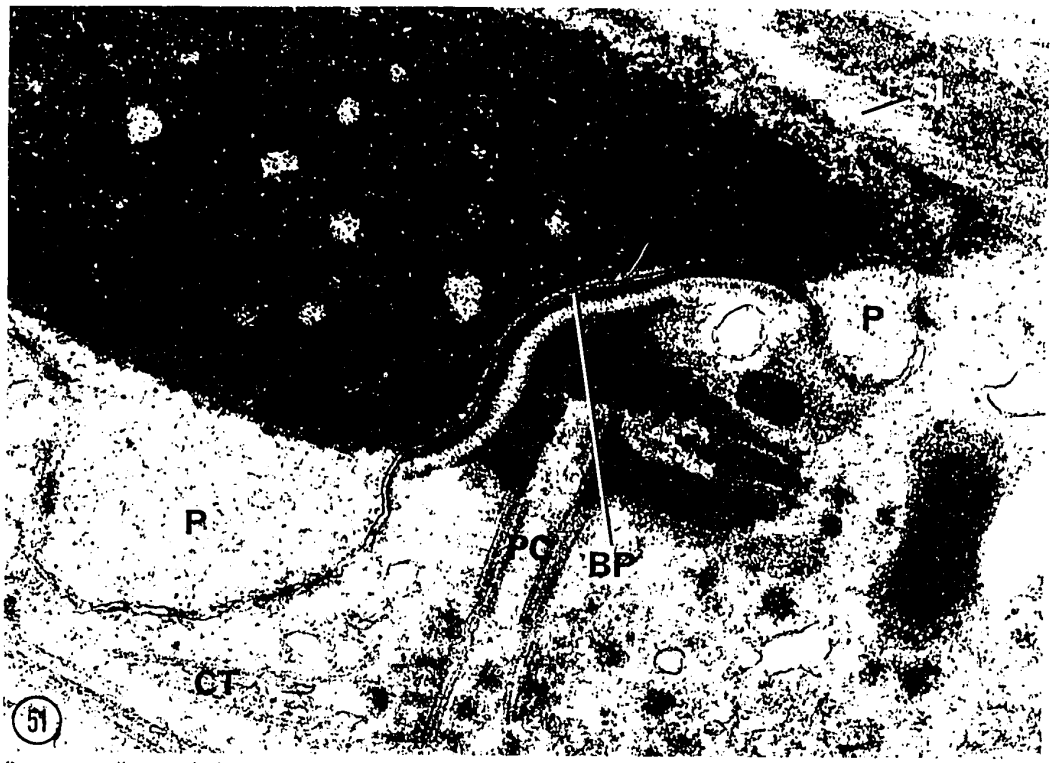
P
P
PC
BP
CT
51

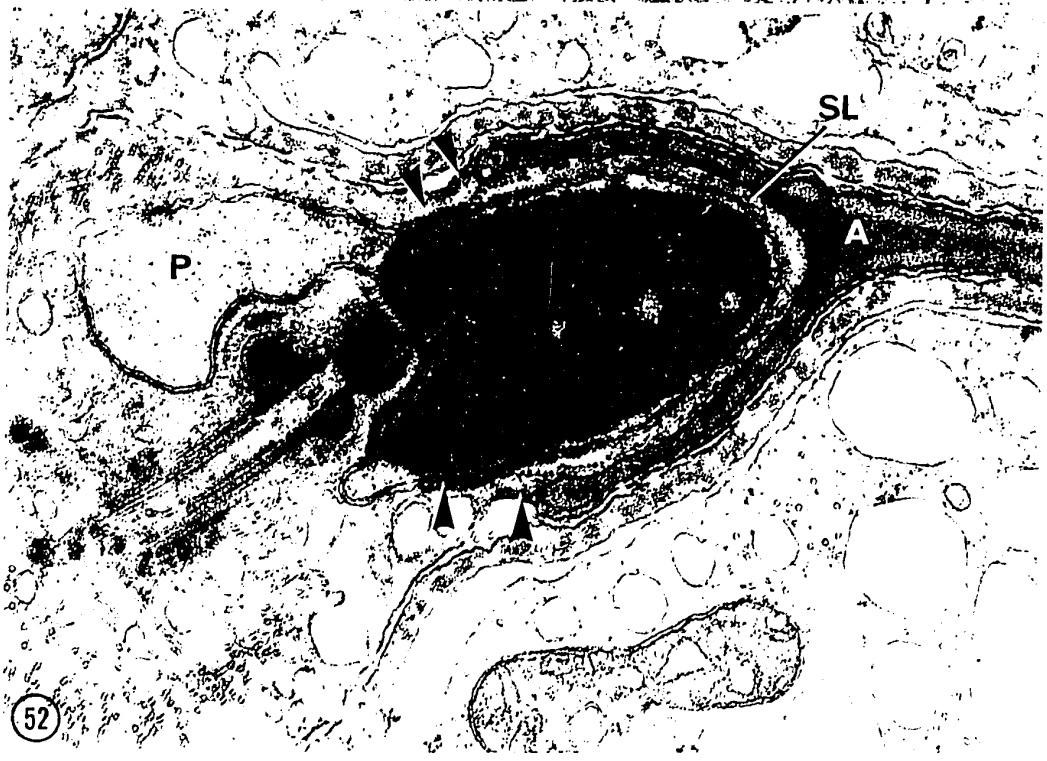
SL
A
P
52

Fig. 53 Sections through various levels of the head of step 17 spermatids. The two sections at the top are from the apical third of the spermatids, the middle section goes through the mid-portion of a spermatid and the lower section goes through the caudal third of the spermatid. These sections demonstrate the triangular shape of the anterior part of the head in this step. A space continuous with the subacrosomic layer is present around and anterior to the tip of the nucleus. A, acrosome; Fl, flagellum; HC, head cap; P, nuclear protrusion; SL, subacrosomic layer; VHC, ventral head cap. (25,000 X)

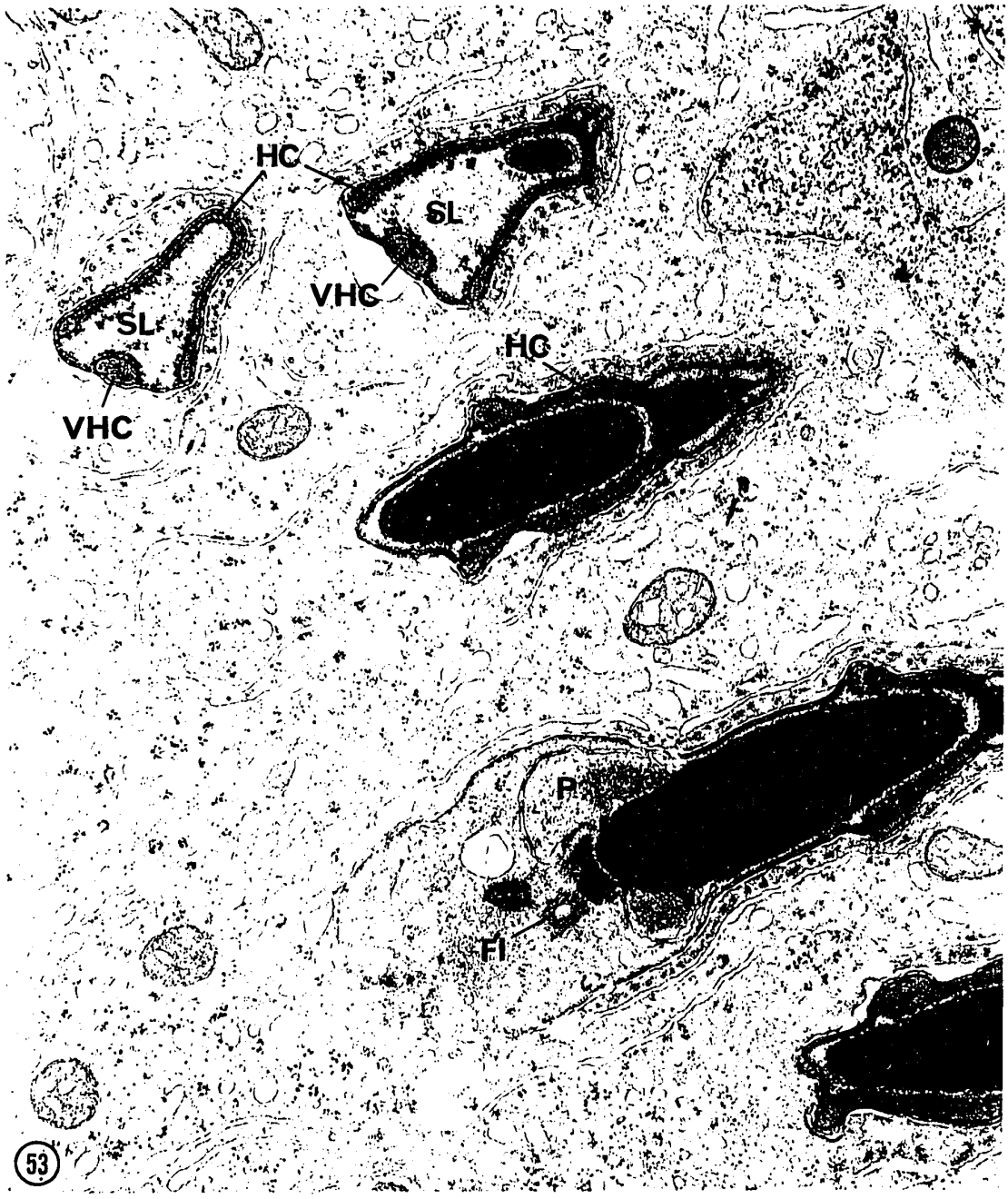
HC
SL
VHC
SL
VHC
HC
P
Fl
53

Figs. 54-57 Cross sections through the anterior triangular portion of the head of step 17 spermatids. The superfluous nuclear envelope (NE) undergoes degenerative changes as indicated by the myelin figures seen close to (Figures 55, 56) or associated with the nuclear membrane (Figure 57). Note that the subacrosomic layer (SL) has an area of increased density along the inner acrosomic and plasma membrane. A, acrosome; HC, head cap; N, nucleus; VHC, ventral head cap. (Figure 54: 30,000 X; Figures 55-57: 20,000 X)

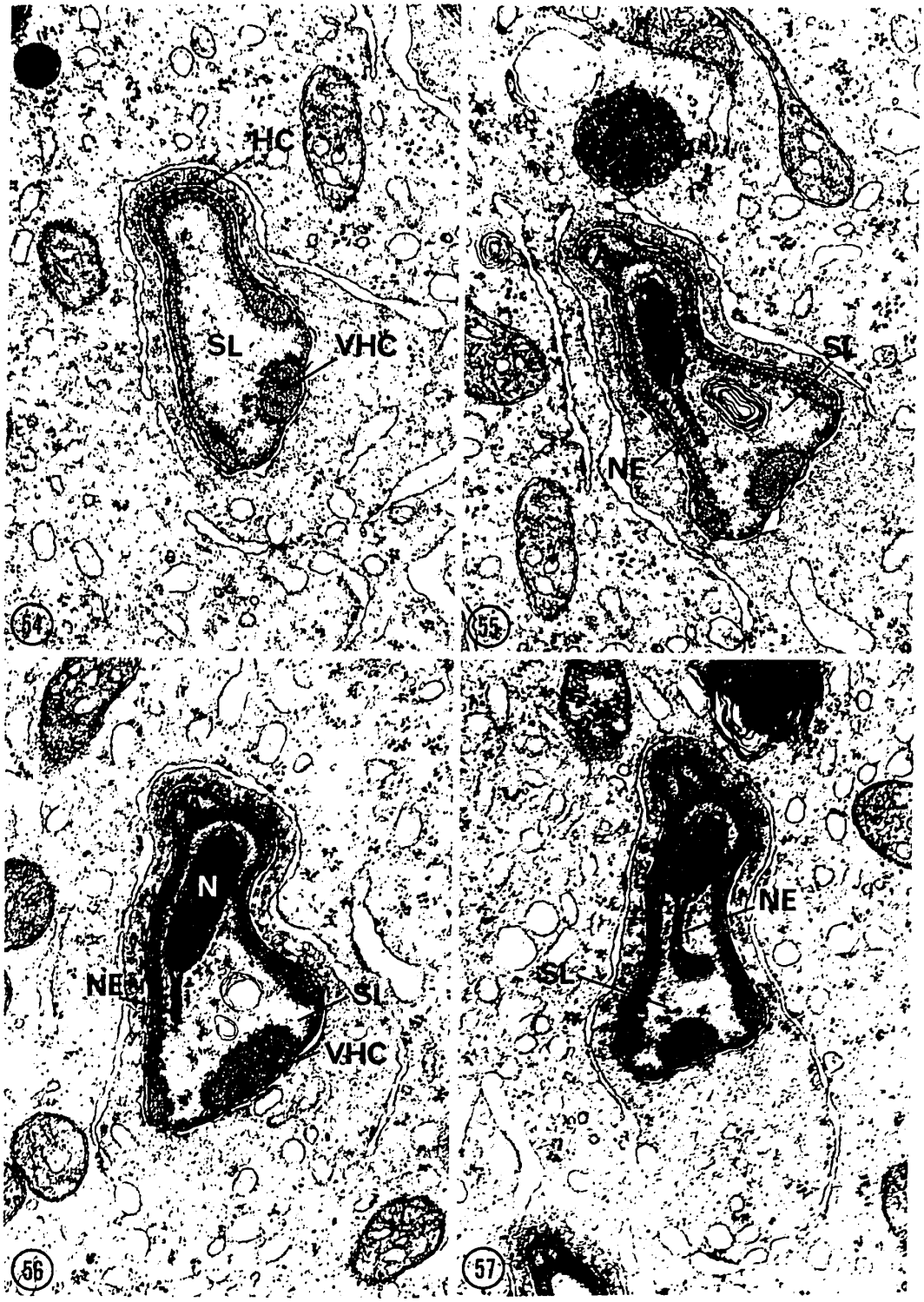
HC
SL
VHC
54
SL
NE
55
N
NE
SL
VHC
56
NE
SL
57

Figs. 58, 59 Sections through the middle portions of the head of step 17 spermatids. The acrosome (A) is very prominent in this region. The layer of material, which surrounds the nucleus ventral to the head cap, shows an area of increased density against the nuclear envelope and against the plasma membrane (arrows). A small nuclear protrusion (P), without pores, is sometimes present in this region. HC, head cap; SL, subacrosomic layer. (40,000 X)

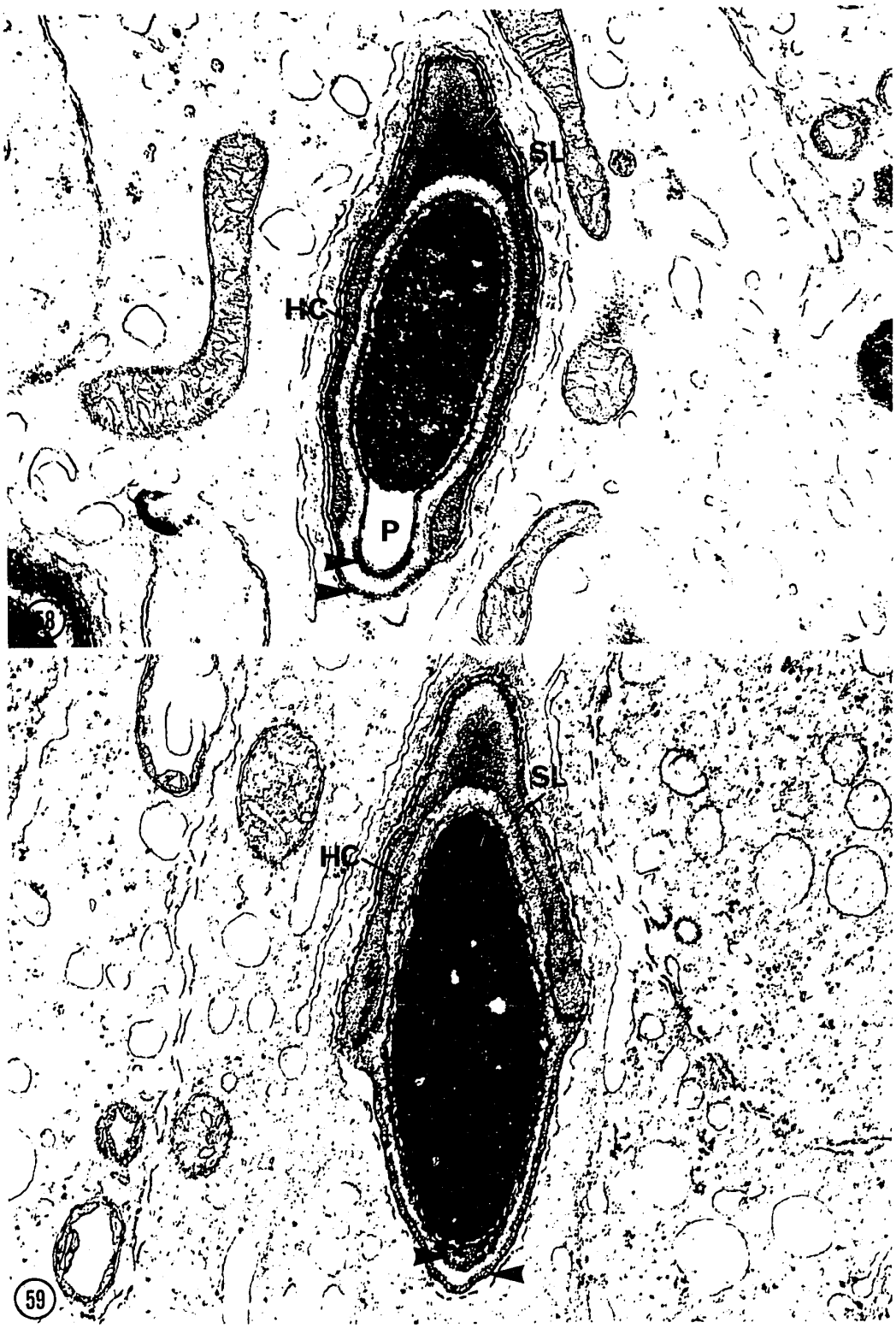
SL
HC
P
58
SL
HC
59

Fig. 60 This section of a step 17 spermatid is at the level just anterior to the implantation fossa and shows the large nuclear protrusion (P) in this area. Note that the nuclear protrusion contains nuclear material of varying densities. Nuclear pores, although indistinct in this section, are present in the protruded nuclear membrane. Note also that the subacrosomic layer plus the layer on the lateral surface of the head ventral to the head cap are continuous with the spermatid cytoplasm. The protruded nuclear envelope degenerates into myelin type figures (asterisk) which are commonly seen in this step of development. A, acrosome; CIR, remnant of caudal tube insertion ring; HC, head cap; SL, subacrosomic layer. (45,000 X)

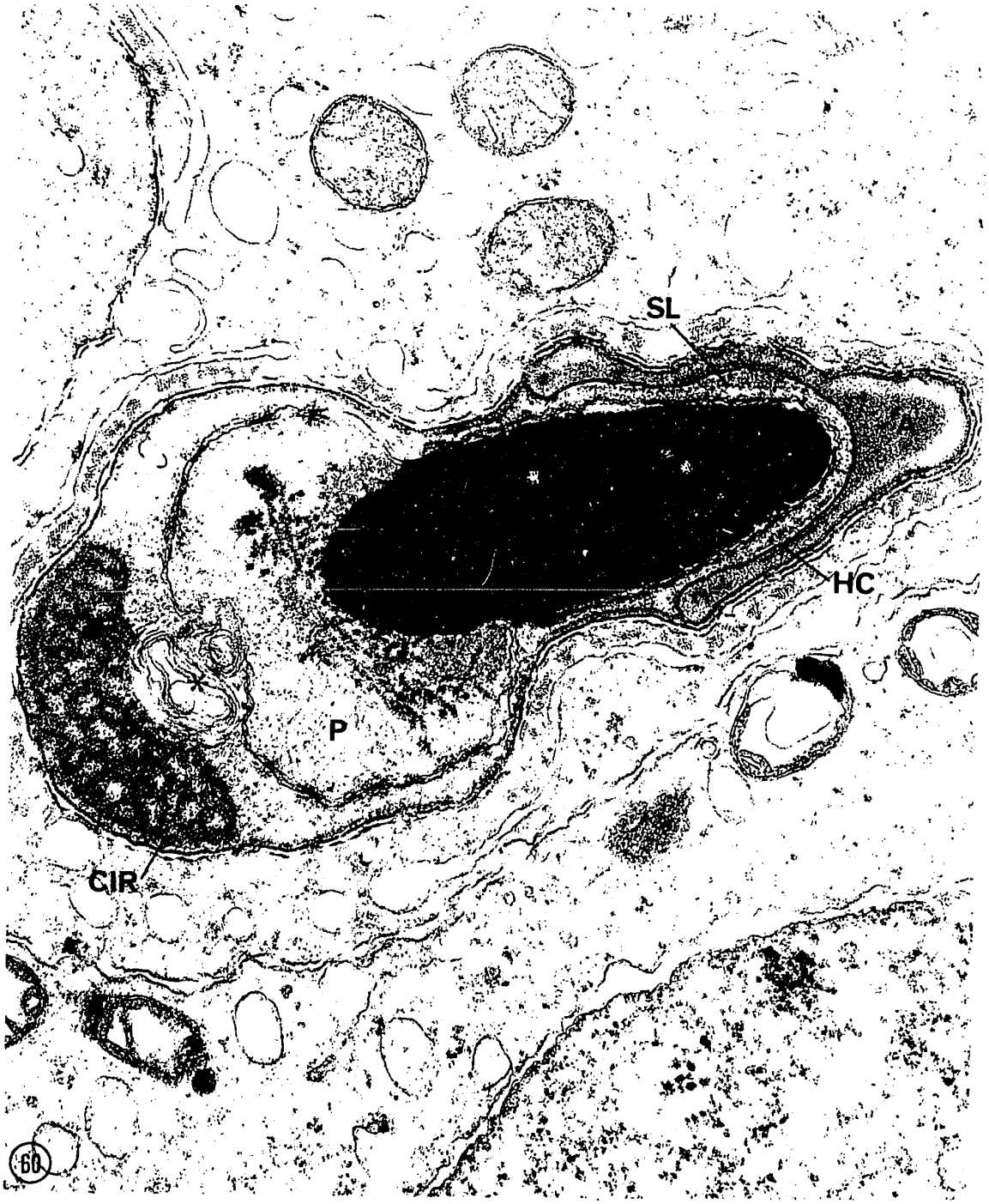
SL
HC
P
CIR
60

Fig. 61 A section through the head of a step 17 spermatid anterior to the insertion of the flagellum. The large nuclear protrusion (P) contains nuclear pores (NP). The granules of chromatin in this spermatid nucleus have fused to form a homogeneous dense mass containing some vacuoles. Some cross sections through the microtubules (M) of the caudal tube are still present along with a remnant of the caudal tube insertion ring (CIR). Fl, flagellum of an adjacent step 17 spermatid. (45,000 X)

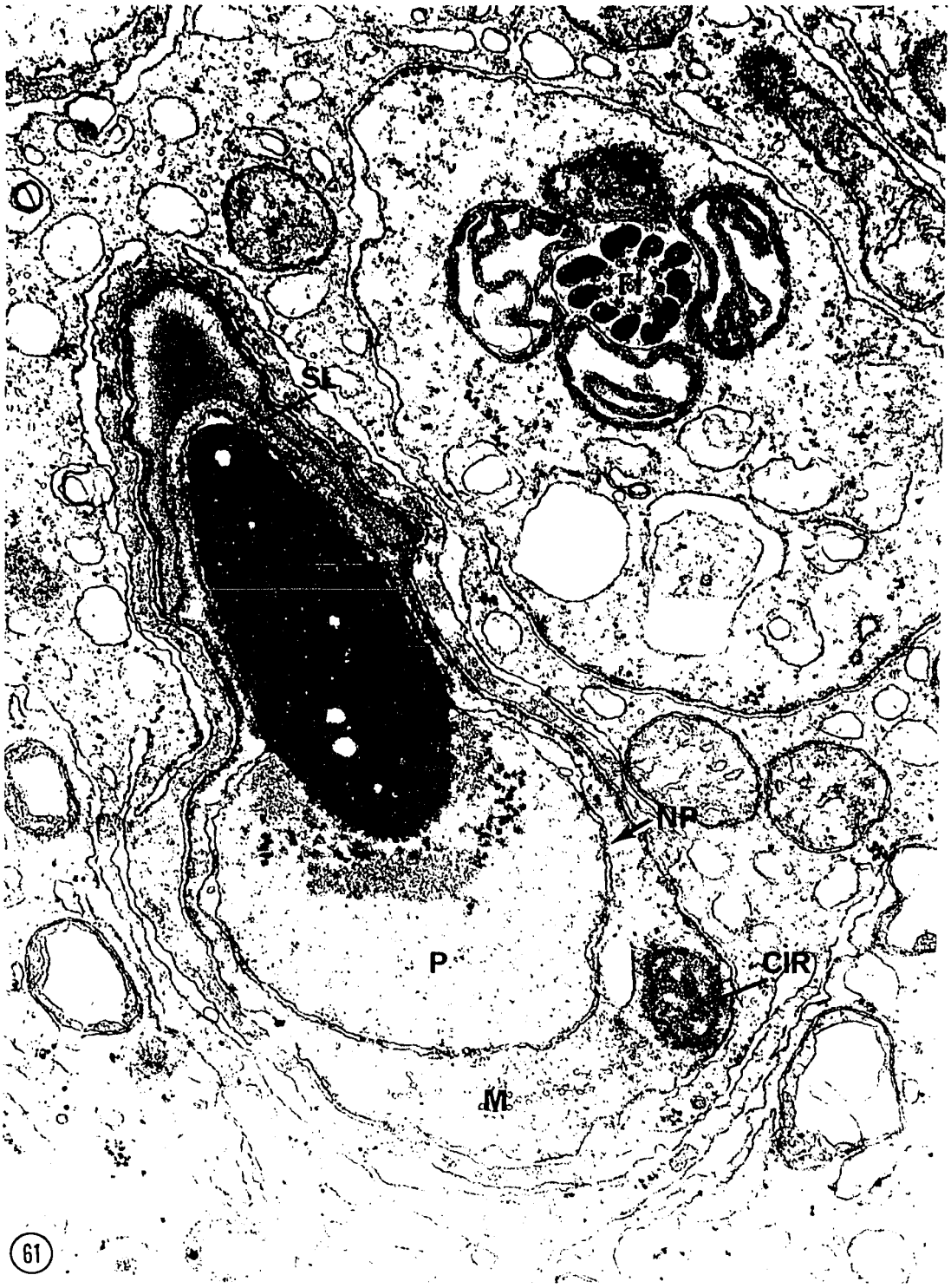

61

Fig. 62 A cross section through the caudal part of a step 17 spermatid showing a section of the caudal part of the nucleus and middle piece of the flagellum (Fl). Three components of the perinuclear theca can be seen on this section: (1) the subacrosomic layer (SL), (2) the layer on the lateral surface of the head ventral to the head cap (asterisk); this layer was covered by caudal tube earlier in spermiogenesis, and (3) the layer against the caudal surface of the nucleus (arrow) which was never covered by acrosomic system or caudal tube. (45,000 X)

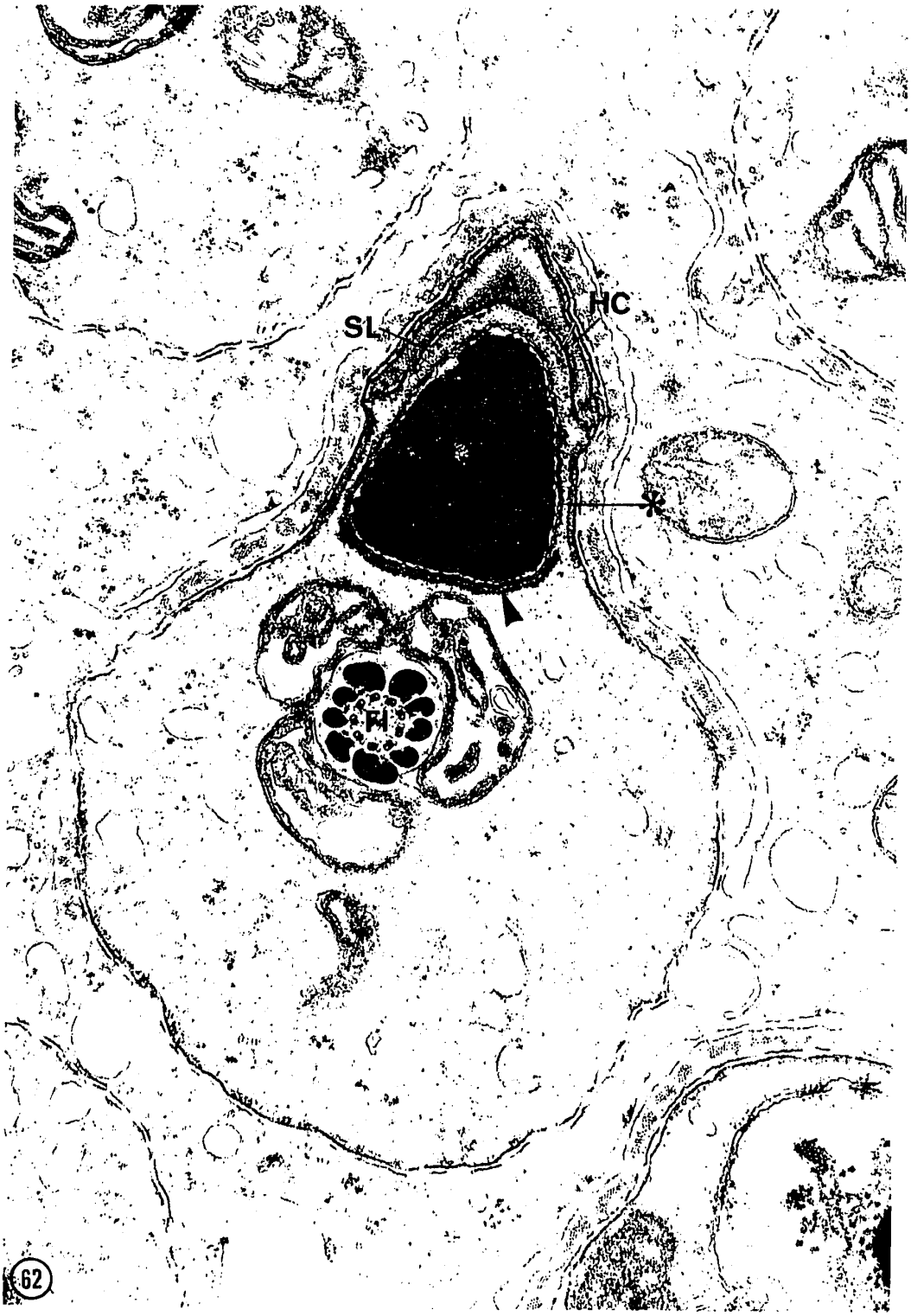

62

Fig. 63 A section through the anterior tip of the head of an early step 19 spermatid. The subacrosomic material increases in density and takes the appearance of the perinuclear theca (PT) of the fully formed spermatid. Double walled tubules (T) are seen in the Sertoli cell cytoplasm (SC). (40,000 X)

Fig. 64 A section through the mid-portion of the head of an early step 19 spermatid. The chromatin of the nucleus (N) is a fully condensed homogeneous mass. A tubule (T) in the Sertoli cell cytoplasm (SC) is associated with the spermatid. A, acrosome; HC, head cap; PT, perinuclear theca. (40,000 X)

Fig. 65 A section through the anterior triangular part of the head of an early step 19 spermatid showing the associated Sertoli cell. Microtubules (M) and tubules (T) are present in the cytoplasm of the Sertoli cell. PT, perinuclear theca; SC, Sertoli cell cytoplasm. (40,000 X)


PT
T
SC
63

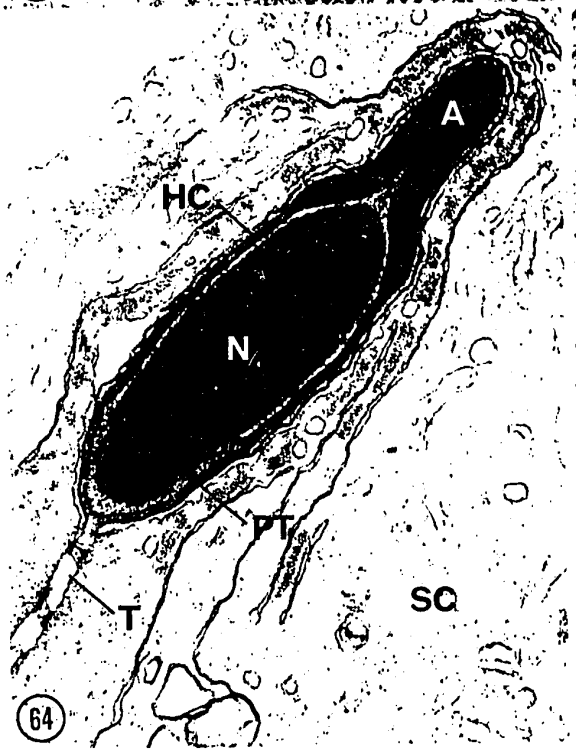
A
HC
N
PT
T
SC
64

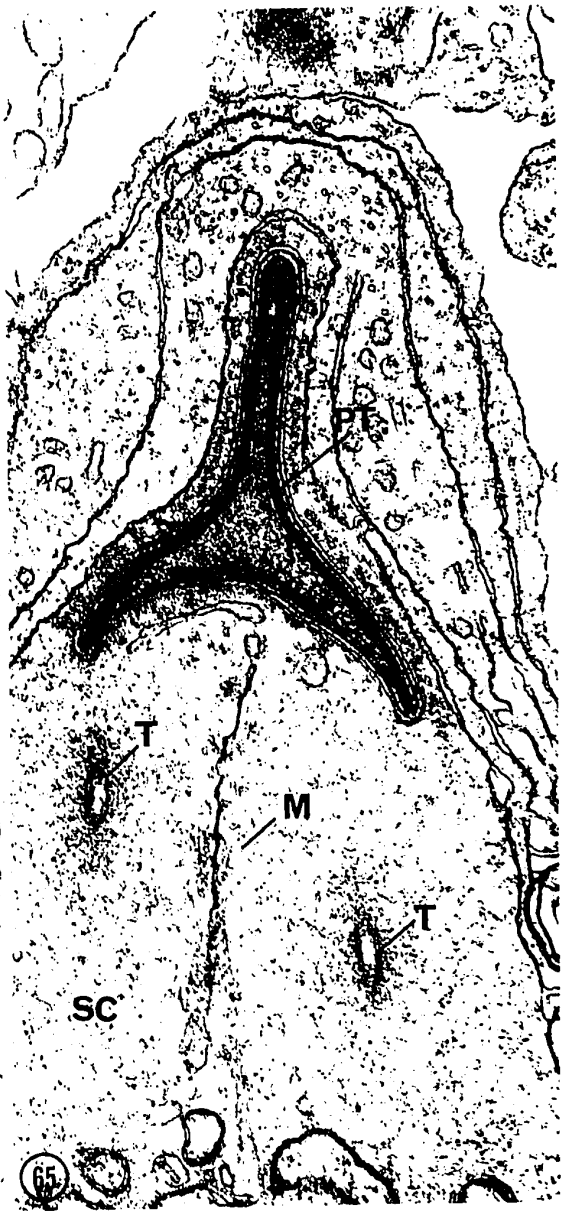
PT
T
M
T
SC
65

Figs. 66-69 Sections through various levels of the head of early step 19 spermatids. The nuclear chromatin has condensed to a homogeneous mass in all spermatids by this step of development. Many areas of rarefactions are seen in the chromatin. The material surrounding the nucleus has not yet condensed completely into the dense granular material that forms the perinuclear theca (PT). In Figures 68 and 69 there are some areas of the perinuclear theca that are more electron dense than others. The ventral spur (VS) becomes recognizable at this step of development. The nuclear protrusion (P) in the area of the implantation fossa contains some coarse granular nuclear material. A, acrosome; HC, head cap; NP, nuclear pore; VHC, ventral head cap. (Figures 66 and 67: 40,000 X; Figures 68 and 69: 30,000 X)

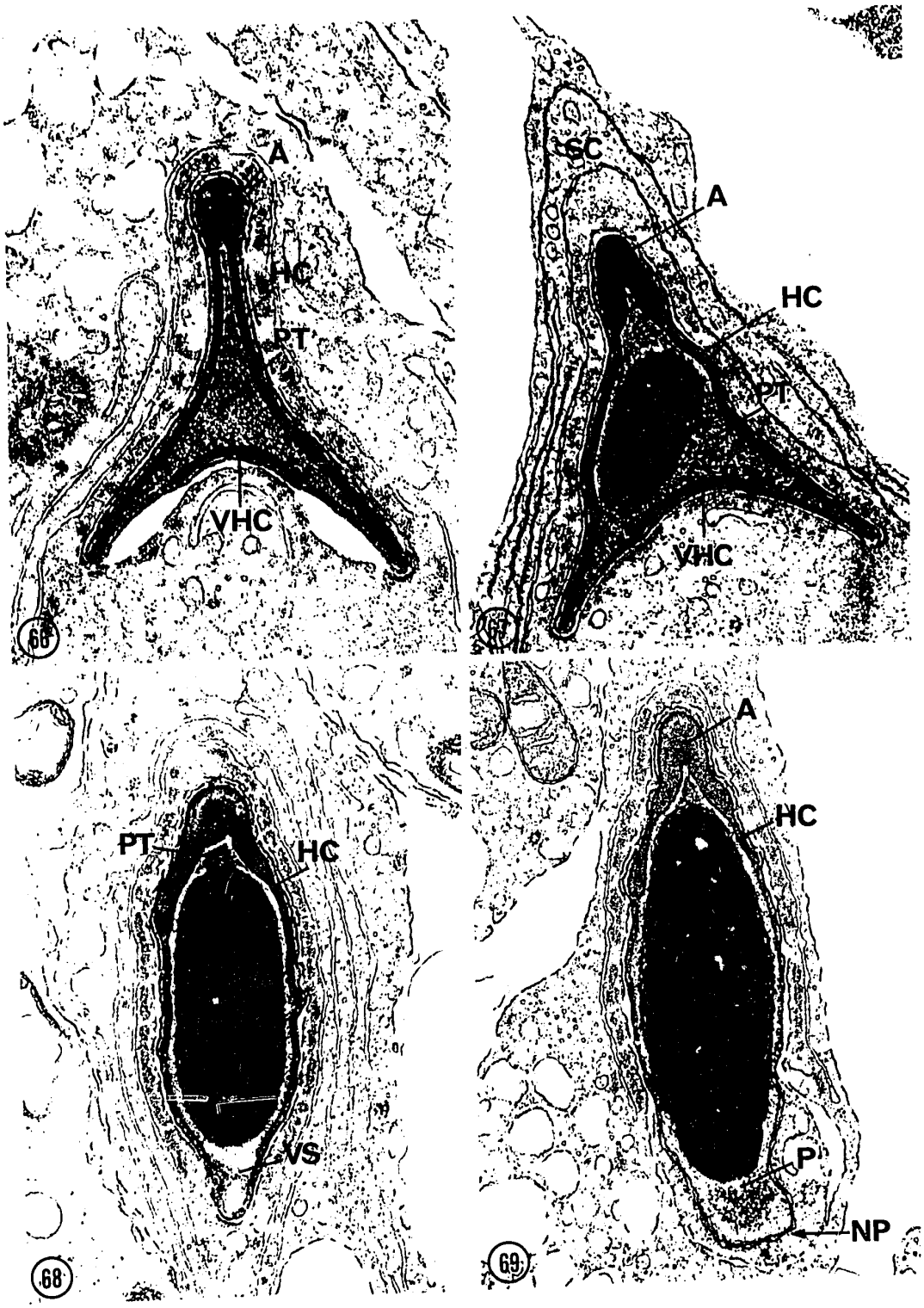
A
HC
PT
VHC
68
SC
A
HC
PT
VHC
PT
HC
VS
68
A
HC
P
NP
69

Figs. 70-72 Sections through the mid and caudal regions of the step 19 spermatid. The Sertoli cell cytoplasm (SC) is beginning to dissociate from the head of the spermatid. The perinuclear theca (PT) is more condensed than in Figures 66-69. Residual cytoplasm of the spermatid is present around the nuclear protrusion (P) and the flagellum (Fl). A, acrosome; HC, head cap. (40,000 X)

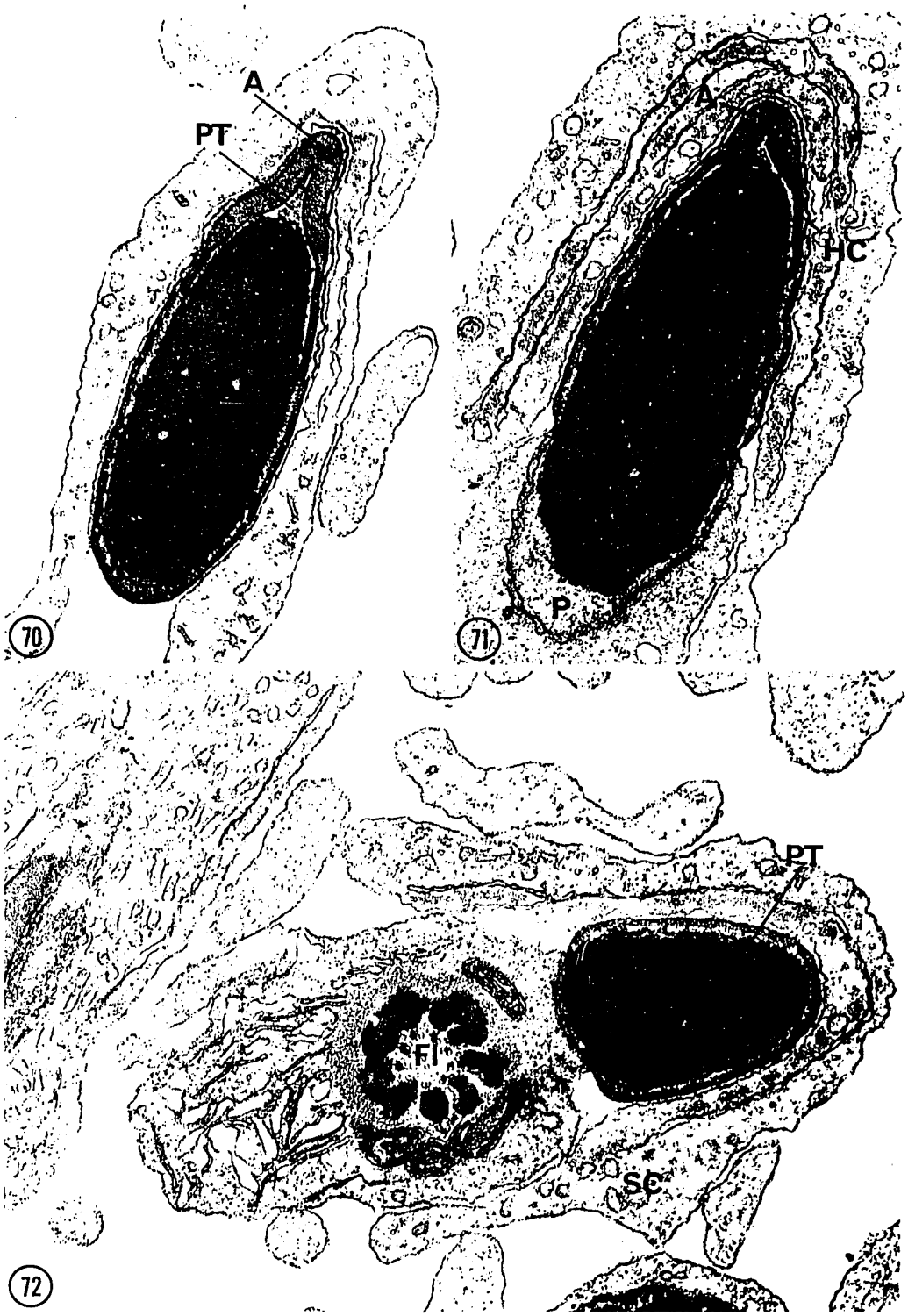
A
PT
70
A
HC
P
71
PT
Fl
SC
72

Figs. 73-76 Sections of late step 19 spermatids at the point of being released into the lumen of the seminiferous tubule as spermatozoa. The acrosomic system is similar in appearance to that of caput epididymal spermatozoa. The perinuclear theca (PT) is similar in appearance and density to that of a mature spermatozoon. Two different densities of the perinuclear theca can be seen in the ventral spur (VS) in Figure 74. Streamers of Sertoli cell cytoplasm (SC) are still attached to some areas of the spermatid. A, acrosome; HC, head cap. (Figure 73: 50,000 X; Figures 74-76: 37,500 X)

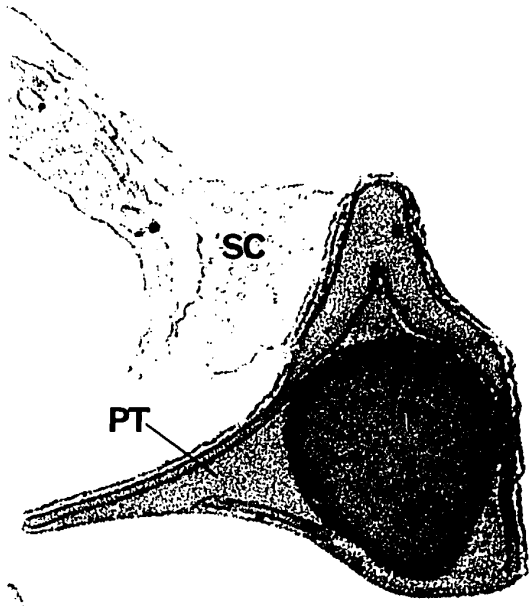

73

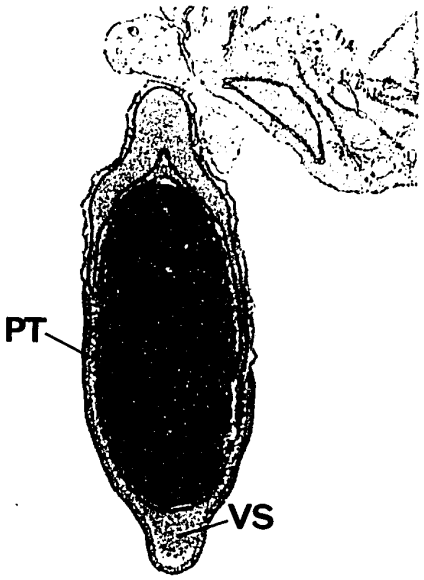

74

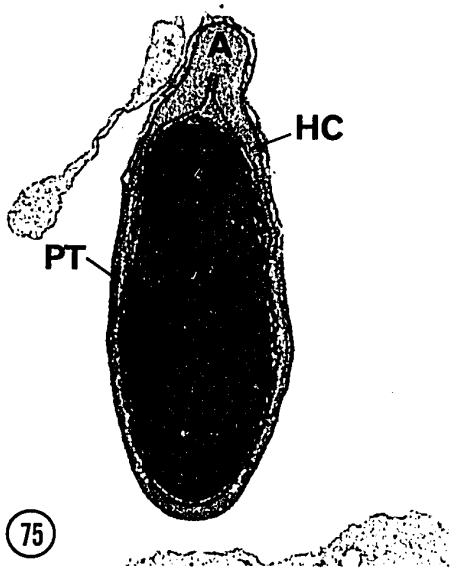

75

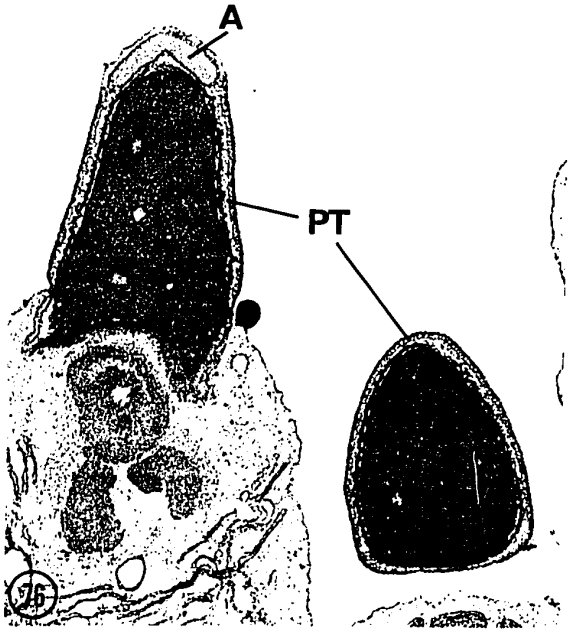

76